5-2022

A Foraminiferal Perspective on Holocene Environments of the Eastern Tropical Pacific

Maria Angelica Zamora-Duran

A Foraminiferal Perspective on Holocene Environments of the Eastern Tropical Pacific

by

Maria Angelica Zamora-Duran

A dissertation submitted to the College of Engineering and Science of
Florida Institute of Technology
in partial fulfillment of the requirements
for the degree of

Doctor of Philosophy
in
Biological Sciences

Melbourne, Florida
May, 2022

We the undersigned committee hereby approve the attached dissertation,
"A Foraminiferal Perspective on Holocene Environments of the Eastern Tropical Pacific."

by
Maria Angelica Zamora-Duran

_____
Richard B. Aronson, Ph.D.
Department Head and Professor
Ocean Engineering and Marine Sciences
Major Advisor

_____
Mark Bush, Ph.D.
Professor
Ocean Engineering and Marine Sciences

_____
Toby S. Daly-Engel, Ph.D.
Assistant Professor
Ocean Engineering and Marine Sciences

_____
Steven Lazarus, Ph.D.
Professor
Ocean Engineering and Marine Sciences

_____
Robert van Woesik, Ph.D.
Professor
Ocean Engineering and Marine Sciences

_____
Lauren T. Toth, Ph.D.
Research Oceanographer
United States Geological Society

Abstract

A FORAMINIFERAL PERSPECTIVE ON HOLOCENE ENVIRONMENTS OF THE EASTERN TROPICAL PACIFIC

by Maria Angelica Zamora-Duran, M.S., Florida Institute of Technology

Chairperson of Advisory Committee: Richard B. Aronson, Ph.D.

Climate change is the primary threat facing coral reef ecosystems. How marginal reef systems responded to past climatic variability provides clues to their prospects for persisting through contemporary climate change. Reefs along the Pacific coast of Panamá are dominated by branching corals of the genus *Pocillopora*. These reefs experience a natural gradient of nutrients, pH, and temperature because of stronger seasonal upwelling in the Gulf of Panamá (GoP) than in the Gulf of Chiriquí (GoC). The shallow reefs within both of the gulfs of Panamá They are also strongly affected by climatic variability due to the El Niño–Southern Oscillation (ENSO). It is hypothesized that ENSO variability at the beginning of the Late Holocene ~4000 year ago caused a 2000-year hiatus in reef-building in Pacific Panamá. Nevertheless, the environmental conditions that drove the shutdown and continued to suppress reef development were inferred from the geochemistry of a limited number of coral samples. Foraminifera are good

indicators of reef-ecosystem condition because they are abundant in reef settings, secrete calcium carbonate, host symbionts, respond rapidly to environmental variation, and persist in the absence of corals. In addition, unlike some other benthic taxa, the diversity of benthic Foraminifera and scleractinian corals reflect regional differences in oceanographic conditions in the ETP. Both taxa are approximately half as diverse in the ETP as they are in the Caribbean.

The composition of contemporary foraminiferal assemblages and their geochemistry track environmental variations in the eastern tropical Pacific. Temperature loggers deployed from 2016 to 2019 showed that water temperatures were lower on average and more variable in the GoP due to stronger seasonal upwelling. To determine how regional oceanography and climatic drivers influence modern foraminiferal assemblages between the two gulfs, I examined benthic Foraminifera in surface sediments. Contemporary and subfossil samples from both gulfs were dominated by heterotrophic Foraminifera, which was likely the result of overall nutrient enrichment due to upwelling—even in the weakly upwelling GoC—combined with ENSO effects. However, the GoC had higher abundances of symbiont-bearing taxa than the GoP. Since the Gulf of Chiriquí experiences weaker upwelling than the Gulf of Panamá, it is more characteristic of an oligotrophic reef environment. Geochemical analysis of contemporary, symbiont-bearing miliolids, *Sorites marginalis*, revealed that foraminiferal Mg/Ca ratios were lower in the GoP than in the GoC. The elemental ratio of magnesium to calcium in tests of benthic Foraminifera has been used successfully as a proxy for ocean temperature because

more magnesium is incorporated into the test during its construction with increasing temperature. The offset in foraminiferal Mg/Ca was consistent with the lower mean annual temperature observed in the GoP due to stronger seasonal upwelling.

Since contemporary foraminiferal assemblages were shown to be modulated by environmental variations, I sought to test whether the climatic changes leading up to the shutdown of reef accretion also led to shifts in the foraminiferal assemblages over the same period. I sampled Foraminifera from two cores from reef-framework within the GoP (Saboga and Contadora) and one core from the GoC (Canales de Tierra). I also used Mg/Ca-based temperature reconstructions to evaluate past environmental change. Similar to assemblages found in contemporary sediments, heterotrophic foraminifers dominated at all sites, and Canales de Tierra was characterized by a greater number of symbiotic Foraminifera than those sites in the GoP. The density of symbiotic Foraminifera tracked *Pocillopora* growth through time at all sites, decreasing from ~15 individuals/gram of sediment to ~2 ind/g during the hiatus in reef growth (~4000 cal yr BP to ~2000 cal yr BP).

I conducted geochemical analyses on foraminiferal tests within the cores to determine Mg/Ca ratios over time. At all sites, Mg/Ca ratios were more variable during the hiatus period. However, attempts to reconstruct temperature using Mg/Ca proxies from foraminiferal shells proved difficult in this study since shell Mg/Ca ratios from Contadora suggested an unrealistic temperature range of 8–64°C (107–247 mmol/mol) even after two rounds of analyses. At Saboga and Canales de

Tierra, Mg/Ca ratios did not show as much variability as those from Contadora, ranging from 135 to 150 mmol/mol and 101 to 203 mmol/mol, respectively. Based on the cores from Saboga and Canales de Tierra, I hypothesize that the greater variability of Mg/Ca during is likely a result of higher variability in ENSO. Strong La Niñas at the inception of the hiatus would result in cooler water temperatures which would account for the lower Mg/Ca ratios. Stronger El Niño events during the hiatus are most likely represented by higher Mg/Ca ratios. Reef accretion resumed ~2000 cal BP at which time Mg/Ca-based reconstructions of temperature stabilized at all sites. A local effect on Mg/Ca concentrations in Contadora could suggest a reason for the increased concentrations of Mg/Ca during the hiatus but the cause of the anomalously high Mg/Ca values is unclear.

Predicting the long-term behavior of ENSO with ongoing climate change is difficult due to conflicting evidence from paleoclimate proxies and model projections. However, the models that best capture key ENSO dynamics also tend to project an increase in future ENSO-driven sea-surface temperature variability and magnitude under ongoing warming particularly in the ETP. Based on the history of reef development in Pacific Panamá, it is likely that increased warming and ENSO variability could result in the collapse of Pacific reef ecosystems and a shift toward an increasingly heterotrophic state.

TABLE OF CONTENTS

List of Figures

List of Tables

Acknowledgments

I am very thankful for all of the people who have helped me achieve this long-awaited ambition. To all of the friends, family, and teachers that have offered me guidance and assistance throughout the years in the form of words, lessons, and/or embraces: your encouragement and efforts have truly helped me get to where I am today and you will never be forgotten. To the friends I have made in Melbourne, both from and outside of Florida Tech, thank you for making this once-unfamiliar place feel like home.

To my advisor Rich Aronson, I appreciate not only your advice and support, but also your challenging me to become a better scientist and communicator. To Mark Bush and Robert van Woesik, thank you both for your suggestions and guidance on statistical approaches that thoroughly strengthened my dissertation and that I will carry with me throughout my future endeavors. Thank you to Toby Daly-Engle and Steven Lazarus for your advice, support, and encouragement that allowed me to push forward even through difficult moments. To Lauren Toth, your insight on this project has been indispensable both in the field and the lab. I am extremely grateful that you introduced me to and helped me obtain the supplemental grant that allowed me to work at USGS and broaden my scope from a strictly biological background to a geological perspective. You and Phil Gravinese were always such generous hosts during my stays in St. Petersburg and I cannot thank you both enough.

To the other scientists that I had the pleasure of working with at USGS, thank you for walking me through geochemical analyses that were paramount to this project. To Julie Richey and Caitlin Reynolds, I would not have been able to complete this dissertation without your expertise on foraminiferal geochemistry and assistance with methodological procedures. To Jennifer Flannery, thank you for working with me over the years to complete the entirety of my geochemical analysis, especially in these challenging times that we've recently experienced.

I am thankful for the financial support offered to me by assistantships from the Department of Ocean Engineering and Marine Sciences and the National Science Foundation, without which I would not have been able to conduct this research. To Dee Dee Van Horn, thank you for your administrative support and encouragement. It is a wonder how you can keep track of all these students (and professors) and hold the department together. I am also thankful for the organizations and people that allowed the fieldwork in Panamá to be successful: The Smithsonian Tropical Research Institute and Liquid Jungle lab for their facilities, and Guillermo Schuttke for being our captain, dive safety officer, travel guide, and friend.

This experience has shaped the person I am today and will undoubtedly allow me to strive for great things in the future. For all who were involved, thank you.

Dedication

To my parents,

Your love and support have been unyielding, throughout this process and in my life. I love you both.

Chapter 1: Scope of Research

INTRODUCTION

The rate of projected loss of coral reefs due to climate change and other human disturbances is alarming (Hoegh-Guldberg, 1999; Walther et al., 2002; Hoegh-Guldberg et al., 2007; Carpenter et al., 2008; Hughes et al., 2007). Although reef systems occupy less than one percent of the biosphere, they provide over $300 billion per year in goods and services (Ahmed et al., 2007; Andersson, 2007). They serve as a critical food source for half-a-billion people and buffer shorelines from storm damage and erosion, protecting lives and property (Cesar et al., 2003). To predict how reefs will respond to ongoing climate change, it is increasingly important to understand the local and global forces that affect their growth and development. Benthic Foraminifera are valuable indicators of environmental conditions in marine ecosystems (Uthicke and Nobes, 2008; Willard and Cronin, 2007) and have been used previously to determine if environmental conditions are suitable for reef growth (Hallock et al., 2003; Oliver et al., 2014). In addition, the geochemistry of foraminiferal tests can help us reconstruct past changes in climate

(Henderson, 2002; Scheibner and Speijer, 2008; Eiler, 2011). The use of modern analogs, in which assemblages found in contemporary ecological conditions calibrate reconstructions of past oceanographic and climatic variability, is a well-proven technique. Such analyses improve our understanding of the major influences on coral-reef development that establish modern patterns.

As climate change and other human disturbances continue to degrade coral reefs globally (Glynn, 1984; Hughes et al., 2003; Hoegh-Guldberg et al., 2007; Baker et al., 2008), it is becoming increasingly important to determine how oceanographic patterns modulate the trajectories of reef biotas. This study explores how regional oceanography and climatic variability influence foraminiferal assemblage structure and reef growth from the mid-Holocene to the present. With a better understanding of these controls on reef-ecosystem development, it will be possible to hypothesize reasons for intermittent reef accretion.

Reefs along the Pacific coast of Panamá span a natural gradient of nutrients, pH, and temperature because of stronger seasonal upwelling in the Gulf of Panamá relative to the Gulf of Chiriquí (Fig. I.1). The ecosystems are not only influenced by dynamic regional oceanography but are affected by climatic variability due to the El Niño–Southern Oscillation (ENSO).

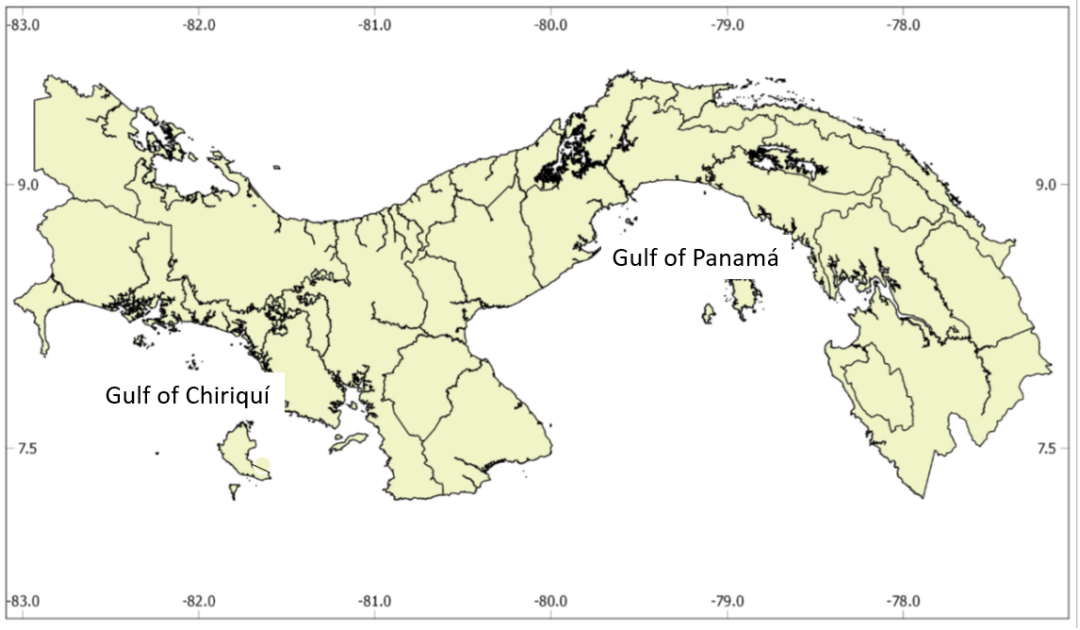

Figure 1.1: Outline map of Panamá with the two gulfs of study labeled.

Despite the high levels of climatic and oceanographic variability, and species composition varying, species diversities of most benthic taxa in the eastern tropical Pacific (ETP) do not differ from Caribbean reef environments (Chesher, 1972; Jones & Hasson, 1985; Allmon et al., 1993, Glynn, 2004; Cortés et al., 2017). Scleractinian corals (Glynn, 1972; Glynn & Ault, 2000; Toth et al., 2017) and benthic Foraminifera (Buzas & Culver, 1991; Collins 1999; Humphreys et al., 2019) are notable exceptions: both taxa are approximately half as diverse in the ETP as they are in the Caribbean. These differences in diversity primarily reflect regional differences in oceanographic conditions (Cortés 1997; Buzas & Culver, 1998; Manzello 2010; Toth et al., 2013, 2017).

OCEANOGRAPHIC AND CLIMATIC VARIABILITY OF REEF ECOSYSTEMS IN PACIFIC PANAMA

Off the Pacific coast of Panamá, the Gulfs of Panamá and Chiriquí experience seasonal differences in oceanography due to wind-driven upwelling. During the dry season, from December to April, the Intertropical Convergence Zone (ITCZ) migrates south of the Isthmus of Panamá, strengthening the trade winds from the Caribbean over Central America (D'Croz & O'Dea, 2007; Alexander et al., 2012). These northeast trade winds form wind jets where the topography of the isthmus is low, driving strong upwelling in the Gulf of Panamá (D'Croz & O'Dea, 2007; Alexander et al., 2012). Upwelling in the Gulf of Panamá is associated with thermocline-shoaling, nutrient enrichment, and decreased pH from CO_2 enrichment (Legeckis, 1988; Xie et al., 2005; D'Croz & O'Dea, 2007). The Gulf of Chiriquí does not experience the same degree of intense, wind-driven upwelling that occurs in the Gulf of Panamá; however, thermocline-shoaling does occur in the Gulf of Chiriquí during the dry season (D'Croz & O'Dea, 2007; Wyatt et al., 2019). During the non-upwelling, wet season from April to December, the two gulfs experience similar oceanographic conditions and stratification of their water columns (D'Croz & O'Dea, 2007).

During the wet season, sea-surface temperatures (SSTs) in both gulfs range from 27.5 to 29 °C, and salinities range from 29.5 to 33.5 ppt (D'Croz & O'Dea,

2007). In the Gulf of Panamá, upwelling during the dry season (December–April) decreases SSTs to a monthly average of 18–24 °C. *In situ* measurements of temperature in both locations from 2016–2018 showed that daily SSTs fluctuated up to 8.2 °C in the Gulf of Panamá and 5.8 °C in the Gulf of Chiriquí from January to April (Randall et al., 2020). At the peak of upwelling (February–March), nutrients are enriched, with chlorophyll-a concentrations reaching a monthly average of up to 10 mg m^{-3} in the Gulf of Panamá, while remaining stable around 1 mg m^{-3} on average in the Gulf of Chiriquí (Randall et al., 2020). Salinities in both gulfs increase to ~33 ppt during the dry season (Glynn & Maté, 1997). This regime of wind-gap upwelling has persisted in Pacific Panamá throughout the Holocene as shown by palaeoceanographic reconstructions (Martínez et al., 2006; Toth et al., 2015 a, Toth et al., 2015b). Toth et al. (2015b) showed that the intensity of this upwelling varied significantly over the past 7000 years, with the strongest upwelling occurring around 4000 years ago but then had weakened to approximate modern conditions 2000 years.

In addition to seasonal upwelling, reef environments of the ETP experience interannual to decadal-scale climatic variability because of ENSO events. During El Niño years in Pacific Panamá, SSTs increase and seasonal upwelling is reduced. By contrast, La Niña results in cooler SSTs, increased precipitation, and stronger upwelling in the ETP leading to increased nutrient inputs. The shallow reefs within both gulfs of Panamá, which are dominated by colonies of branching corals of the genus *Pocillopora* (Glynn & Maté, 1997; Glynn et al., 2017; Toth et al., 2017),

respond strongly to these ENSO events (Wang & Fielder, 2006; Toth et al., 2012; Reymond et al., 2016; Fieldler et al., 2017; Glynn, 2017; Glynn et al., 2017; Manzello et al., 2017). For example, during the 1982–1983 El Niño event, Glynn et al. (2001) documented 85% mortality of corals in the Gulf of Panamá and 75% mortality in the Gulf of Chiriquí. On a millennial scale, strong variability in ENSO apparently led to a 2,500-year hiatus in coral growth during the Holocene, about 4,100 cal yr BP (calibrated calendar years before present, where 'present' is 1950; Toth et al., 2012). The environmental conditions that drove the shutdown and continued to suppress reef development are uncertain however, in part because there are limited samples available for coral-based climate reconstructions. Nevertheless, stronger La Niña events are thought to have caused the initial shutdown of reef accretion whereas enhanced variability in ENSO may have suppressed coral growth for over 2,000 years (Toth et al., 2015, Toth et al., 2017). Because ENSO events are known to affect foraminiferal composition in reef environments (Kelmo and Hallock, 2013; Humphreys et al., 2019), analyses of foraminiferal abundances could be used to investigate environmental variability at a fine resolution and in the absence of corals.

TAXONOMY AND BIOLOGY OF BENTHIC FORAMINIFERA

Antoine van Leuwenhoek and Carl von Linné first described the complexity of Foraminifera, initially classifying them as mollusks. Dujardin (1835) aided in the

classification by concluding that Foraminifera were unicellular. Most studies completed in the 19th century on Foraminifera did not focus on their biology but instead investigated their geology, with over 50,000 fossil species described (Pawlowski and Holzmann, 2008). Approximately 3,000–5,000 species of Foraminfera are estimated to be living today (Goldstein, 2002).

Foraminifera are currently classified according to the mechanism by which they build their tests, which leads to differences in composition and morphology of the test (Sen Gupta, 2002). Foraminifera build their tests by adding chambers separated by partitions connected by a hole, or foramen. Most species of Foraminifera are multilocular, building their tests with multiple chambers. Multilocular species intermittently add a new chamber by forming a cyst made of sediment or other foreign material filled in with an organic lining, ultimately resulting in calcification of the chamber and the whole test (Goldstein, 2002). Some species are unilocular, building their test with a single chamber. During growth, the unilocular forms increase the size of their single chamber by adding material to the inner organic lining of the test (Goldstein and Barker, 1988).

During the earliest Cambrian the first agglutinating foraminifera made their first appearance in the geologic record. These "primitive" forms built their test of foreign particles held together by an organic cement. This organic cement may have been secreted by the foraminifer in cytoplasmic vacuoles as is the case with Recent agglutinating foraminifera. Yet, the capability to biomineralize calcite did not evolve until after another 60 million years when the fusulinids

developed their microgranular wall. Calcitic cemented agglutinates occur even later, at the base of the Carboniferous. The agglutinated species construct their tests by cementing particles from their environment, such as organic matter and sand grains, with proteins, iron oxide, or calcium carbonate. Although ubiquitous in marine environments, agglutinated foraminifers dominate in areas with reduced levels of calcium carbonate, where calcareous foraminifers are stressed (Murray, 2006). The few agglutinated taxa that use a calcareous cement to form their tests, like those in the order Textulariida, are common in carbonate-saturated environments like open shelves and/or coral reefs.

The other groups of Foraminifera secrete certain forms of calcite to build their test and are subdivided into three major groups: microgranular, porcelaneous, and hyaline. Microgranular-walled taxa secrete subspherical grains of low-magnesium calcite that are equal in dimension. Porcelaneous species secrete imperforate tests made of rods of high-magnesium calcite randomly arranged into inner and outer surface layers, enclosing a thick middle layer of crystal laths that do not contain pores. The hyaline Foraminifera add a new lamella to the test when forming new chambers and have perforate shells comprised of interlocking crystals of low-magnesium calcite. Studies on the phylogeny of these taxa support their current distinction based on morphology, indicating that the porcelaneous taxa and the hyaline taxa diverged early in the evolutionary history of these lineages (Longet and Pawlowski, 2007). Lee (1990) elevated Foraminifera from Order to Class within the Phylum Sarcomastigophora, and currently 16 orders are recognized

(Loeblich and Tappan, 1992; Sen Gupta, 2002). All extant orders of Foraminifera are benthic except for one suborder of the Order Rotaliida: the Globigerinida. Some benthic Foraminifera, however, can have planktonic reproductive stages (Goldstein, 2002).

There are three dominant orders of benthic Foraminifera that produce calcite shells: Miliolida, Rotaliida, and Buliminida (Sen Gupta, 2002). Of the calcite-producing species, many use energy to exclude magnesium (Mg) ions during precipitation. Porcelaneous species in the Order Miliolida, however, precipitate their shells close to equilibrium with seawater, resulting in shells that contain as much as 130–150 ppm of Mg in shallow tropical waters (Mores and Mackenzie, 1990). Because tests containing more than 80 ppm of Mg are relatively soluble under reduced carbonate saturation, miliolids are good indicators of carbonate supersaturation and will be the most susceptible to ocean acidification (Hallock, 2000). The Rotaliida include some of the most stress-tolerant generalists, such as members of the genus *Ammonia*, which can survive in hypoxic or highly polluted habitats (Schafer, 2000). Rotaliids also comprise some of the most highly specialized species including those that host algal endosymbionts. Rotaliids thrive and produce vast volumes of carbonate sediments in oligotrophic environments that are sensitive to anthropogenic pollution (Hallock, 2003).

Benthic foraminifers exhibit a variety of feeding strategies, including grazing, suspension feeding, deposit feeding, carnivory, parasitism, direct uptake of dissolved organic carbon, and symbiosis (Goldstein, 2002). Heterotrophic forms

feed on detritus, bacteria, algae, or a combination thereof. Species that live in muddy sediments, within and below the photic zone, can use their reticulopodia (individual pseudopodia that form complex, branched nets) to construct feeding cysts (Hofker, 1927; Nyholm, 1957; Goldstein and Corliss, 1994). In this process, the reticulopodia gather material including sediment, algal cells, bacteria, and organic detritus and partition the material into small bundles, which the foraminifer then ingests by phagotrophy from the terminal chamber (Goldstein and Corliss 1994). In areas of high organic matter and decomposition, increased hypoxia/anoxia and sulfidic conditions limit the depth in the sediments to which Foraminifera can live (Alve, 1995; Sen Gupta, 2002). In oligotrophic environments, food availability is the dominant factor that limits the depth at which Foraminifera live (Hallock, 2003).

Several families of Miliolida and Rotaliida have coevolved with marine algae, diversifying and morphologically specializing to the benefit of their symbiotic relationship. These symbiotic Foraminifera can increase greatly the amount of fixed carbon available to them compared with the purely heterotrophic organisms that share the same environment (Hallock, 2002; Lee, 2006). Foraminifers, especially those that host endosymbionts, are common in reef ecosystems including reef flats, lagoons, reef slopes, and oceanic banks (Murray, 2006). As shown in Table 1, all genera in reef environments within the same order share the same feeding strategy (either heterotrophic or symbiont bearing), though the type of symbiont can differ among genera.

Members of the living families within the Order Miliolida have been documented to host a vast range of algal symbionts (Table 1; Lee, 2006). The superfamily Soritacea includes a clade of reef-dwelling, porcelaneous, benthic foraminifers that host dinoflagellate endosymbionts similar to the zooxanthellae found in scleractinian corals (Pochon et al., 2007). Members of this clade are most commonly found in the Indo-Pacific in reef-flat environments. A second clade hosts chlorophyte (green-algae) endosymbionts, whereas a third hosts rhodophytes (red algae). These species are abundant on seagrass, macroalgae, and reef rubble in western Atlantic and Caribbean reef flats and lagoons. The Alveolinidae, a separate family of milioline Foraminifera, host diatom endosymbionts. Miliolid diversity is high in reef ecosystems because their warm, saline waters are typically carbonate-supersaturated, which promotes enhanced rates of precipitation of their high-Mg-calcite, porcelaneous shells.

Rotaliid families, including Amphisteginidae, Calcarinidae, Asterigerinidae, and Nummulitidae, predominantly host diatoms (Table 1; Lee, 2006). These rotaliid species are usually more dominant than the Miliolida in reef environments, yet their diversity is lower. Of the rotaliids, *Amphistegina* typically dominates foraminiferal assemblages in reef margins and slopes. In the Indo-Malay region, however, the Calcarinidae can be more abundant than Amphisteginidae (Hohenegger, 2006). The Asterigerinidae are relatively small and morphologically simple. By contrast, the Nummulitidae include individuals that are among the largest foraminifers documented. They have highly specialized internal structures

to accommodate symbionts, gather light, and aid in cytoplasmic exchange among the internal chambers and the environment (Hottinger, 2000, 2006).

Table 1.1 Overview of the phylogeny of the most common orders found in reef environments and their feeding strategies (Based on Hallock, 2003).

Order	Family	Genera	Feedi strategy
Buliminida	Reussellidae	*Reussella*	Heterotrophic
	Bolivinidae	*Bolivina*	Heterotrophic
Trochamminida	Trochamminidae	*Trochammina*	Heterotrophic
Textulariida	Lituolidae	*Ammobaculites*	Heterotrophic
Rotaliida	Nonionidae	*Nonionoides*	Heterotrophic
		Nonion	Heterotrophic
		Haynesina	Heterotrophic
	Planorbulinidae	*Planorbulina*	Heterotrophic
	Elphididae	*Cribroelphidium*	Heterotrophic
		Elphidium	Heterotrophic
	Rosalinidae	*Rosalina*	Heterotrophic
	Rotaliidae	*Ammonia*	Heterotrophic
	Cibicididae	*Lobatula*	Heterotrophic
	Acervulinidae	*Discogypsina*	Heterotrophic
	Discorbidea	*Discorbis*	Heterotrophic
	Amphisteginidae	*Amphistegina*	Symbiotic: Diatom
	Asterigerinidae	*Asterigerina*	Symbiotic: Diatom
	Nummilitidae	*Heterostegina*	Symbiotic: Diatom
Miliolida	Cornuspiridae	*Cornuspira*	Heterotrophic
	Fischerinidae	*Vertebralina*	Heterotrophic
		Wiesnerella	Heterotrophic
	Hauerinidae	*Hauerina*	Heterotrophic
		Miliolinella	Heterotrophic
		Pyrgo	Heterotrophic
		Quinqueloculina	Heterotrophic
		Schlumbergerina	Heterotrophic
		Triloculina	Heterotrophic
	Miliolidae	*Pseudohauerina*	Heterotrophic
	Spiroloculinidae	*Spiroloculina*	Heterotrophic
	Tubinellidae	*Articulina*	Heterotrophic
	Alveolinidae	*Borelis*	Symbiotic: Diatom
		Alveolinella	Symbiotic: Diatom
	Peneroplidae	*Laevipeneroplis*	Symbiotic:
		Peneroplis	Rhodophyte
	Soritidae	*Archais*	

		Cyclobiculina *Broeckina* *Sorites*	Symbiotic: Rhodophyte Symbiotic: Chlorophyte Symbiotic: Chlorophyte Symbiotic: Chlorophyte Symbiotic: Dinoflagellate

Most foraminifers are microscopic, but some species can grow to several centimeters in diameter, with the extinct *Lepidocyclina elephatina* being the largest ever reported at 14 cm (Grell, 1973). The algal-symbiont-bearing foraminifers are often referred to as larger benthic Foraminifera because many species attain large adult sizes, some exceeding 10 cm in diameter. Size is proportional to lifespan in Foraminifera, with small taxa living for days and larger taxa licing for years. Growth and calcification of substantial-sized shells over periods of months to years can only be sustained by relatively predictable environments in which juvenile and adult mortality are low and access to sunlight is predictable (Hallock, 1985).

The life cycle in Foraminifera is more varied than any other group of protists, with other protist groups exhibiting binary fission, various forms of budding, and morphological dimorphism associated with their reproductive cycle (Goldstein, 2002). Benthic Foraminifera undergo alternation of generations (Goldstein, 2002). Foraminifera can have one or more asexual generations that typically reproduce by multiple fission, producing broods of tens to thousands of juveniles from the cytoplasm of the parent cell (Cushman, 1928). The young

produced by meiosis are haploid and grow to become uninucleate adults, producing gametes by mitosis (Le Calvez, 1946, 1950). Since meiosis can occur before asexual reproduction, the juveniles produced may be genetically distinct from the parent cell. Most species of Foraminifera also sexually reproduce by expelling biflagellated gametes directly into the water (Goldstein, 1997). Of the 30 species whose life cycles have been studied, most exhibit this general theme of alternation of generations. Some species exhibit obligatory alternation of generations, going through meiosis before multiple fission (Lee et al., 1991; Goldstein, 1997). Other species of Foraminifera show facultative alternation of generations, which includes asexual cycles that reproduce by multiple fission (Bradshaw, 1957; Schnitker, 1974).

FORAMINIFERA AS ENVIRONMENTAL INDICATORS

Planktonic Foraminifera have proven to be invaluable assets to paleoceanographical and paleoclimatological research (Murray, 1991; Verhallen, 1991; Schlesinger, 1991; Gooday, 2003) because isotopic analysis of foraminiferal tests can provide reliable reconstructions of paleotemperature (Naqvi et al., 1994; Waelbroeck et al., 2002, Groeneveld et al., 2019). The elemental ratio of magnesium to calcium in tests of benthic Foraminifera has been used successfully as a proxy for ocean temperature (Rosenthal et al., 1997; Lear et al., 2000; Billups and Schrag, 2002; Martin et al., 2002; Elderfield et al., 2000). Trace amounts of

magnesium are substituted for calcium in foraminiferal calcite during construction of the test, and Mg/Ca increases with increasing temperature. In addition, studies have recognized correlations between shell type, depth, and salinity, allowing the structure and morphogroup distribution of assemblages of benthic Foraminifera to be used to infer paleoenvironments and sediment types (Murray, 2006; Willard and Cronin, 2007). Paleoecological data from foraminiferal tests provide valuable historical perspectives to ecologists and restoration planners (Alve, 1991; Gooday, 2003; Willard and Cronin, 2007).

Foraminifera have also been used as environmental bioindicators of contemporary water quality (Havach and Collins, 1997; Ishman et al., 1997; Thomas et al., 2000; Gibson et al., 2000; Karlsen et al., 2000; Hallock, 2003; Kelmo and Hallock, 2013; Alves Martins et al., 2015 a, b). They are an effective tool because of their pervasive distributions, high abundances, short generation times, reliable fossil record, and sensitivity to certain environmental factors (Buzas et al., 1970; Schönfeld et al., 2012). Researchers have used the assemblage structure of Foraminifera to develop indices for evaluating ecosystem conditions (Sen Gupta et al., 1996; Hallock et al., 2003; Bouchet, 2012), which resource managers can then use to evaluate restoration efforts.

Coral reefs thrive in oligotrophic waters, where mixotrophic nutrition is advantageous (Birkeland 1977, 1988; Hallock and Schalger, 1986). Slightly higher nutrient flux promotes phytoplankton blooms in the water column, limiting light penetration to the benthos. Light attenuation promotes the dominance of the

benthos by heterotrophic suspension-feeding animals, such as sponges and ascidians, and of detritus-feeding echinoderms and crustaceans that do not directly require sunlight for survival. Benthic foraminiferal assemblages respond similarly to nutrient flux (Hallock, 1987, 1988). In very-low-nutrient marine environments, including many coral reef systems, large benthic Foraminifera that host symbionts completely dominate the sand-sized sediments (e.g., McKee et al., 1956; Hallock, 1981a). As nutrient supplies increase, bioeroded coral fragments, calcareous algae, molluscan debris, and smaller herbivorous and detritivorous foraminifers become more common as sedimentary constituents (Hirschfield et al., 1968; Hallock, 1988; Cockey et al., 1996). When the environment becomes unsuitable for the survival of symbiotic foraminifers, their dead tests become rare in the sediments, and remnants become increasingly corroded (e.g., Cottey and Hallock, 1988). These changes occur with high nutrient loading that does not result in a measurable increase in dissolved nutrients in the water column because the planktic and benthic communities can incorporate and utilize all available nutrients (e.g., Laws and Redalje, 1979). True eutrophication results in further changes in benthic-community structure, including domination by stress-tolerant taxa that can survive episodic anoxia (e.g., Alve, 1995).

On coral reefs that are subject to significant nutrient loading, populations of smaller heterotrophic foraminifers proliferate, and their shell numbers overwhelm those of symbiotic large benthic Foraminifera (Hirshfield et al., 1968; Cockey et al., 1996). It is becoming increasingly important to have indicators of conditions of

water quality that will support reef development, especially with the increase of multiple stressors that are causing coral mortality. Populations of large benthic Foraminifera are immune to coral-specific diseases and recover much more quickly from physical impacts than long-lived coral populations. Therefore, large benthic Foraminifera can serve as sensitive indicators of water-quality conditions that support reef development. Reef-building corals and large benthic Foraminifera share physiological traits as both groups depend on algal symbionts to enhance growth and calcification (e.g., Lee and Anderson, 1991). Physiological studies of corals (Falkowski et al., 1993; Steven and Broadbent, 1997) and large benthic Foraminifera (Lee, 1998) demonstrated that fixed-nitrogen limitation is crucial to maintaining the host-symbiont relationship.

The Foraminifera in Reef Assessment and Monitoring Index ("FORAM" Index or FI; Hallock, 2003) applies observations from the 1970s suggesting that healthy coral reefs had abundant mixotrophic foraminifers (McKee et al., Hallock 1981a, 1988). Specifically, the FORAM Index is used to determine whether water quality in the environment is adequate to support coral-reef growth or recovery and is calculated as the proportion of symbiont-bearing taxa to heterotrophic and stress-tolerant taxa that can tolerate intermittent hypoxia. The FORAM Index is based on observations that symbiont-bearing foraminifers and zooxanthellate, reef-building corals require similar water quality (Hallock, 1996, 2003). Foraminiferal assemblages in sediment samples from the northwest Atlantic and Caribbean areas were originally used to create the FORAM Index, so it cannot be assumed to be

appropriate in other biogeographic regions. However, many studies have successfully implemented the FORAM Index in marginal and non-reefal environments in the subtropical north- and southwestern Atlantic, Mediterranean, and Indo-Pacific to show diminishing water quality in those areas (e.g., Barbosa et al., 2009, Dimiza et al., 2016). Though the FORAM Index has proved useful in reef environments outside of the Caribbean and the northwest Atlantic, it would not be practical to use in this study. Both the Gulfs of Panamá and Chiriquí exhibit seasonal upwelling and are therefore subject to higher productivity than most oligotrophic reef environments. Heterotrophs dominate in both gulfs due to the relatively high nutrient loads. For this reason, both gulfs inherently show low, but subtly different, FORAM Index numbers even though reefs persist in these conditions.

The relationship of foraminiferal assemblage composition to productivity has been examined in upwelling zones (e.g., Lutze and Coulbourn, 1984; Altenbach and Sarnthein, 1989) and inferred from the geologic record (e.g., Van der Zwaan, 1982; Woodruff, 1985; Loubere and Banonis, 1987). These studies show that the composition of benthic foraminiferal assemblages correlates with sedimentary organic-carbon content. In fact, nutrient increases led to the rapid rebound of heterotrophic taxa in Bahía, Brazil following the strong La Niña from 1999–2000 (Kelmo & Hallock, 2013).

Changes in sea level also influence shifts in foraminiferal assemblages. A recent study completed by Johnson et al. (2019) determined that benthic

foraminiferal assemblages responded to effects caused by reef-shallowing to keep up with sea level, including changes in hydrodynamic energy, light availability, and the carbonate content of reef-matrix sediments. This study showed the foraminiferal composition of nearshore reef communities were resistant to change, even as anthropogenic pollution and runoff continued to diminish water quality.

RESEARCH GOALS

For this research, I sought to identify how climatic and oceanographic variability controlled coral-reef ecosystem development in the Pacific Panamá. I collected samples of contemporary sediments, and sought to characterize their foraminiferal composition to determine whether environmental drivers led to differences in foraminiferal assemblages between gulfs. I then used paleoecological analyses of foraminiferal assemblages combined with records from cores of coral-reef frameworks to analyze the conditions that led to the cessation and recovery of reef development in Pacific Panamá after ~4100 cal yr BP. I address the following research goals through this study.

1. In Chapter 2, I explore differences in contemporary foraminiferal assemblages between the Gulfs of Panamá and Chiriquí, and I determine that there is not only a difference in assemblages, but that the difference reflects differences in mesoscale oceanography.

2. In Chapter 3, I investigate whether foraminiferal composition changed in reef frameworks throughout the Holocene and conclude that there were significant shifts in heterotrophs and symbiotic taxa through time.
3. In Chapter 4, I seek to determine whether the geochemistry of foraminiferal tests relates to environmental variability, specifically temperature, and whether geochemical proxies show significant changes in temperature leading up to the hiatus in coral-reef growth and/or reef recovery following the hiatus.

By answering these questions, I determined that regional oceanography led to heterotrophic dominance in both gulfs, yet the Gulf of Chiriquí was characterized by greater symbiont density than the Gulf of Panamá because of weaker seasonal upwelling. I also found that Mg/Ca was highly variable in Contadora during the hiatus in reef growth, potentially due to increased variability in ENSO.

Chapter 2: Surface characterization of foraminiferal species composition

INTRODUCTION

Coral-reef ecosystems of the eastern tropical Pacific (ETP) are subject to some of the most stressful environmental conditions experienced by reef systems across the tropics (Cortés, 1997; Glynn & Ault, 2000). Reefs of the ETP are centered at the convergence of equatorial currents and countercurrents, experience varying levels of seasonal, wind-driven upwelling, and are strongly influenced by the El Niño-Southern Oscillation (ENSO; Wang & Fiedler, 2006; Reymond et al., 2016; Fiedler & Lavin, 2017; Glynn, 2017; Glynn et al., 2017; Manzello et al., 2017; Wang et al., 2016). As a result, temperature, salinity, and nutrient levels are highly variable in these environments (Fiedler 1992, 2002). For these reasons, the marginal marine environments of the eastern tropical Pacific (ETP) serve as an ideal natural laboratory to study how oceanographic and climatic variability influence coral-reef ecosystems.

Foraminifera are effective bioindicators of water quality in the tropics, as elsewhere (Cockey et al., 1996, Havach & Collins, 1997; Hallock, 2000; Hallock et al., 2003, Martínez-Colón et al., 2009; Parker and Gischler, 2011; Kelmo & Hallock, 2013; Fajemila et al., 2015). Hallock et al. (2003) categorized foraminiferal genera into three functional groups: phototrophic, symbiont-bearing

taxa (hereafter referred to as symbiotic); stress-tolerant, heterotrophic taxa (hereafter referred to as tolerant); and other heterotrophic taxa (hereafter referred to as heterotrophic). As discussed in Chapter 1, the relative abundances of these three functional groups can be used to calculate the FORAM Index, which was developed to indicate whether or not an area should be expected to support reef growth: assemblages tend to shift from dominance of larger, symbiont-bearing taxa to smaller, faster-growing heterotrophs as nutrient levels increase (Hallock, 2000; Hallock et al., 2003).

In this study, I characterized the contemporary foraminiferal assemblages in shallow-reef environments off the Pacific coast of Panamá, both taxonomically and in terms of functional groups. This baseline information will help us to interpret variability in foraminiferal assemblages in the subfossil record and project the future of environments supporting coral reefs under ongoing climate change, nutrient enrichment, and ocean acidification. My goal was to determine the imprint of regional oceanography on assemblage structure. I also evaluated how the elemental composition—the ratio of magnesium to calcium (Mg/Ca)—of a large, symbiont-bearing foraminifer, *Sorites marginalis*, varied in response to differences in water temperature between gulfs. I address the following research questions and hypotheses:

1. Does contemporary foraminiferal composition differ between the two gulfs, and if so is that a reflection of differences in mesoscale oceanography?

- H_1: Genera that are more characteristic of coral-reef environments (symbiont-bearing foraminifers) are dominant in the Gulf of Chiriquí whereas heterotrophs dominate in the Gulf of Panamá due to increased nutrients and oceanographic variability there.

2. Do the Mg/Ca ratios of contemporary foraminiferal tests relate to differences in mean annual SSTs between the two gulfs?
    - H_2: Because the incorporation of Mg as an impurity to calcite occurs at higher temperatures, Mg/Ca ratios from foraminifers within the Gulf of Chiriquí are higher than those from specimens from the Gulf of Panamá because the mean annual SSTs are lower in the Gulf of Panamá as a result of seasonal upwelling.

METHODS

SAMPLING PROCEDURES

Reefs off the coasts of three islands in each of Panamás gulfs were chosen as collection sites for this study (Fig. 2.1): Pedro González, Saboga, and Contadora in the Gulf of Panamá; and Coiba, Uva, and Canales de Tierra in the Gulf of Chiriquí.

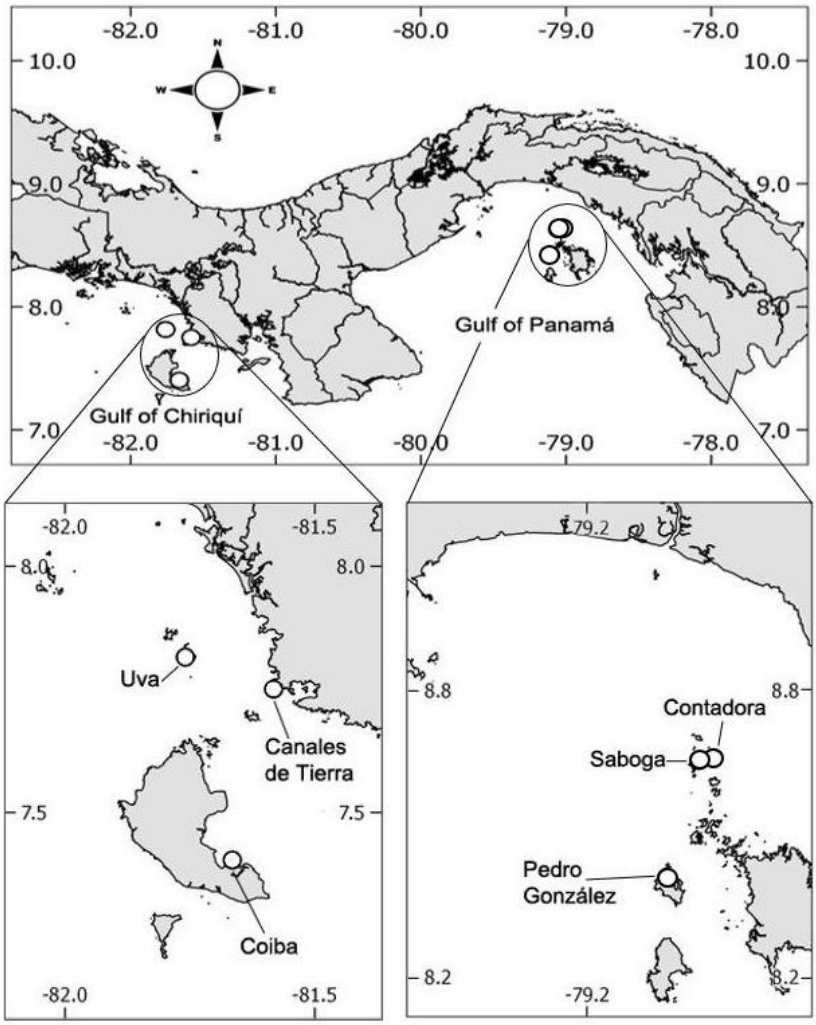

Figure 2.1 Locations of sampling sites in the Gulf of Panamá and the Gulf of Chiriquí.

To examine seasonal differences in temperature between the two gulfs, multi-year temperature records were collected on the shallow reef slopes at 3 m below mean sea level at each site using Seabird Electronics SBE56 temperature recorders (0.002 °C accuracy, 0.0001 °C resolution, <10 sec response time) mounted just above the reef surface on reinforcing rods driven into the substrate. Instruments were programmed to sample at 2-min intervals during deployment

durations of ~6–12 months, with instruments changed out at those intervals to achieve near-continuous temperature records from December 2015 to March 2019.

Samples of surface sediment were taken in March 2019, during an ENSO-neutral year. The ETP experienced a strong El Niño event from the summer of 2015 through the spring of 2016. The El Niño gave way to more neutral conditions late in 2016 and La Niña conditions in late 2017 to early 2018 (https://www.esrl.noaa.gov/psd/gcos_wgsp/Timeseries/Nino3/). These samples, therefore, were collected 2–3 years after as strong El Niño event and one year after a La Niña event.

At each of the three sites within each gulf, five sediment samples were collected within stands of *Pocillopora* spp. at locations at least 5 m apart (n=30 total samples). The samples were collected at a depth of ~3 m relative to mean sea level using SCUBA. Sediment samples were scooped and placed in plastic bags to a volume of 10–20 cm^3. The samples were processed following the procedures described by Hallock et al. (2003). Half the sediment from each sample was washed with fresh water over a 63-µm mesh sieve to remove silt and clay, and then dried on filter paper at ~40 °C overnight. Subsamples were weighed to the nearest mg (typically 200–500 mg) and examined for foraminiferal tests under a stereomicroscope. The sediment samples were comprised mainly of carbonate sand, with little silt and clay, so the mud fraction was not included in this study. All of the identifiable foraminifers from each subsample were picked, transferred to micropaleontological slides, identified to the genus-level, and counted. If fewer

than 250–300 foraminifers were found in the subsample, the process was repeated for additional subsamples until at least 250–300 individuals or the whole subsample were picked. The total weight in grams of the sand-sized sediment that was picked was recorded and used to calculate foraminiferal densities.

MG/CA ANALYSIS

I used symbiont-bearing miliolids, *Sorites marginalis*, for Mg/Ca analysis because of their abundance and relatively large size. *Sorites marginalis* construct its tests of high-Mg calcite (van Dijk et al., 2017). Very few studies have investigated the Mg/Ca-temperature relationship in shallow-benthic Foraminifera with high-Mg calcite, and the temperature sensitivity of *S. marginalis* is presently unknown. However, a culture study showed a temperature sensitivity of 1.7% $°C^{-1}$ in another high-Mg-calcite, shallow-benthic species, *Operculina ammonoides* (Evans et al., 2015). I applied the Mg/Ca relationship for *O. ammonoides* to the Mg/Ca data for *S. marginalis* to determine whether variability in the ratio in the latter species provided a reasonable estimate of the temperature difference between the Gulfs of Chiriquí and Panamá.

For this analysis, 10–20 individuals of *S. marginalis* were picked from each sediment sample. The tests were lightly crushed and cleaned using a modified procedure from Barker et al. (2003), which involved a clay-removal step (using MilliQ water and methanol rinses), an oxidation step to remove organic material, and a weak acid-leach to remove any adsorbed contaminants. Cleaned samples were dissolved in 2% HNO_3 to achieve a target concentration of 20 ppm Ca.

Samples were analyzed for Mg/Ca using a PerkinElmer 7300 DV Inductively Coupled Plasma-Optical Emission Spectrometer (ICP-OES) at the United States Geological Survey's Coastal and Marine Science Center in St. Petersburg, FL, USA. The Mg/Ca ratios were corrected for instrumental drift and noise using the internal gravimetric standard (IGS) method developed by Schrag (1999). The mean corrected IGS precision for Mg/Ca was 0.033 mmol/mol (1σ, n = 223). Three samples were analyzed for Mg/Ca concentrations from each of the six sites; however, only the samples that had concentrations of Ca within the QA/QC range of 10–30 ppm Ca were used for statistical analyses. Only one sample from Canales qualified, whereas two samples from each of the other sites were within range and could be used.

STATISTICAL ANALYSES

I calculated 30-day running means of the *in situ* temperatures from each site from January 2016 to March 2019. The data were plotted for each gulf to highlight the differences between gulfs in seasonal temperature variability. A nested analysis of variance (ANOVA), in which sites were nested within gulfs, was used to determine if the Mg/Ca ratios of *S. marginalis* tests were significantly different among sites and/or between gulfs.

Raw counts of foraminiferal genera were recorded, and their densities in individuals per gram (ind/g) of picked sediment were calculated. The genera were categorized into the three functional groups of Hallock et al. (2003): symbiotic, tolerant, and heterotrophic. A nested ANOVA was used to examine differences in

total foraminiferal density and, separately, the densities of the dominant foraminiferal orders—Miliolida and Rotaliida—between gulfs and among sites, with sites nested within gulfs. After square-root transformation, the data met the assumptions of normality and homogeneity of variances required for the ANOVA. The ANOVAs were calculated using the "aov" function in the R statistical package (Chambers et al., 1992).

Analysis of Similarity (ANOSIM) was used to evaluate the variability of foraminiferal assemblages between gulfs based on the densities of functional groups and, separately, based on the densities of all taxa. The ANOSIMs used square-root-transformed Bray-Curtis dissimilarities, and sites were nested within gulfs. The genera that contributed the most to the differences between gulfs were identified using Similarity Percentage (SIMPER) analysis. The ANOSIMs and the SIMPER analysis were calculated using Primer v.7 (PRIMER-e 2017, Quest Research Ltd., Auckland, New Zealand).

The functional-group composition of the two gulfs was also compared using the FoRAM Index, FI, which was calculated using the following equation:

$$FI = (10*P_s) + (P_t) + (2*P_h) \quad (1)$$

where P_s is the proportion of symbiotic species, P_t is the proportion of tolerant species, and P_h is the proportion of heterotrophic genera. Based on the thresholds proposed by Hallock et al. (2003) for Caribbean reef sediments, foraminiferal assemblages composed of at least 25–30% symbiotic foraminiferal specimens and no more than 75% heterotrophic taxa have FI ≥ 4, suggesting that

water quality is suitable for reef growth. The FI values between 2 and 4 suggest that environmental conditions are marginal for reef growth and may be unsuitable for reef recovery following disturbances. An FI ≤ 2 characterizes environments where stress-tolerant taxa are common and conditions are generally unsuitable for reef growth (Hallock et al., 2003). For descriptive purposes, I averaged the FI over all samples from all sites within each gulf.

RESULTS

IN SITU TEMPERATURE MEASUREMENTS

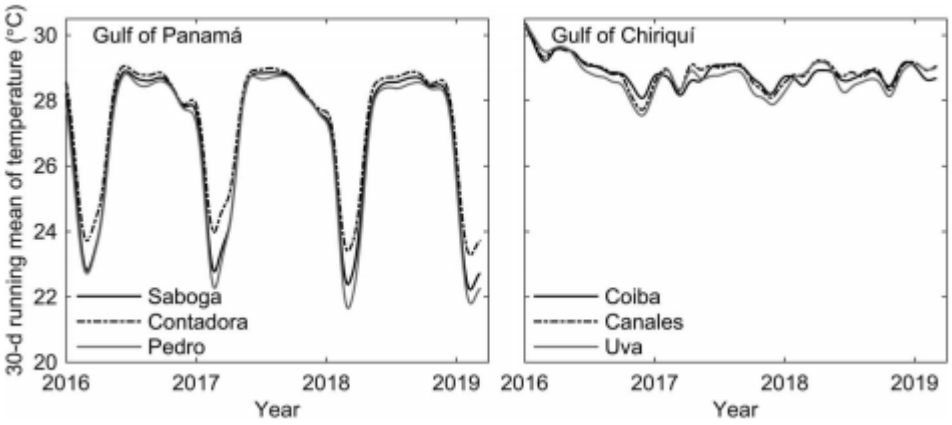

Figure 2.2 Plot showing 30-day running-means of temperatures, measured by in situ data loggers placed within the reef sites at 3 m depth 'Pedro' refers to Pedro González Island and 'Canales' refers to Canales de Tierra Island.

Averaged over sites within gulfs, the mean temperature calculated from the *in situ* data loggers during the period February 2016–March 2019 was 26.9 °C ± 0.38 SE in the Gulf of Panamá and 28.8 °C ± 0.08 SE in the Gulf of Chiriquí. Plots of the 30-day running means show greater temperature variability in the Gulf of Panamá than in the Gulf of Chiriquí due to seasonal upwelling (Fig. 2.2). The minimum mean temperature in the Gulf of Panamá was 21.6 °C ± 1.8 SE during the upwelling season, whereas the minimum mean temperature in the Gulf of Chiriquí was 27.5 °C ± 0.24 SE.

FORAMINIFERAL ASSEMBLAGES

Table 2.1 Taxonomy and functional groups of Foraminifera in samples from Pacific Panamá.

Order	*Family*	*Genus*	*Functional Group*
Buliminida	Bolivinidae	*Bolivina*	Tolerant
	Reussellidae	*Reussella*	Heterotrophic
Miliolida	Alveolinidae	*Borelis*	Symbiotic
	Hauerinidae	*Quinqueloculina*	Heterotrophic
		Triloculina	Heterotrophic
		Miliolinella	Heterotrophic
	Miliolidae	*Pseudohauerina*	Heterotrophic
	Peneroplidae	*Peneroplis*	Symbiotic
	Soritidae	*Sorites*	Symbiotic
	Spiroloculinidae	*Spiroloculina*	Heterotrophic
	Tubinellidae	*Articulina*	Heterotrophic
Rotaliida	Amphisteginidae	*Amphistegina*	Symbiotic
	Elphidiidae	*Elphidium*	Tolerant
	Nonionidae	*Haynesina*	Tolerant
		Nonionella	Heterotrophic

	Planorbulinidae	*Planorbulina*	Heterotrophic
		Cymbaloporetta	Heterotrophic
	Rosalinidae	*Rosalina*	Heterotrophic
		Neoconorbina	Heterotrophic
	Uvigerininae	*Uvigerina*	Heterotrophic
Textulariida	Textulariidae	*Textularia*	Heterotrophic

A total of 21 genera of Foraminifera were identified in the sediment samples from both gulfs (Table 2.1). A nested ANOVA, with sites nested within gulfs, showed that the mean density of foraminiferal tests per gram of sediment was not significantly different between gulfs ($F_{1, 4} = 16.94$, p=0.195); however, there were significant differences among sites ($F_{4, 26} = 2.41$, p=0.003; Fig. 2.3). An *a posteriori* Tukey honestly significant difference (HSD) test showed that the mean density at Contadora (Gulf of Panamá) was significantly lower than at Saboga (Gulf of Panamá; p=0.039), Uva (Gulf of Chiriquí; p=0.004), and Canales de Tierra (Gulf of Chiriquí; p=0.001). The other pairwise differences between sites were not significant.

Functional Groups

Symbiotic foraminifers were represented by four genera (Table 2.1), comprising 3.3% of the foraminiferal composition in the Gulf of Panamá and 17.6% in the Gulf of Chiriquí. Tolerant taxa were represented by three genera,

amounting to 8.1% and 7.2% of the foraminiferal composition in the Gulf of Panamá and the Gulf of Chiriquí, respectively.

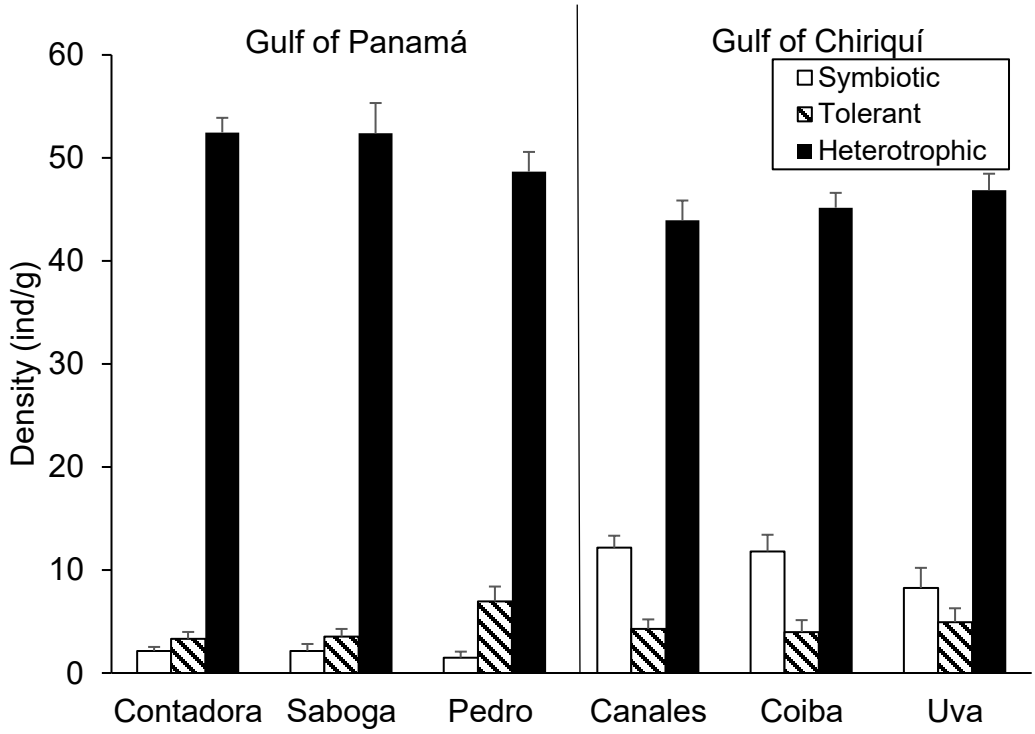

Figure 2.3 Mean densities of symbiotic, tolerant, and heterotrophic Foraminifera at each site. Error bars represent standard errors.

Thirteen genera comprised the dominant functional group, heterotrophs, accounting for 88.6% of the foraminiferal composition in the Gulf of Panamá and 75.2% in the Gulf of Chiriquí. The densities of these functional groups are shown for each gulf in Figure 2.3.

A nested ANOSIM on the densities of the functional groups showed a large degree of separation between gulfs, but this result was not significant (ANOSIM: R=0.85, p=0.1), likely due to low sample size. Nevertheless, a bivariate plot of symbiotic against heterotrophic taxa (the latter including tolerant genera) shows

that, although foraminiferal assemblages in both gulfs were dominated by heterotrophs, the sites in the Gulf of Chiriquí were characterized by relatively higher densities of symbionts (Fig. 2.4).

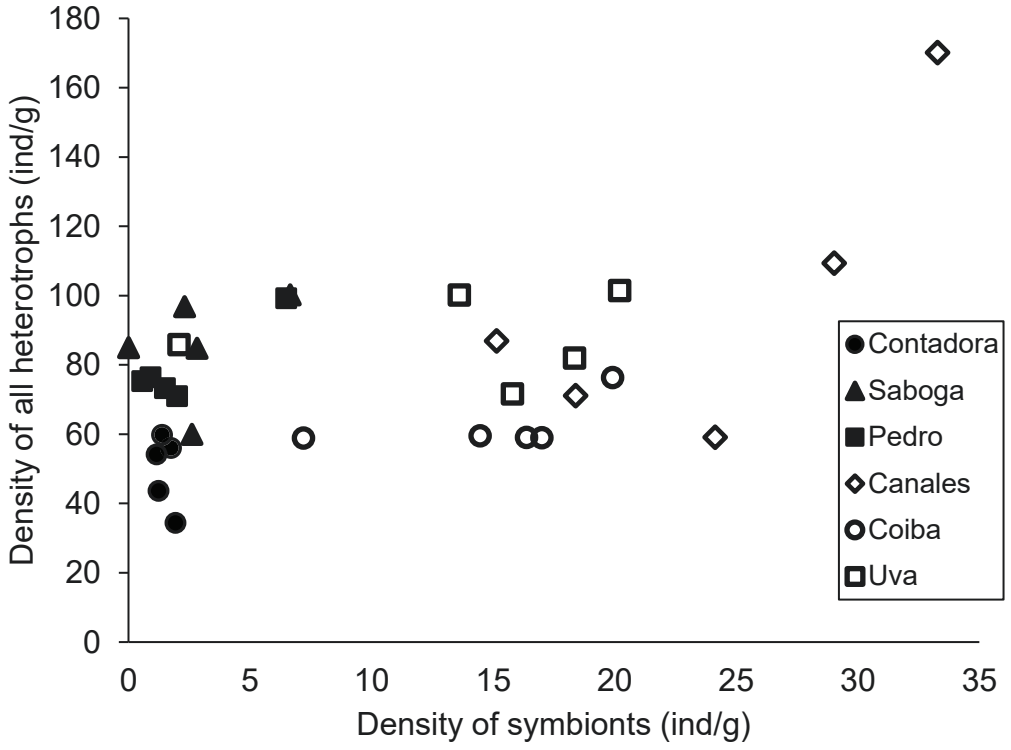

Figure 2.4 Bivariate plot of the densities of symbionts against the summed densities of heterotrophs and stress-tolerant heterotrophs. Solid shapes represent samples from the Gulf of Chiriquí, and open shapes represent samples from the Gulf of Panamá.

There was a significant difference in assemblages at the site-level ($p=0.001$), but the degree of separation was relatively low ($R=0.28$). The SIMPER analysis suggested that the gulfs were 19% dissimilar based on functional groups, with symbiont-bearing genera contributing most (10%) to the dissimilarity between the two gulfs.

Averaged across samples and sites, the mean FORAM Index for the Gulf of Panamá was 2.2 ± 0.05 SE (n=15) and the mean FORAM Index for the Gulf of Chiriquí was FORAM Index of 3.3 ± 0.12 SE (n=15). In both gulfs, therefore, the mean FORAM Index suggests that environmental conditions were marginal for reef growth, reflecting elevated nutrient levels compared with other tropical-reef environments such as those common in the Caribbean. The preponderance of heterotrophic taxa in both gulfs is consistent with some degree of upwelling in the Gulf of Chiriquí, as well as strong upwelling in the Gulf of Panamá.

Foraminiferal Taxa

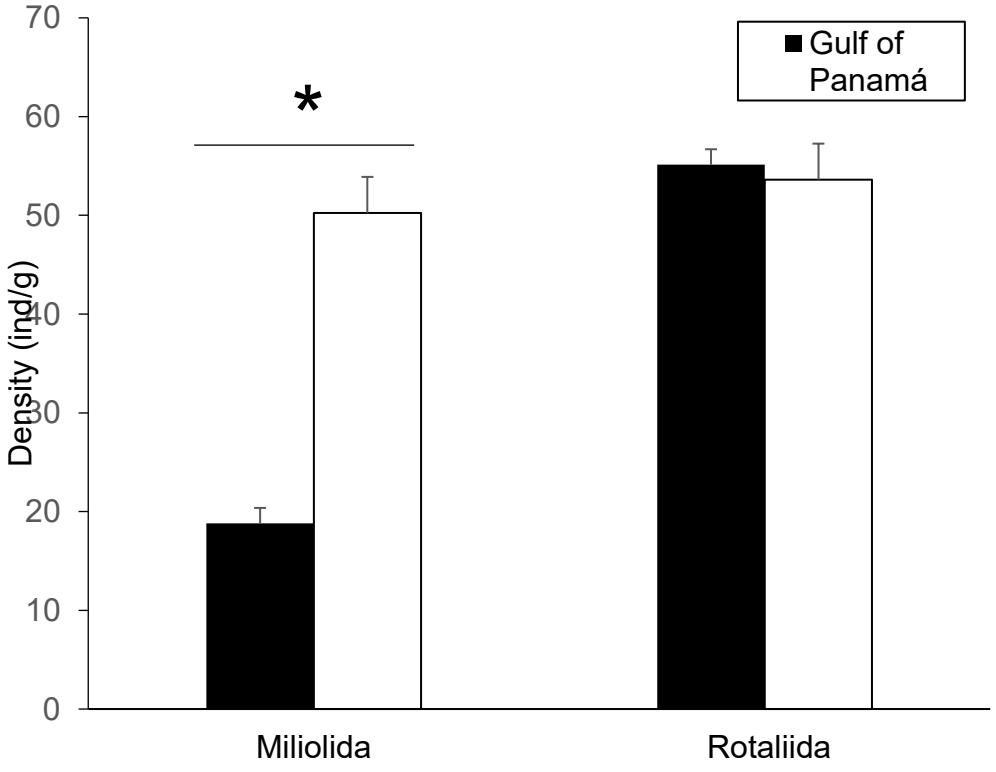

Figure 2.5 Mean densities of the two most abundant orders (Miliolida and Rotaliida) of Foraminifera in each gulf. Error bars represent standard errors. The asterisk indicates that the difference between gulfs is statistically significant for the Miliolida (p=0.007).

The Miliolida and Rotaliida were the two dominant orders represented in the samples, with the heterotrophs *Quinqueloculina* and *Rosalina* being the most abundant genera in the respective orders. These genera comprised >80% of the foraminiferal tests in the Gulf of Panamá and >60% of those in the Gulf of Chiriquí. Nested ANOVAs showed that the density of miliolids was significantly lower on average in the Gulf of Panamá than in the Gulf of Chiriquí ($F_{1, 4} = 69.6$, $p=0.007$; mean densities were 18.8 ind/g ± 1.6 SE and 50.3 ± 9.6 SE, respectively), but rotaliid densities were not significantly different between the two gulfs ($F_{1, 4} = 0.018$, $p=0.9$; densities were 55.1 ind/g ± 3.6 SE and 53.6 ± 13.5 SE; Fig. 2.5).

A nested ANOSIM did not show significant differences in generic composition between gulfs (ANOSIM: $R=0.85$, $p=0.1$) or sites (ANOSIM: $R=0.004$, $p=0.5$), likely because of the low sample size. The high R value when comparing gulfs suggests that there is a great degree of separation between the foraminiferal abundances in each gulf. The mean dissimilarity of foraminiferal assemblages between the two gulfs was 35% based on SIMPER analysis.

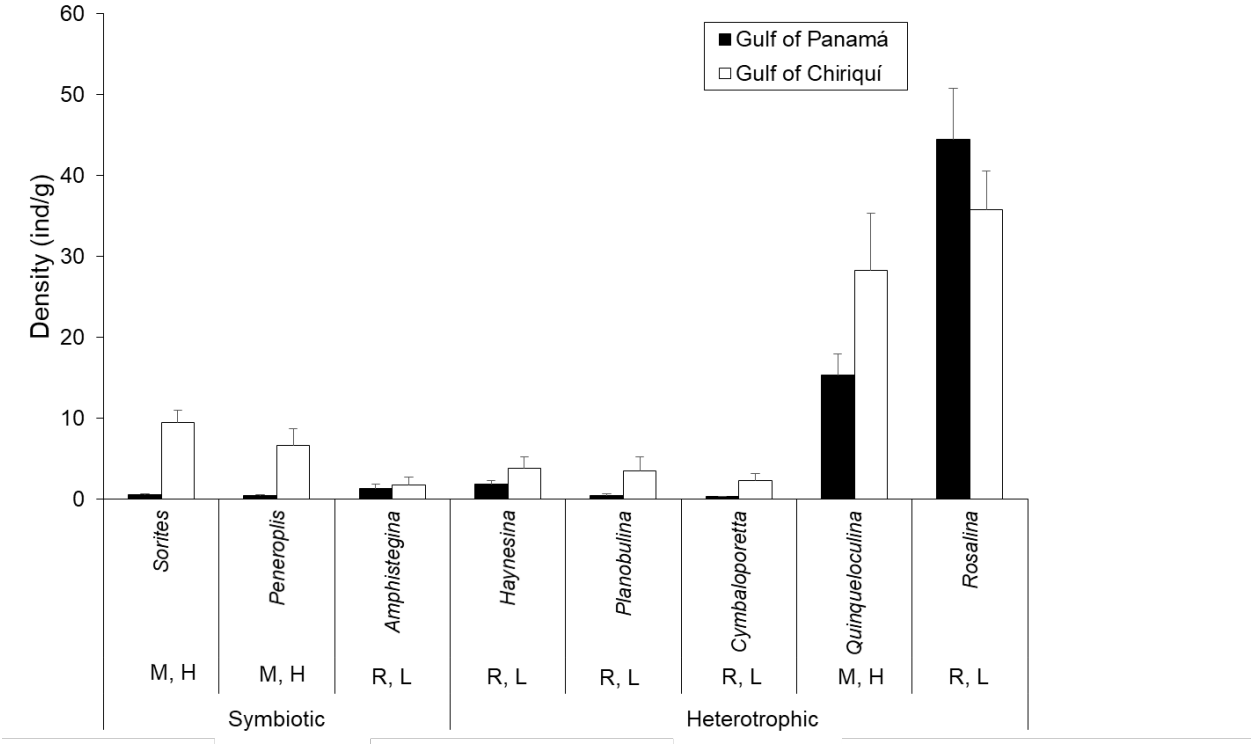

Figure 2.6 Mean foraminiferal densities of the eight genera that contributed ~70% of the dissimilarity between gulfs, based on SIMPER analysis. Error bars represent standard errors. Genera are coded by order (M, Miliolida; R, Rotaliida) and magnesium content of the shell (H, high-magnesium calcite; L, low-magnesium calcite).

Eight genera contributed ~70% to that difference (Fig. 2.6): *Sorites*, *Quinqueloculina*, *Peneroplis*, *Rosalina*, *Haynesina*, *Planorbulina*, *Cymbaloporetta*, and *Amphistegina* (listed in descending order of their contributions to mean dissimilarity). Of these, three were symbiont-bearing (*Sorites*, *Peneroplis*, and *Amphistegina*), and the rest were heterotrophic. *Sorites marginalis*, which was more abundant in the Gulf of Chiriquí, contributed 14% to the dissimilarity, the largest contribution of all the genera. The two most abundant genera, *Quinqueloculina* and *Rosalina*, contributed 8.1% and 7.3% to the dissimilarity,

respectively. *Quinqueloculina* was more abundant in the Gulf of Chiriquí (nested ANOVA, p=0.030), whereas there was no significant difference between gulfs in the density of *Rosalina* (p=0.353).

MAGNESIUM/CALCIUM ANALYSIS

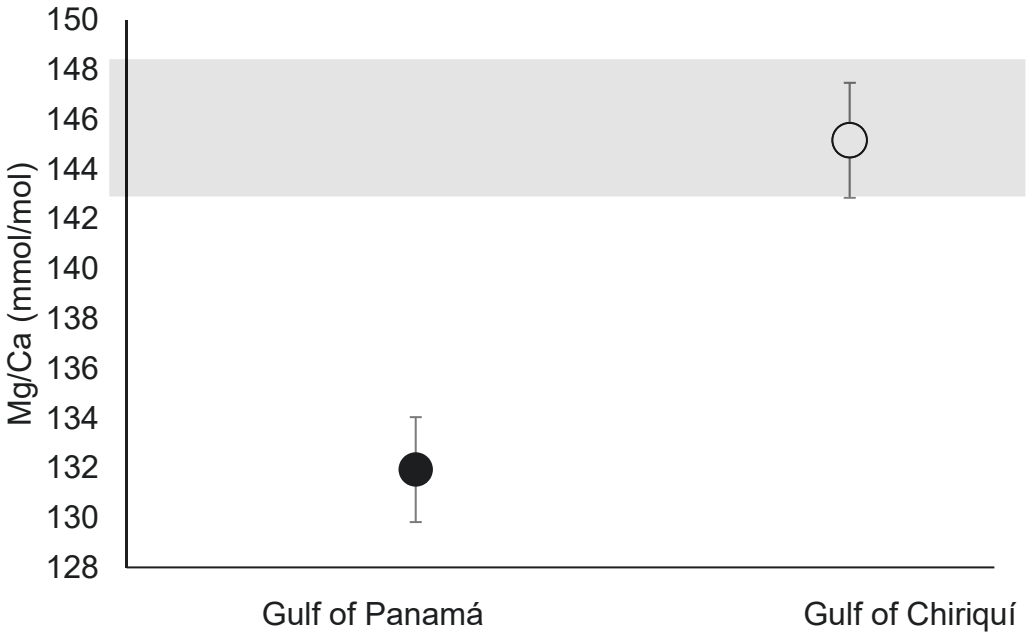

Figure 2.7 Plot showing mean Mg/Ca ratios of *Sorites marginalis* tests from each gulf. Error bars represent standard errors. Filled in circle represents Gulf of Panamá whereas open circle represents Gulf of Chiriquí. Shaded box represents the range of Mg/Ca measurements published for *S. marginalis* in culture, 143–148 mmol/mol at 25 ºC (van Dijk et al., 2017).

A nested ANOVA of the mean Mg/Ca ratios of *S. marginalis* tests from each site showed that Mg/Ca ratios were significantly lower in the Gulf of Panamá than in the Gulf of Chiriquí ($F_{1,4}$=27.07, p<0.001; Fig. 2.8), but there was no significant difference among sites ($F_{1,26}$=2.53, p=0.13). The mean Mg/Ca

concentration for *S. marginalis* in the Gulf of Panamá was 131.9 mmol/mol ± 2.10 SE versus 145.2 ± 2.30 SE in the Gulf of Chiriquí (Fig. 2.7).

DISCUSSION

The contemporary assemblages of benthic Foraminifera in both gulfs of Pacific Panamá were dominated by heterotrophic genera, but the Gulf of Chiriquí was characterized by higher densities of symbiotic genera. The Gulf of Panamá is seasonally cooler, more acidic, and more nutrient-rich than the Gulf of Chiriquí as a result of wind-driven upwelling during the dry season (D'Croz & O'Dea, 2007; Manzello et al., 2008; Randall et al., 2019). Although rates of carbonate production do not differ between the two gulfs, Reijmer et al. (2012) suggested that the taxa responsible for producing sediments reflect the difference in upwelling intensity. Seasonally nutrient-enriched conditions in the Gulf of Panamá result in heterotrophic sedimentary assemblages characterized by balanids, echinoderms, and mollusks, whereas the sediments in the Gulf of Chiriquí are characterized by phototrophic assemblages dominated by corals and rhodoliths. The depositional environments of both gulfs, however, suggested mesotrophic to eutrophic conditions rather than purely tropical or purely cool-water environments (Reijmer et al., 2012). The dominance of heterotrophic Foraminifera in this study reflects these mesotrophic conditions, yet symbiotic taxa were more characteristic of assemblages in the Gulf of Chiriquí (Figs. 2.3 and 2.4). Heterotrophic dominance

reflects the fact that both systems are nutrient-enriched compared with more typical, oligotrophic, coral-reef environments (Halfar and Ingle, 2003; Wang & Fiedler, 2006; Klicpera et al., 2015; Reymond et al., 2016). Heterotrophs respond positively to increased nutrient levels as long as there is sufficient oxygen available (Hallock et al., 2003).

Both miliolids and rotaliids are calcareous, but they differ in their calcification pathways. Miliolids precipitate calcite intracellularly, and their tests have high magnesium-to-calcium (Mg/Ca) ratios of 100–150 mmol/mol (Fig. 2.8; Bentov & Erez, 2006; van Dijk et al., 2017). The porcelaneous tests of miliolids are opaque with no perforations. In contrast, most rotaliids precipitate calcite extracellularly and have Mg/Ca ratios of only ~1–30 mmol/mol: they are composed of low-Mg calcite (Toyofuku et al., 2000; van Dijk et al., 2017). The hyaline tests of rotaliids are clear or translucent with small pores. Mesoscale differences in pH might explain the lower densities of miliolids in the Gulf of Panamá.

Strong upwelling in the Gulf of Panamá increases the concentration of CO_2 in shallow waters, lowering the pH (D'Croz & O'Dea, 2007, Manzello et al., 2008). A recent culturing experiment suggests that some miliolids, including *S. marginalis*, can continue to calcify under elevated pCO_2 levels as high as 1200 ppm (van Dijk et al., 2017); however, magnesium increases carbonate solubility (Knorr et al., 2015), and fewer (high-Mg-calcite) miliolids in the Gulf of Panamá could have resulted from an increased cost of calcification (Bentov & Erez, 2006). In fact, Manzello et al. (2008) reported lower cementation percentages and higher

bioerosion rates for reefs in the Gulf of Panamá compared with the Gulf of Chiriquí. Miliolids contributed ~26% of the mean foraminiferal density in the Gulf of Panamá, compared with 48% in the Gulf of Chiriquí, consistent with the idea of an environmental bias against Foraminifera with high-Mg-calcite tests.

The contribution of miliolids in the Gulf of Panamá was similar to that in the southern Galápagos, an upwelling zone also dominated by heterotrophic species, where the overall contribution of miliolids was on average 20% (Humphreys et al., 2019). Upwelling strength in the Gulf of Panamá has varied considerably in the past and appears to have affected reef growth (Toth et al., 2012, 2015b). I expect that miliolids would have been less abundant during times of strong upwelling. It should be noted, however, that the abundances of almost all genera recorded in this study were lower in the Gulf of Panamá compared with the Gulf of Chiriquí, including all but one genus—*Rosalina*—that secrete low-Mg-calcite tests. In fact, of the 8 genera that contributed most to the dissimilarity between the two gulfs none had a significantly higher density in the Gulf of Panamá (Fig. 2.6). Differences in pH between the gulfs may, therefore, not be the only reason for differences in the densities of particular taxa.

The geochemistry of the tests of benthic Foraminifera is known to track thermal variability (e.g., Lea et al., 2000; Billups and Schrag, 2002, 2003; Lear et al., 2003; Martin et al., 2002; Marchitto and deMenocal, 2003; Skinner et al., 2003). Although no studies have directly evaluated the Mg/Ca-temperature relationship in *S. marginalis*, the preliminary data suggest that this proxy has

promise in Pacific Panamá. During times of seasonal upwelling, mean temperatures in the Gulf of Panamá were lower than in the Gulf of Chiriquí during this study, and that difference was apparently reflected in the Mg/Ca ratios of the tests of *Sorites marginalis* (Figs. 2.2, 2.7). Lower Mg/Ca ratios in *S. marginalis* in the Gulf of Panamá were associated with cooler mean temperatures compared with the Gulf of Chiriquí.

Other species of shallow-benthic Foraminifera exhibit robust relationships between Mg/Ca and calcification temperature (Raitzsch et al. 2010; Toyofuku et al., 2010; Evans et al., 2015; de Nooijer et al., 2017). Evans et al. (2015) developed a linear calibration between Mg/Ca and temperature for the benthic foraminifer *Operculina ammonoides*. That study found a temperature sensitivity of 1.7 % $°C^{-1}$ and a linear relationship between Mg/Ca and temperature (T) as follows:

$$Mg/Ca = 2.55 (\pm 0.39) \times T + 81.7 (\pm 9.0) \quad (2)$$

Operculina ammonoides is a symbiotic, shallow-dwelling, large, benthic species like *S. marginalis*, but it is in the order Rotaliida rather than Miliolida. At a constant 25 °C, van Dijk et al. (2017) determined a mean Mg/Ca ratio of 144 mmol/mol for *S. marginalis*, which is within error of the mean Mg/Ca (145.2 ± 2.30) from the Gulf of Chiriquí (Fig. 2.8) and calibrates to their culture temperature of 25 °C using the equation published for *O. ammonoides* (Evans et al., 2015). This result provides first-order evidence that Equation 2 may also be applicable to *S. marginalis*. When applied to the mean Mg/Ca concentrations of *S. marginalis* tests in this study, the equation yields estimated mean temperatures of 19.7 °C in the

Gulf of Panamá and 25.2 °C in the Gulf of Chiriquí. These Mg/Ca-derived temperatures are lower than the mean annual *in situ* temperatures of 26.9 °C ± 0.38 SE and 28.8 °C ± 0.08 SE for the Gulf of Panamá and Gulf of Chiriquí, respectively, but are similar to the minimum mean temperatures of 21.6 ± 1.8 SE and 27.5 ± 0.24 SE, respectively recorded during the upwelling season. The 5.5 °C difference between the two gulfs estimated from Mg/Ca is also more similar to the 5.9 °C offset observed during the upwelling season than to the difference in mean annual temperatures of 1.9 °C measured *in situ*. Specimens of *S. marginalis* were not distinguished by living vs. non-living individuals, so these samples could be time-averaged across multiple years, which would make the magnitude of the between-gulf difference in Mg/Ca difficult to interpret. Although a culturing study would provide the best way to confirm the relationship between Mg/Ca and temperature for *S. marginalis*, the preliminary data suggest that the calibration of Evans et al. (2015) could be applied to down-core samples of *S. marginalis* to estimate temporal variability in the temperature offsets between the two gulfs.

Foraminiferal assemblages and geochemistry in the Gulfs of Panamá and Chiriquí thus reflect regional oceanography, and they likely respond strongly to climatic variability as well. Studies of reefs in Bahía, Brazil, showed that El Niño events caused dramatic declines in live foraminiferal densities in all shallow-reef environments (Kelmo & Hallock, 2013). The 1997–1998 El Niño resulted in declines of symbiont-bearing taxa, due to bleaching from elevated temperatures and reduced turbidity, while also diminishing heterotrophic taxa due to decreased food

sources. Kelmo & Hallock (2013) noted that the observed rapid recovery of heterotrophs resulted in a significant decline of FORAM Index from ~3.0 during 1995 to 2.5 in 2000. Likewise, densities of heterotrophic taxa in the Gulfs of Panamá and Chiriquí should rebound from El Niño events more quickly than symbiont-bearing taxa, because relatively high nutrient-levels promote blooms of phytoplankton and benthic algae, and the heterotrophs that feed upon them (cf. Hallock et al., 2003).

Dominance by heterotrophic taxa in both gulfs may be a result of not only higher nutrient levels in the ETP in general, but also the influence of La Niña. La Niña strengthens upwelling in the ETP, leading to an increase in nutrients and, in turn, increased densities of heterotrophic Foraminifera. For example, nutrient increases because of La Niña conditions led to the rapid rebound of heterotrophic taxa in live assemblages in Bahía, Brazil, following the strong La Niña from 1999–2000 (Kelmo & Hallock, 2013). Considering that both La Niña and El Niño events are expected to become stronger and more frequent as a result of climate change (Timmerman et al., 1999; Cai et al., 2018), the diversity of Foraminifera could decrease in the ETP due to increased heterotrophic dominance.

Although the FI is currently higher in the Gulf of Chiriquí than the Gulf of Panamá, Randall et al. (2019) suggested that upwelling in the Gulf of Panamá could moderate high temperatures and, hence, bleaching-related coral mortality as the ocean continues to warm, whereas mortality events could become more frequent in the Gulf of Chiriquí. Based upon Caribbean FI thresholds (Hallock et

al., 2003), the FI values for the Gulf of Chiriquí (3.3) suggest that reefs there may not be able to recover as mortality events become more prevalent. Looking retrospectively, the composition of foraminiferal assemblages in the Holocene record of reef frameworks along with temperature reconstructions from test geochemistry could be used in tandem with other proxies (e.g., Toth et al., 2015a, 2015b) to reconstruct past climatological and environmental conditions in the ETP.

As a final note, according to Crouch & Poag (1979), *Amphistegina* species have not been documented in Pacific Panamá in Pleistocene or Holocene sediments, though fossil reworked fossil specimens have been reported in previous studies cited therein. My identification of *Amphistegina* in the sediments I collected was confirmed by P. Hallock (personal communication, 2019), though she could not identify the species nor confirm that the specimens were not reworked fossil material. If the specimens are indeed modern, the occurrence of *Amphistegina* in my samples may represent a new record. As such, future confirmation of live *Amphistegina* may indicate recent expansion of this genus into the ETP.

Chapter 3: Shifts in the structure of foraminiferal assemblages during the hiatus in reef growth in Pacific Panamá

INTRODUCTION

It has been proposed that increasing variability of the El Niño–Southern Oscillation (ENSO) beginning around ~4000 ka led to a shutdown of coral-reef growth in Pacific Panamá that lasted for a period of ~2500 years (Toth, 2012; Toth et al., 2015a, 2015b). These climatic changes may also have led to shifts in the foraminiferal assemblage over the same period. As shown in Chapter 2, the composition of contemporary foraminiferal assemblages in Pacific Panamá responded to local oceanographic variations as well as climatic changes attributable to ENSO effects. Some reef areas in Pacific Panamá, did not show a complete hiatus in reef growth during the period of enhanced climatic variability. Reefs within Saboga Island showed brief resumptions of reef growth during the hiatus, though most of the corals sampled within the hiatus period were in poor taphonomic condition, suggesting that reef growth was stunted during that period.

Under El Niño conditions, sea temperatures in Pacific Panamá are elevated and precipitation is reduced. By contrast, La Niña is associated with cooler SSTs, enhanced precipitation, and intensified upwelling. Like corals, symbiont-bearing

foraminifers exhibit bleaching in response to increased temperatures, including from El Niño events in the eastern Pacific (Kelmo and Hallock, 2013; Prazeres, 2018). El Niño also leads to the decline of heterotrophic foraminifers as a result of decreasing nutrients and, therefore, declining sources of plankton and detritus (Kelmo and Hallock, 2013).

Recurring La Niña events in the eastern Pacific along with seasonal upwelling increase nutrients concentrations above background levels. Nutrient enrichment from seasonal upwelling underlies the heterotrophic dominance in both the Gulf of Chiriquí and the Gulf of Panamá. Furthermore, stronger upwelling induced by La Niña leads to lowered pH, which could also reduce densities of porcelaneous (high-magnesium-calcite) Foraminifera through dissolution. In Chapter 2, I determined that the Miliolida (porcelaneous) and Rotaliida (hyaline) were the two dominant orders in Pacific Panamá in modern sediments. Low pH affects miliolid taxa more negatively than rotaliid taxa due to the higher magnesium content of miliolid tests (Bentov & Erez, 2006).

Since upwelling strength in the Gulf of Panamá has varied considerably in the past and appears to have affected reef growth (Toth et al., 2012, 2015a), it would be expected that upwelling variability would similarly affect foraminiferal composition in this area. In fact, as described in Chapter 2, the density of miliolids is significantly greater in the Gulf of Chiriquí in modern sediments than within the Gulf of Panamá. Stronger upwelling in the Gulf of Panamá results in lower pH which could be the cause of the decreased miliolid density compared with the Gulf

of Chiriquí. By contrast, differences in pH would have had a lesser effect on calcification by the lower-magnesium rotaliids. Hypothesized strong La Niña events or La-Niña-like conditions in Pacific Panamá at the inception of reef shutdown, ~4200 cal BP (Toth et al., 2015a), would be consistent with increased densities of heterotrophs with hyaline tests within foraminiferal assemblages.

By sampling Foraminifera from the same cores used to reconstruct changes in reef accretion, I was able to determine if changes in local oceanographic conditions and the increased variability of El Niño and La Niña affected smaller, more sensitive carbonate producers compared with corals. This chapter will compare two sites within the Gulf of Panamá, where reefs developed in an environment with strong upwelling, with one site in the Gulf of Chiriquí with weak upwelling. By doing this, I will be able to determine whether the patterns in foraminiferal assemblages that were seen in Chapter 2 were persistent across millennial timescales. Studying changes in foraminiferal species composition will help infer oceanographic and climatic changes associated with the shutdown of reef development and/or the beginning of reef recovery. I address the following research questions and hypotheses:

1. Did foraminiferal composition change on reefs in Pacific Panamá during the Holocene when reefs ceased to grow? Can foraminiferal composition be used to infer the environmental conditions that led to reef collapse?

- H_1: The ratio of heterotrophic to symbiotic Foraminifera was greater leading up to and during the hiatus in reef development compared with periods before and after the hiatus, supporting the hypothesis of increased nutrients as a result of stronger La Niña events.
- H_2: Rotaliids were dominant during La Niña events/periods of low pH, whereas miliolids dominated during El Niño periods.

2. Do foraminiferal assemblages from reefs that did not have a defined hiatus differ through time from nearby reefs where the hiatus was continuous?
    - H_3: The ratio of heterotrophic to symbiotic Foraminifera will be more constant in reefs at Saboga Island, which did not experience a discrete hiatus in reef growth, than the reefs at Contadora Island and Canales de Tierra Island, which did experience a discrete hiatus in reef growth for ~2500 years.

METHODS

SAMPLING PROCEDURES

I analyzed Foraminifera within 5-cm sections of sediment from three reef cores previously collected from Saboga (8°37'35" N, 79°03'10" W) and Contadora

(8°37'54" N, 79°01'42" W) in the Gulf of Panamá, and Canales de Tierra in the Gulf of Chiriquí (7°44'60" N, 81°34'55" W). Each 5-cm section of sediment had been previously washed through a 63-µm sieve and frozen. I defrosted half the sediment from each sample and then dried it on filter paper at ~40 °C overnight. Subsamples of the dried sediment were weighed and then examined by stereomicroscopy. The identifiable foraminifers within the entirety of each subsample were identified to genus-level and tallied. This process was repeated until at least 250–300 individuals were tallied, or until the entirety of the last subsample was completed. The sum of the weights of each subsample analyzed was totaled and used to calculate foraminiferal densities. Foraminiferal genera were separated into functional groups and the total densities of heterotrophs and symbiont-bearing foraminifers were calculated. Since heterotrophs were found to be dominant in both gulfs, the ratio of the densities of heterotrophic to symbiotic Foraminifera was calculated to determine the variability in the proportion of symbiotic foraminifers. Genera were also classified by orders to determine if there were changes in dominance through time for the two most prevalent orders, Rotaliida and Miliolida.

Existing data on coral composition, coral mass, taphonomic condition of the corals, and radiocarbon ages from the same cores were used to compare changes in foraminiferal composition. Almost all the corals within the cores were fragments of *Pocillopora* spp. or *Psammocora stellata*. Taphonomic condition refers to the degree of encrustation, erosion, and boring of the coral fragments. The taphonomic

condition was defined as good, intermediate, or poor referring to fragments that had <20% alteration of the surface, 20–50% alteration of the surface, or >50% alteration of the surface, respectively. The ratios of the weights of *Pocillopora* specimens in good and intermediate taphonomic condition to poor taphonomic condition were calculated to compare the ratios of heterotrophic to symbiotic foraminifers. Using a ratio allowed for comparable analyses of foraminiferal densities and coral-fragment weights. I predicted that symbiotic foraminifera would be more abundant during periods of rapid reef accretion, characterized by dominance of *Pocillopora* in good and intermediate condition, leading to lower ratios of heterotrophic to symbiotic foraminifers.

DATING

Radiocarbon dating of Foraminifera was completed to establish if the timing of shifts in community assemblages aligned with previously established changes in reef growth, and the timing of the hiatus in reef growth. Foraminiferal samples were radiocarbon-dated using accelerator mass spectrometry (AMS). Approximately 10 individuals of *Sorites marginalis* that were in good taphonomic condition were picked from sediment samples corresponding to intervals from before, during, and after the hiatus in reef growth. The tests were sonicated in deionized water to remove any particulate matter and then dried. Samples were sent to the National Ocean Sciences Accelerator Mass Spectrometry (NOSAMS) facility in Woods Hole, MA. I calibrated the conventional radiocarbon ages using the

Marine20 calibration curve from CALIB 8.2 software (Stuvier and Reimer 1993; Stuiver, M., Reimer, P.J., and Reimer, R.W., 2021). Local reservoir corrections (ΔR) from Toth et al. (2012), updated for the Marine20 calibration curve, were applied to age-dated samples. Dates include the 2σ ranges, corresponding to the 95% confidence intervals, and are reported as calibrated calendar years before present (cal BP; 'present' refers to the year 1950 C.E.). The confidence intervals account for uncertainties within the calibration curve and intrinsic error associated with AMS radiocarbon dating.

STATISTICAL ANALYSES

Statistical analyses were completed on the densities of Foraminifera genera per gram of sediment. Bayesian change-point (BCP) analysis was used to estimate the number and timing of change-points associated with (i) ratio of heterotrophic to symbiotic Foraminifera, (ii) the ratio of *Pocillopora* specimens in good taphonomic condition to poor taphonomic condition, and (iii) the density of symbiotic Foraminifera through time. In addition, BCP analysis was used to determine if there were significant changes of the two most dominant orders, Miliolida and Rotaliida, through time. An assumption of BCP analysis is that an unknown partition of a data series exists within a certain number of blocks such that the mean is constant within each block. The posterior probability shows the location in the sequence versus the relative frequency of iterations that resulted in a change-point. The height of each peak is indicative of the probability that there is a change-point

that specific time. Tall, thin peaks represent relative certainty in the timing of a change-point, whereas shorter and wider peaks indicate a greater deal of temporal uncertainty. A posterior probability of 0.7 (70%) or greater was considered a significant change.

Logarithmic transformation was applied to all datasets to reduce the influence of abundant taxa in the sample faunas. Spearman correlations were used to determine if the functional groups of Foraminifera were associated with *Pocillopora* growth. Detrended Correspondence Analysis (DCA) and Permutational Analysis of Variance (PERMANOVA) were conducted to determine if foraminiferal community structure differed significantly as a function of location and/or before, during, and after the hiatus in reef growth. Similarity Percentage analysis (SIMPER) was used to determine the species that contributed the most to the differences in community composition among sites. Statistical analyses were completed using R v.4.1.2 using the "decorana" function in vegan. Age models were calculated using Bayesian statistics with the age-depth modelling function in the "rbacon" package.

RESULTS

AGE COMPARISONS

Dates of foraminiferal and coral samples completed for this study are shown along with those previously reported in Toth (2012) in Tables 3.1, 3.2, and 3.3.

Conventional ages and local reservoir corrections are presented in Appendix A. For foraminferal samples collected from Contadora Island, the 2σ age ranges generally correspond to those of corals from the same depth interval (Table 3.1). At depth interval 220–225 cm, however, the foraminiferal sample shows a date range of 1700–1400 cal BP. This date range conflicts with the date of the coral sample from the depth interval above it, as well as adjacent foraminiferal sample dates, and was therefore removed from the model. Based on the core I analyzed from Contadora (EP08-26), *Pocillopora* growth was halted for ~3000 years from 4384–3909 until 1205–827 cal BP. Symbiotic Foraminifera and *Psammocora* were still present during the hiatus within the 170–180 cm interval, with ages of 3067–2867 and 3165–2779, respectively. At 55–60 cm, the top of a massive *Porites* coral head was sampled and dated, showing a range of 673–376 cal BP. This interval falls between two modern dates, one from *Pocillopora* samples and the other from foraminiferal samples. The older age of the *Porites* sample could suggest that it began to grow first, and the *Pocillopora* and Foraminifera subsequently filled the reef around it.

Table 3.1**.** Calibrated radiocarbon dates from Contadora Island (core EP08-26). Radiocarbon dates that are highlighted in red samples that were rejected and excluded from further analysis. In addition, new/existing refers to dates that were analyzed from samples collected for this study versus dates that were previously completed and reported in Toth (2013) and recalibrated in this study.

Depth in core (cm)	Sample material	New/Existing	Median Age (cal BP)	2σ range
40–45	*Pocillopora*	New	Modern	Modern
55–60	*Porites*	Existing	534	673–376
60–65	Foraminifera	New	Modern	Modern
85–90	*Pocillopora*	Existing	919	1117–723
115-120	*Pocillopora*	New	834	968–684
150–155	*Pocillopora*	Existing	1016	1205–827

170–175	Foraminifera	New	2632	3067–2867
175–180	*Psammocora*	Existing	2974	3165–2779
180–185	*Pocillopora*	Existing	4142	4384–3909
220–225	Foraminifera	New	1569	1719–1399
260–265	Foraminifera	New	4420	4611–4227
260–265	*Pocillopora*	New	4794	4977–4589
305–310	*Pocillopora*	Existing	5244	5441–5035

The Bayesian age model for Contadora (Fig. 3.1) there may have been two distinct periods of interrupted reef growth during the hiatus between 150–170 cm and 170–180 cm. There is a difference of ~1600 cal BP between the median ages from 150–170 cm (2632–1016 cal BP), although it must be noted that samples from the intervals of 160–170 cm were not dated. The *Psammocora* and *Pocillopora* samples dated between 175–185 cm show a difference of ~1200 cal BP (4142–2974 cal BP). It could be argued that this hiatus is a result of sampling different carbonate material; however, the fact that the dates of foraminiferal samples align with coral samples in the interval 170–180 cm and overlap with coral samples within another interval (260–265 cm) suggest that the apparent hiatus is valid.

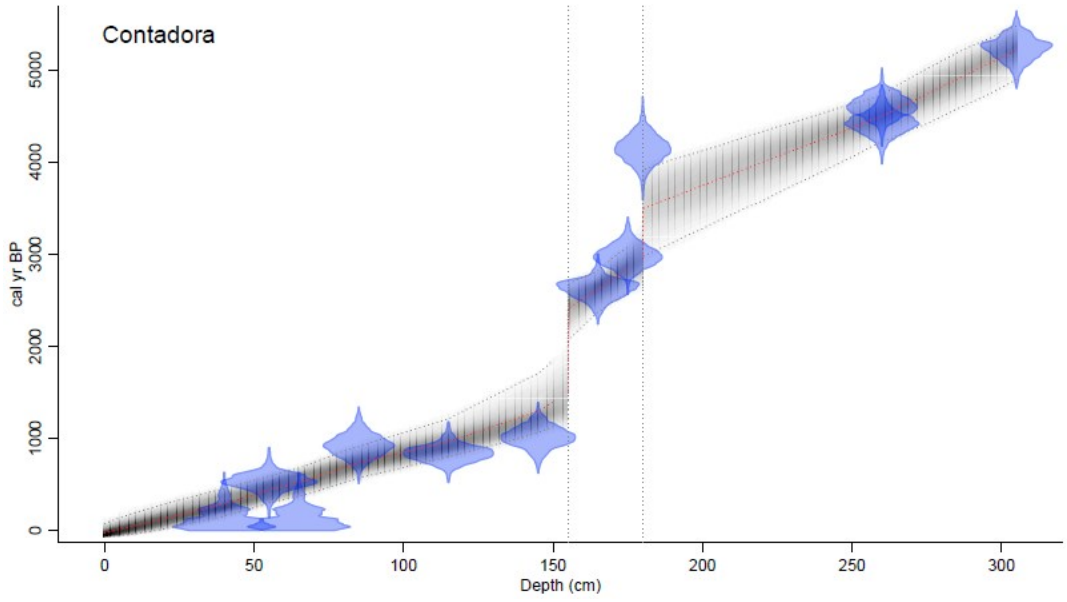

Figure 3.1. Bayesian age model for Contadora. Blue shaded shapes represent the probabilities of the ages and depth ranges based on the radiocarbon dates given to the model. Gray shading represents the 95% confidence interval.

At Saboga Island (Table 3.2), the initiation of the hiatus in reef growth occurred around 4368–3886 cal BP and reef growth was paused for ~2000 years. A few of the foraminiferal samples are younger than corals taken from the same intervals. For example, the median age of foraminiferal samples taken from the 80–85 cm interval is 807 cal BP. In contrast, the median age of the *Pocillopora* samples dated within the same interval is 2621 cal BP, about ~1800 years older. I removed the coral date from the data set because it conflicts with the coral date-range above it. An apparent age reversal seems to occur at the 190–195 cm interval when comparing the dates of the foraminiferal samples to adjacent *Pocillopora* samples. The age range of the foraminiferal samples is 3070–2740 cal BP which shows a ~1500-year difference between coral samples, both up-core and down-

core. In addition, these age data show that the ages of the foraminiferal samples taken from 190–195 cm are effectively the same age as those taken from 125–130 cm, even though those taken from 125–130 cm align with the *Psammocora* dates taken at the same interval as well as the hiatus in reef growth. The dates of samples from Foraminifera and *Pocillopora* taken from the bottom of the core align. Because of this conflict, the radiocarbon dates from the foraminiferal samples at 190–195 cm were removed from the model.

Table 3.2 Calibrated radiocarbon dates from Saboga Island (core EP09-33). Radiocarbon dates that are highlighted in red represent were rejected and excluded from further analysis. In addition, new/existing refers to dates that were analyzed from samples collected for this study versus dates that were previously completed and reported in Toth (2013) and recalibrated in this study.

Depth in core (cm)	Sample material	New/Existing	Median Age	2σ range
25–30	*Psammocora*	New	157	183–1
80–85	Foraminifera	New	807	1045–667
80–85	*Pocillopora*	New	2621	2289–2086
105–110	*Pocillopora*	Existing	2175	2351–1963
125-130	*Psammocora*	Existing	2149	2358–1899
125–130	Foraminifera	New	2934	3109–2764
160–165	*Pocillopora*	Existing	4122	4368–3886
190–195	Foraminifera	New	2897	3070–2740
200–205	*Pocillopora*	Existing	4531	4807–4265
210–215	*Pocillopora*	New	4424	4619–4225
220–225	Foraminifera	New	4596	4794–4414

The Bayesian age model for Saboga (Fig. 3.2) shows a similar pattern as that for Contadora, with two disruptions in reef growth between the intervals of 80–110 cm (~1300 cal BP difference in median ages) cm and 125–160 cm (~1200 cal

BP difference in median ages). These disruptions occur around 2600 and 4100 cal BP at Contadora and ~2100 and 4100 cal BP in Saboga.

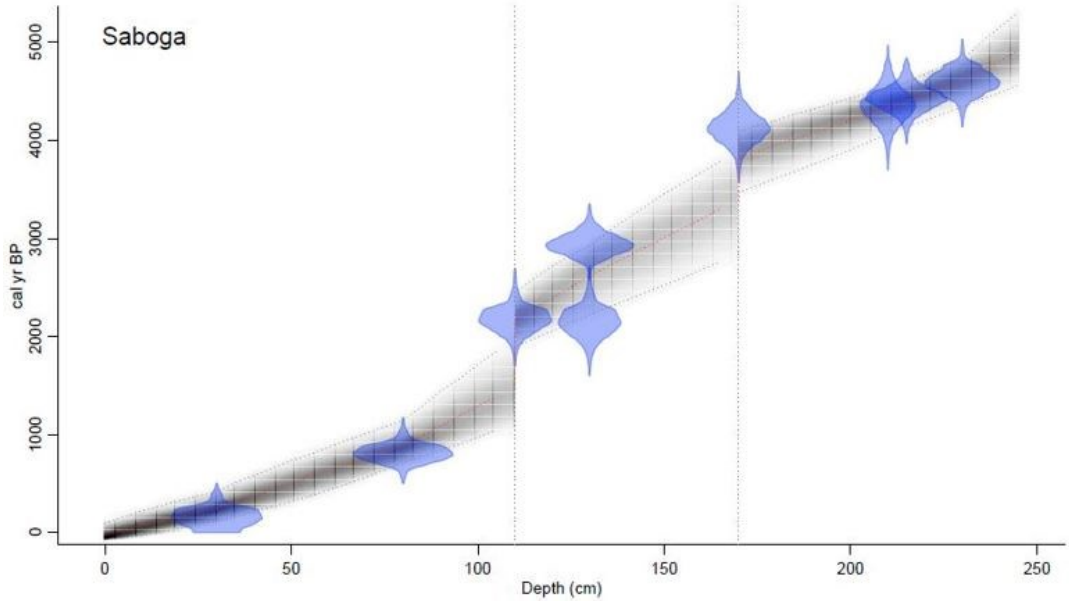

Figure 3.2. Baysian age model for Saboga. Blue shaded shapes represent the probabilities of the ages and depth ranges based on the radiocarbon dates given to the model. Gray shading represents the 95% confidence interval.

At Canales de Tierra Island (Table 3.3), there are two reversals when comparing the ages of foraminiferal samples to coral samples, namely between 120–145 cm and 260–270 cm. When comparing just the foraminiferal dates, however, they do not show any reversals. The initiation of the hiatus in reef growth occurred at 4392–4001 cal BP and lasted for ~2700 years until 1522–1374 cal BP. I expected the dates of the foraminiferal samples between 185–190 cm to fall within the range of the hiatus, yet the actual dates show that the samples are more closely aligned with coral samples taken at the termination of the hiatus. This result could

suggest that symbiotic Foraminifera were not growing during the hiatus in reef growth. Surprisingly, foraminiferal samples from the 265–270 cm interval show radiocarbon dates that fall within the hiatus in reef growth. The foraminiferal samples within the 140–145 cm interval also show a younger date range than the adjacent corals. The dates of the coral samples do not exhibit any significant age reversals, and adjacent dates align with each other. I chose not to remove any dates from the age model for Canales.

Table 3.3 Calibrated radiocarbon dates from Canales Island (core EP11-41). Radiocarbon dates that are highlighted in red represent were rejected and excluded from further analysis. In addition, the study period refers to dates that were analyzed from samples collected for this study versus dates previously completed and reported in Toth (2013) and re-calibrated in this study.

Depth in core (cm)	Sample material	New/Existing	Median Age	2σ range
40–45	*Pocillopora*	New	332	473–164
100–105	*Pocillopora*	Existing	376	516–236
115–120	*Pocillopora*	New	361	500–220
115–120	Foraminifera	Existing	547	661–430
120–125	*Pocillopora*	New	1363	1524–1226
140–145	Foraminifera	New	856	1002–705
165–170	*Pocillopora*	Existing	1506	1522–1374
185–190	Foraminifera	New	1450	1598–1303
225–230	*Pocillopora*	Existing	4198	4392–4001
260–265	*Pocillopora*	New	4316	4502–4163
265–270	Foraminifera	New	3250	3400–3071
290–295	*Pocillopora*	New	4341	4517–4152
365–370	*Pocillopora*	Existing	4930	5208–4706

The Bayesian age model for Canales de Tierra (Figure 3.3) shows a distinct hiatus between 185–230 cm, where the median calibrated dates run from ~4200 to ~1500 cal BP. The model was queried for the possibility of a second hiatus, yet there were not enough dates between 190 cm and 230 cm to determine if a second

hiatus is apparent. The modeled dates suggest continuous age intervals until 230 cm, where the modeled median age goes from 2342 cal BP at 225 cm to 3728 cal BP at 230 cm. This hiatus date is younger than the measured radiocarbon median age (4198 cal BP), most likely because the foraminiferal sample between 265–270 cm is younger than the adjacent coral samples.

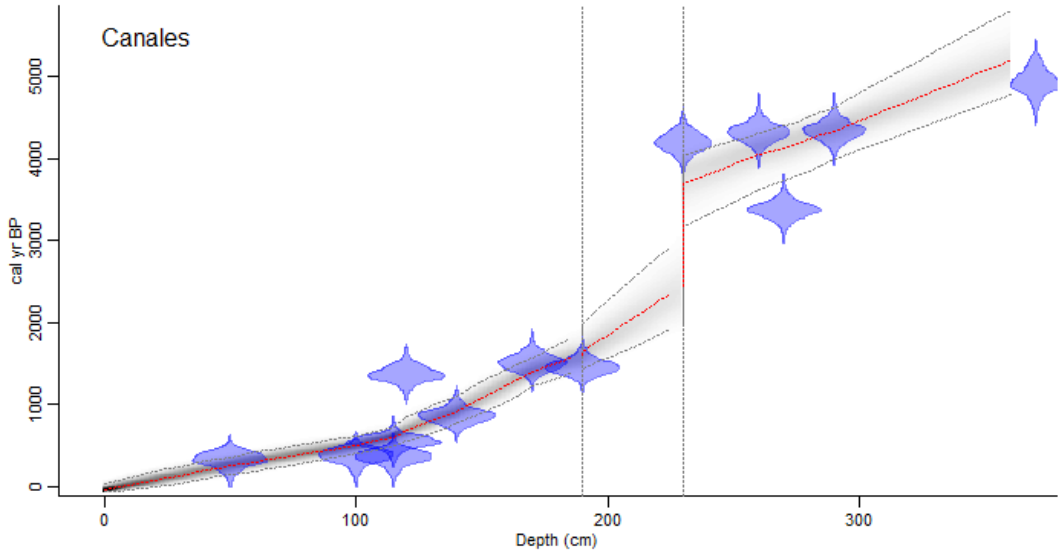

Figure 3.3. Bayesian age model for Canales de Tierra. Blue shaded shapes represent the probabilities of the ages and depth ranges based on the radiocarbon dates given to the model. Gray shading represents the 95% confidence interval.

All three cores show a distinct hiatus in *Pocillopora* growth starting ~4100 cal BP. Paired models of all three cores using the dates before the hiatus show a start-date between 4000–4250 cal BP with a median date of 4130 cal BP. In contrast, the termination of the hiatus in *Pocillopora* growth was different for each site: 1205–827 cal BP at Contadora, 2351–1963 cal BP at Saboga, and 1522–1374 cal BP at Canales de Tierra.

FORAMINIFERAL ASSEMBLAGES AND REEF ACCRETION

Functional Groups

Similar to the modern assemblages, heterotrophic Foraminifera dominated in each of the three sites during the Holocene, with heterotrophs accounting for 72–100% of total foraminiferal densities in Contadora, 81–99% in Saboga, and 72–99% in Canales de Tierra. The core diagrams and calculated masses of *Pocillopora* (Figs. 3.4, 3.8, and 3.12) and the dates corresponding to the core logs previously developed by Toth (2013) are used here to examine foraminiferal assemblage composition through time. At each site, the density of symbiotic foraminifers tracks the ratio of *Pocillopora* in good taphonomic condition to poor taphonomic condition, suggesting that during periods of reef growth, symbionts proliferate. In addition, the ratio of heterotrophic Foraminifera to symbiotic Foraminifera peaks during periods when reefs were not present.

At Contadora (Fig. 3.1), the density of symbiotic Foraminifera peaked at 26 individuals/gram around 4000–4400 cal BP increasing from 1.5 individuals/gram leading up to the hiatus in reef growth. After reef growth resumed, the density of symbiotic Foraminifera increased to 12.9 ind/g, corresponding to a peak of 60.58 g for *Pocillopora* in good and intermediate taphonomic condition within the 125–130 cm interval deposited around 968–648 cal BP. The density of symbiotic Foraminifera and the mass of *Pocillopora* in good and intermediate taphonomic

condition subsequently declined to zero between the 65–75 cm interval before rebounding in the top intervals of the core.

Although heterotrophic Foraminifera at Contadora dominated at all times, the ratio of heterotrophic to symbiotic Foraminifera remained between 5 and 20 before increasing greatly at the initiation of the hiatus in reef growth and peaking at 173.5:1 within the 155–160 cm interval corresponding to 3067–2867 cal BP. The ratio of heterotrophic to symbiotic Foraminifera declined as *Pocillopora* and symbiotic Foraminifera increased within the 125–130 cm interval. The ratio then peaks at 255:1, coupled with a decline in *Pocillopora* and symbiotic Foraminifera at 65–75 cm.

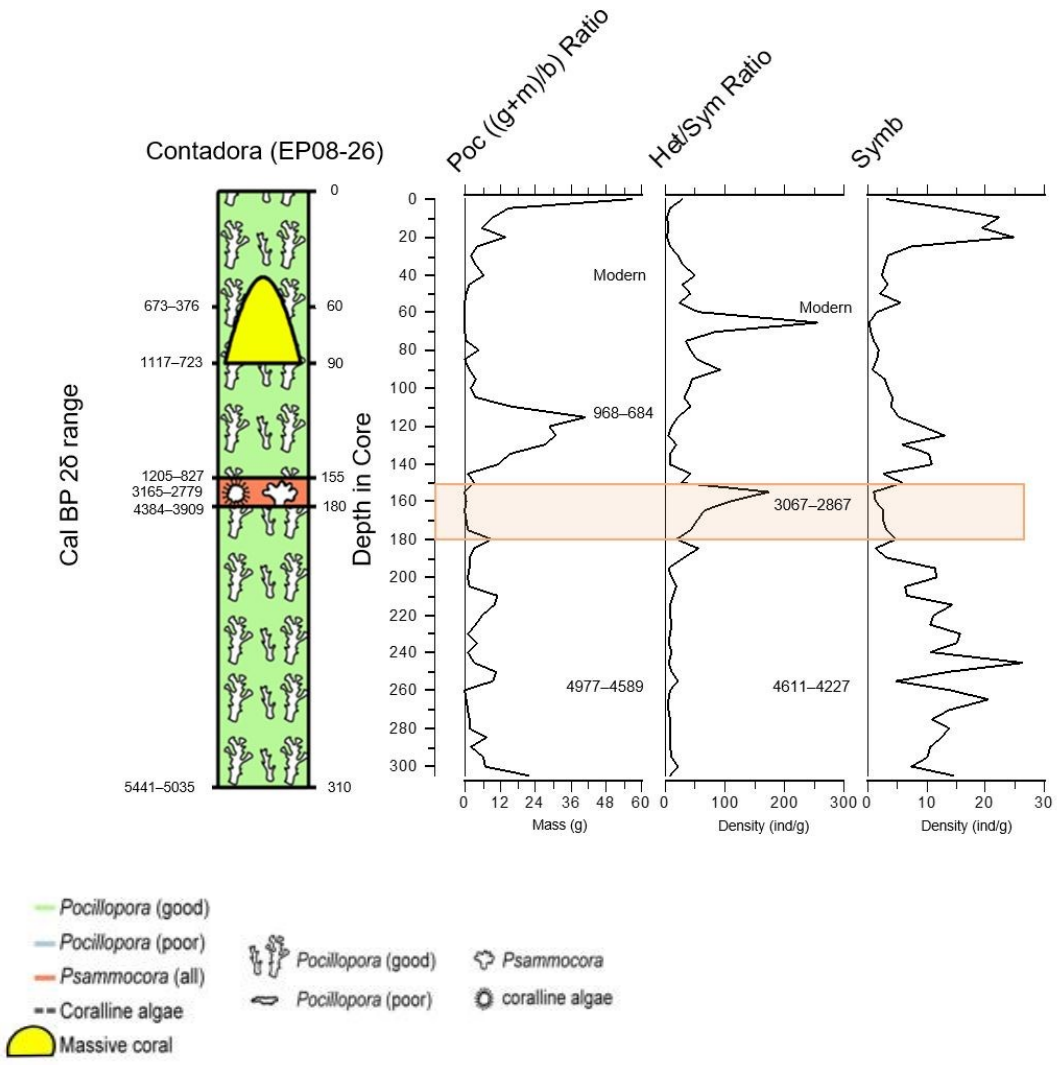

Figure 3.4 Core log for Contadora Island (core 08-26). The legend refers to the core diagram showing coral genera and taphonomic condition. Ages within the *Pocillopora* ratio graph refer to corals dated for this study. Ages within the heterotroph to symbiont ratio graph refer to foraminifers dated for this study.

The Bayesian change-point (BCP) algorithm was used to calculate the locations where there is a shift in coral growth and foraminiferal densities within each core (Fig. 3.5). The tallest peaks in the change-point analysis for the *Pocillopora* ratio compared with the foraminiferal ratio are out of phase (Fig. 3.4, Fig. 3.5). Using the 70% significance threshold, there are two significant change

points according to BCP analysis on the *Pocillopora* ratio: immediately following the hiatus and at the top of the core, where there were only corals in good and intermediate condition present and none in poor condition. After the hiatus in reef growth, the ratio of *Pocillopora* in good and intermediate taphonomic condition to poor condition begins to increase ~1200–800 cal BP to its peak at 43:1 and then subsequently declines to 3.6:1 ~1000–700 cal BP.

There are three significant change points in the ratio of heterotrophs to symbionts within the core. The first significant peak occurs around 160 cm, representing the increase in the heterotrophs compared to symbionts during the hiatus in reef growth ~3000–2800 cal BP. The next change-point occurs due to the subsequent decline in the ratio of heterotrophs to symbionts from its peak at 103:1 to 7.5:1 toward the termination of the hiatus in reef growth, ~1000–800 cal BP. Finally, there is a drastic increase in the ratio of heterotrophs to symbionts at 60–65 cm. There are no significant change-points associated with the density of symbionts in the core, yet at 20–25 cm, there is an increase in symbiont density with a posterior probability of 89%.

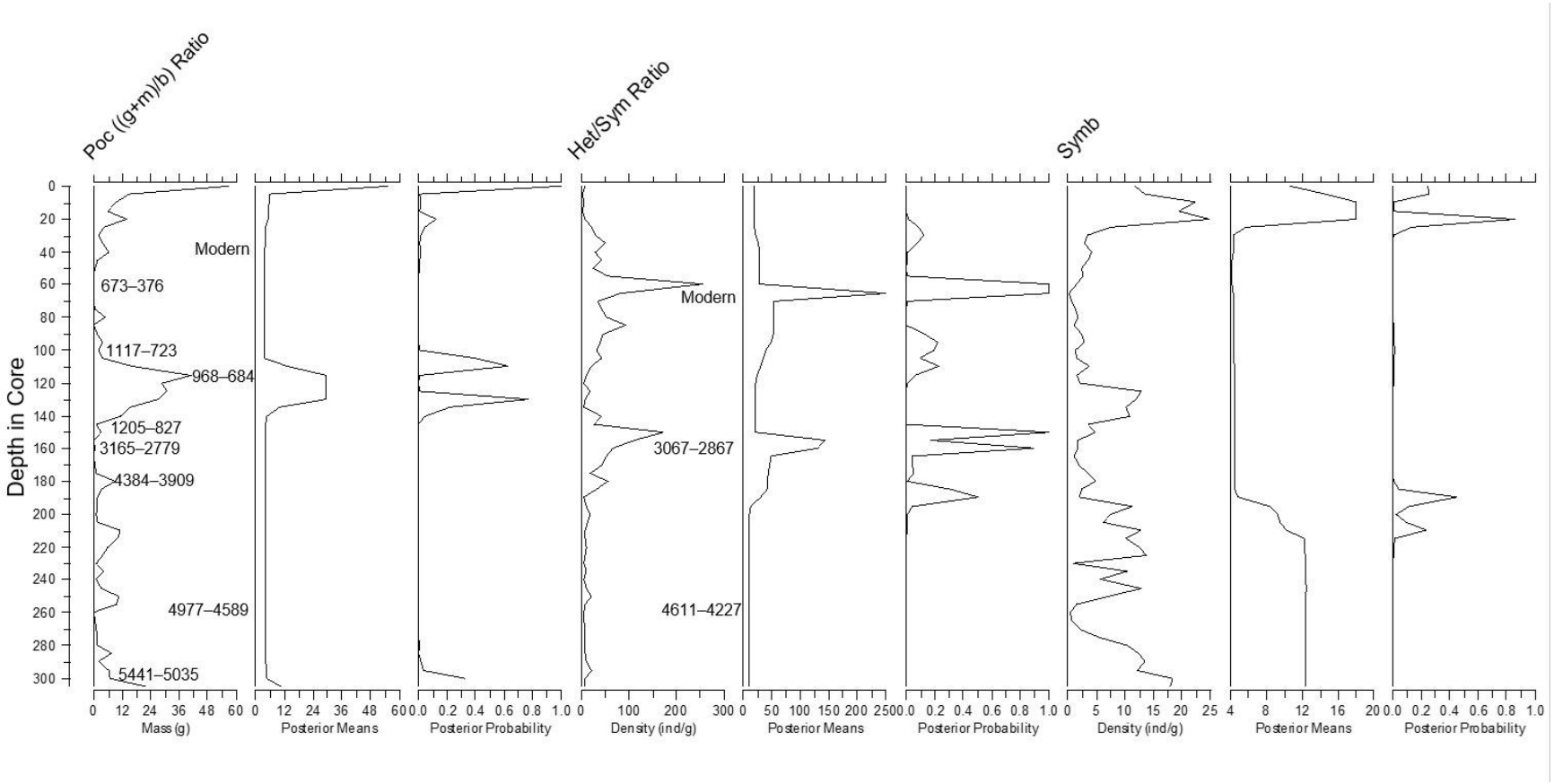

Figure 3.5 Contadora core log plotted with the Bayesian change-point algorithms for the ratio of *Pocillopora* in good and intermediate condition to poor condition, the ratio of heterotrophic to symbiotic Foraminifera, and the density of symbionts. Ages posted on the right side of the columns reflect radiocarbon dates analyzed for this study. Ages that are skewed to the left side of the *Pocillopora* ratio column represent previous Ages reported in Toth (2013).

Since the peaks in *Pocillopora* growth seem to be correlated with symbiotic foraminiferal density, I completed a Spearman correlation to test the relationship between the two.

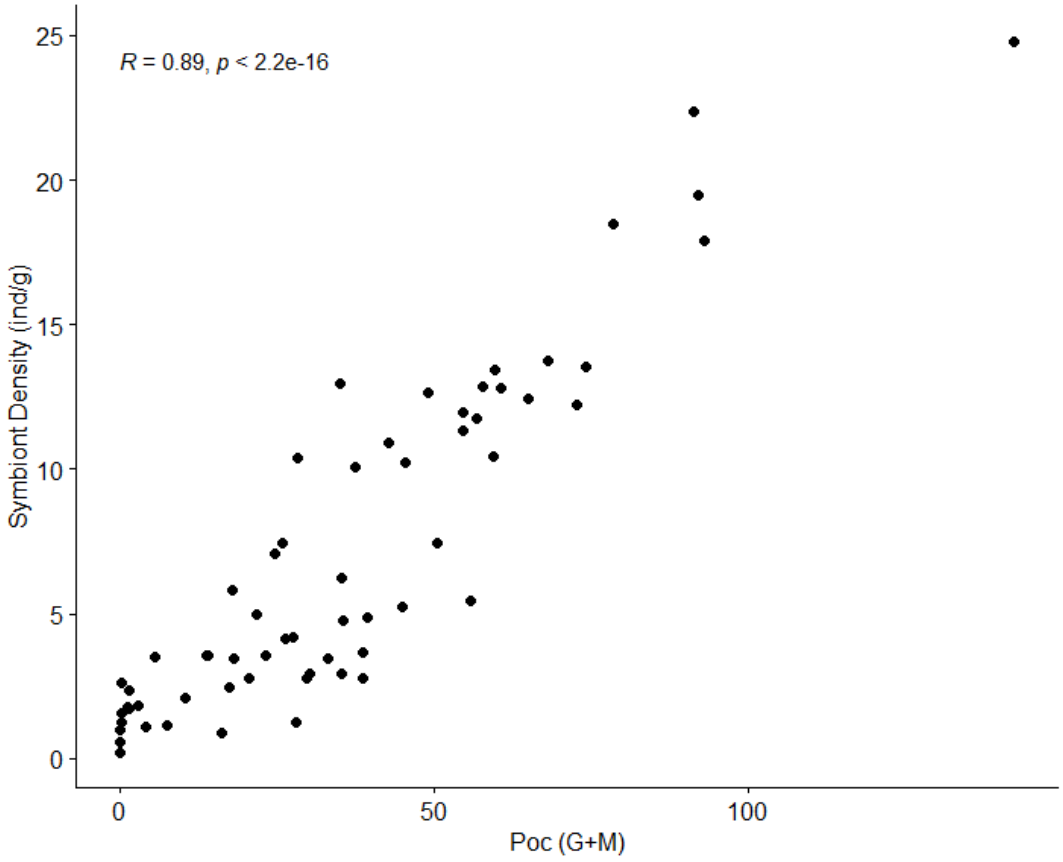

Figure 3.6 Spearman correlation between the mass of *Pocillopora* in good (G) and intermediate (M) taphonomic condition and symbiotic foraminiferal density at Contadora.

The core logs suggest a strong positive correlation between *Pocillopora* in good and intermediate taphonomic condition and symbiotic foraminiferal density (r = 0.89, $p < 0.001$; Fig. 3.6). The relationship between the ratio of *Pocillopora* and

symbiotic foraminiferal density is also significant ($p = 6.2x10^{-8}$; Fig. 3.6). Still, the relationship is not as strong as the one above, with an *r*-value of 0.62 compared with 0.89.

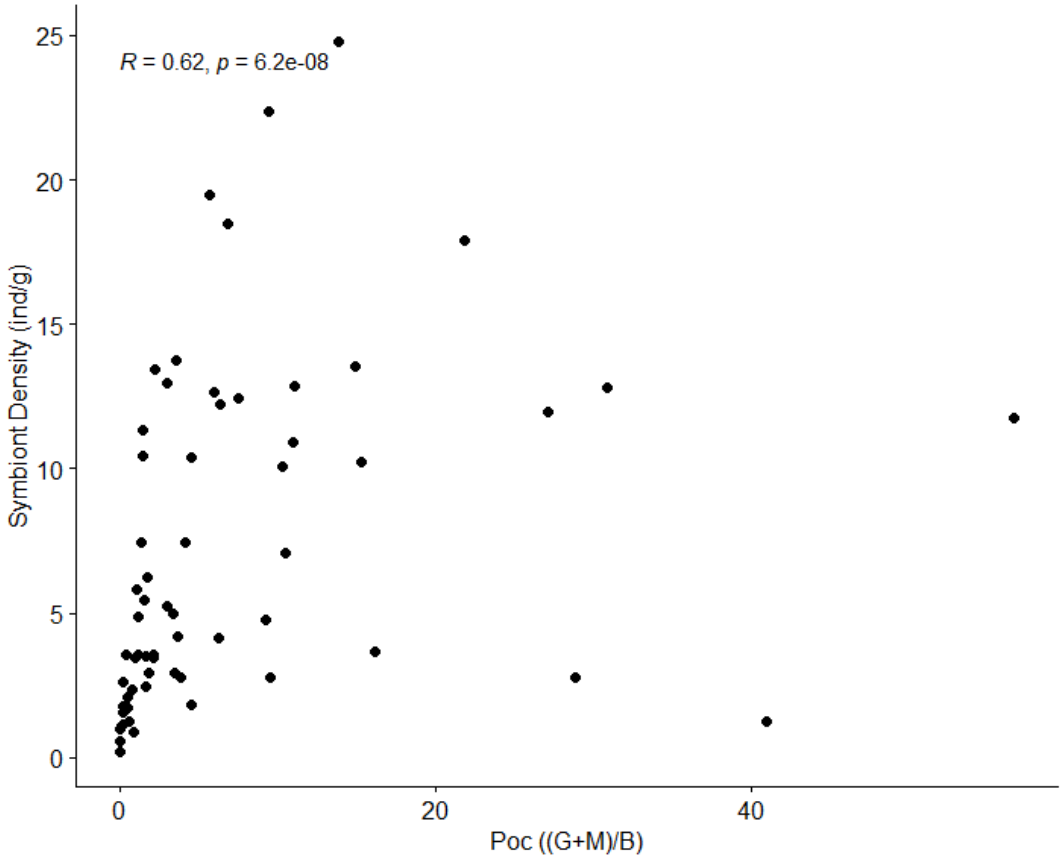

Figure 3.7 Spearman correlation between the ratio of *Pocillopora* in good (G) and intermediate (M) taphonomic condition to *Pocillopora* in poor (B) taphonomic condition and symbiotic foraminiferal density at Contadora.

Neither the relationship between heterotrophic foraminiferal density and *Pocillopora* in good and intermediate condition nor the ratio of *Pocillopora* were significant ($r = -0.2$, $p = 0.11$ and $r = -0.084$, $p = 0.52$, respectively, Fig. 3.7). In

addition, there was not a significant linear association between heterotrophic and symbiotic foraminiferal density (r = -0.045, p = 0.68).

Samples from Saboga Island (Fig. 3.8) show similar patterns to those from Contadora Island, with an inverse correlation between the foraminiferal and coral ratios. The ratio of heterotrophic to symbiotic Foraminifera declined from 64.7:1 to 5.8:1 between the intervals 240–210 cm (~4800–4200 cal BP), most likely caused by a peak in symbiotic Foraminifera from ~2 ind/g up to 15.7 ind/g at 195 cm (~4100 cal BP; Fig. 3.8). Around this same time, the ratio of *Pocillopora* in good and intermediate taphonomic condition to bad taphonomic condition showed a slight increase from 0.3:1 to 16.5:1 at the 200–205 cm interval (~4200 cal BP). During the hiatus in reef growth, the ratio of Foraminifera increased to a peak of 119.6:1 at the 125–130 cm interval, dated to 3109–2764 cal BP. Concurrently, the density of symbiotic Foraminifera dropped from 12.5 ind/g to 0.89 ind/g. There was a rebound of symbiotic Foraminifera and *Pocillopora* in good and intermediate taphonomic condition within the 80–85 cm interval (~1000–700 cal BP), where the density of symbionts increases to 18.9 ind/g and the ratio of *Pocillopora* peaks at 114.2:1. After a decline in the *Pocillopora* ratio at 60 cm, there is a peak in both the *Pocillopora* ratio and symbiotic foraminiferal density in "modern" times at 20–25 cm from 0.5:1 to 51:1 and 3:1 to 25:1, respectively.

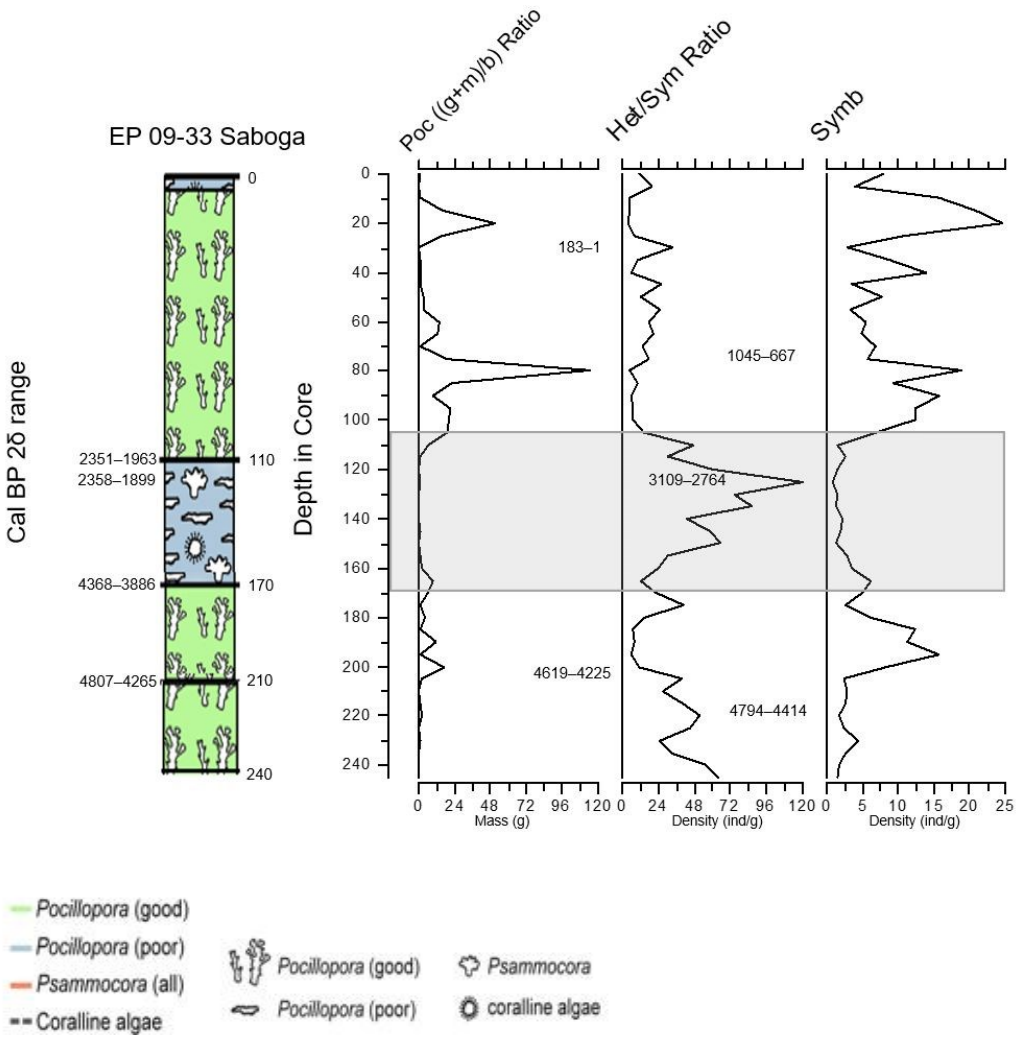

Figure 3.8 Core log for Saboga Island (Core 09-33). The legend refers to the core diagram showing coral genera and taphonomic condition. Ages within the *Pocillopora* ratio graph refer to corals dated for this study. Ages within the heterotroph to symbiont Ratio graph refer to foraminifers dated for this study.

Figure 3.9 depicts the BCP analysis for the Saboga core log. Using the same threshold of significance as for the Contadora core (70% probability), the two significant increases in *Pocillopora* growth occur after the hiatus in reef growth at the 80–85 cm interval and the 20–25 cm interval. The change-points for the heterotroph/symbiont ratio are not significant at the 70% probability threshold. Still, there is a trend of increased heterotrophic Foraminifera beginning at the

inception of the hiatus in reef growth ~4300–3800 cal BP. There are no significant changes in symbiotic foraminiferal density, most likely because their densities are inherently low.

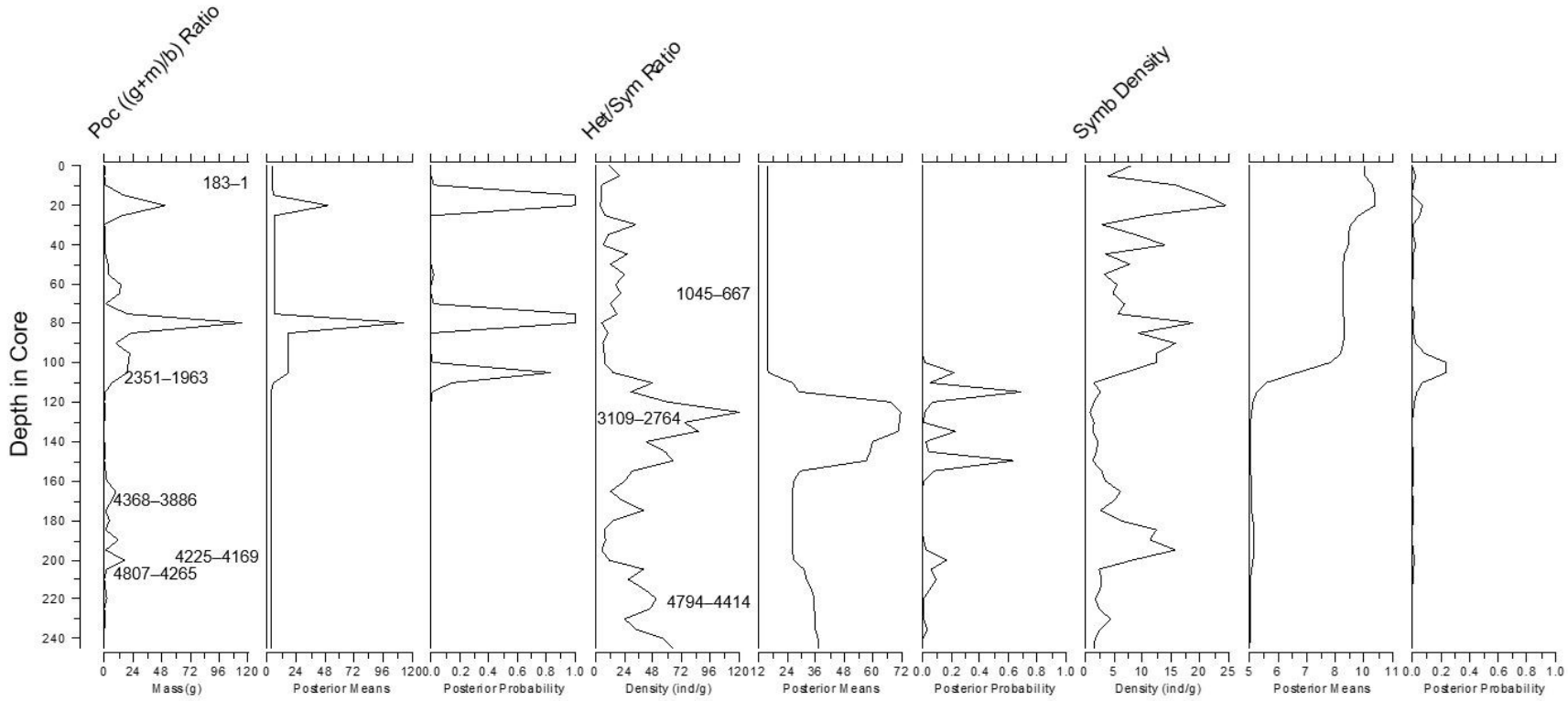

Figure 3.9 Saboga core log plotted with the Bayesian change-point algorithms for the ratio of *Pocillopora* in good and intermediate condition to poor condition, the ratio of heterotrophic to symbiotic Foraminifera, and the density of symbionts. Ages posted on the right side of the columns reflect radiocarbon dates analyzed for this study. Ages that are skewed to the left side of the *Pocillopora* ratio column represent previous ages reported in Toth (2013).

As was the case with Contadora, symbiotic foraminiferal density positively correlated with the mass of good and intermediate *Pocillopora*, (r = 0.86, p = $7.4x10^{-16}$; Fig. 3.10) as well as the *Pocillopora* ratio (r = 0.7, p = $1.4x10^{-8}$; Fig. 3.11).

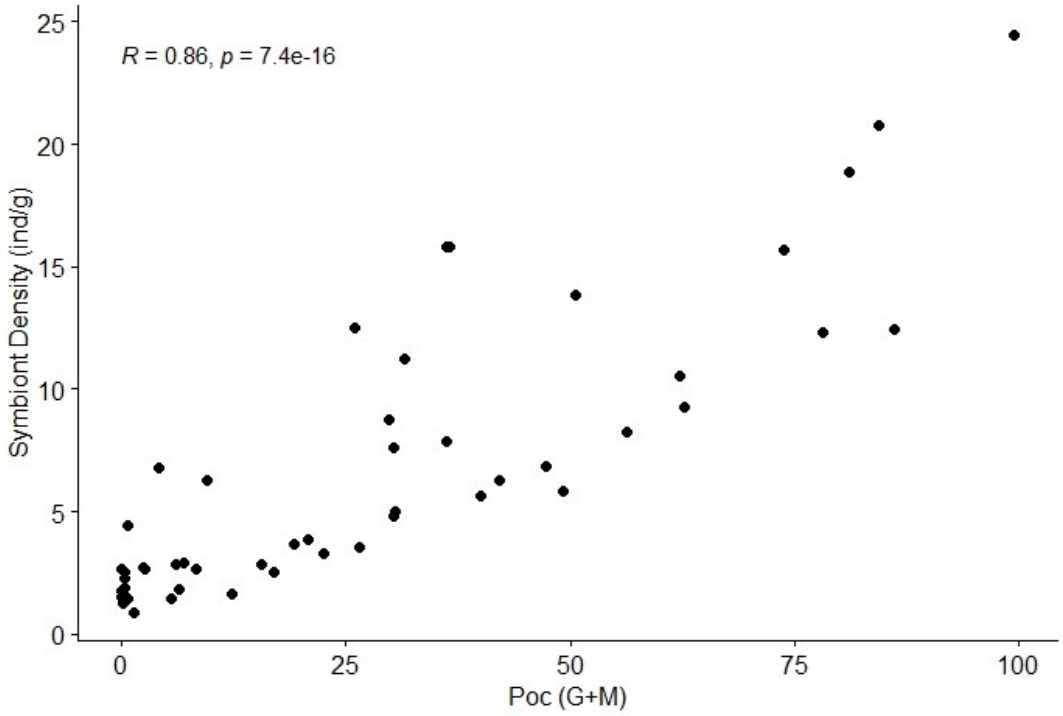

Figure 3.10 Spearman correlation between the mass of *Pocillopora* in good (G) and intermediate (M) taphonomic condition and symbiotic foraminiferal density at Saboga.

There was not a significant association between heterotroph density and symbiotic foraminiferal density (r = -0.12, p = 0.39). Similarly, neither the association between the ratio of heterotrophs to symbiotic forams and *Pocillopora* in good and intermediate condition (r = -0.13, p = 0.38), nor the *Pocillopora* ratio were significant (r = -0.0087, p = 0.95).

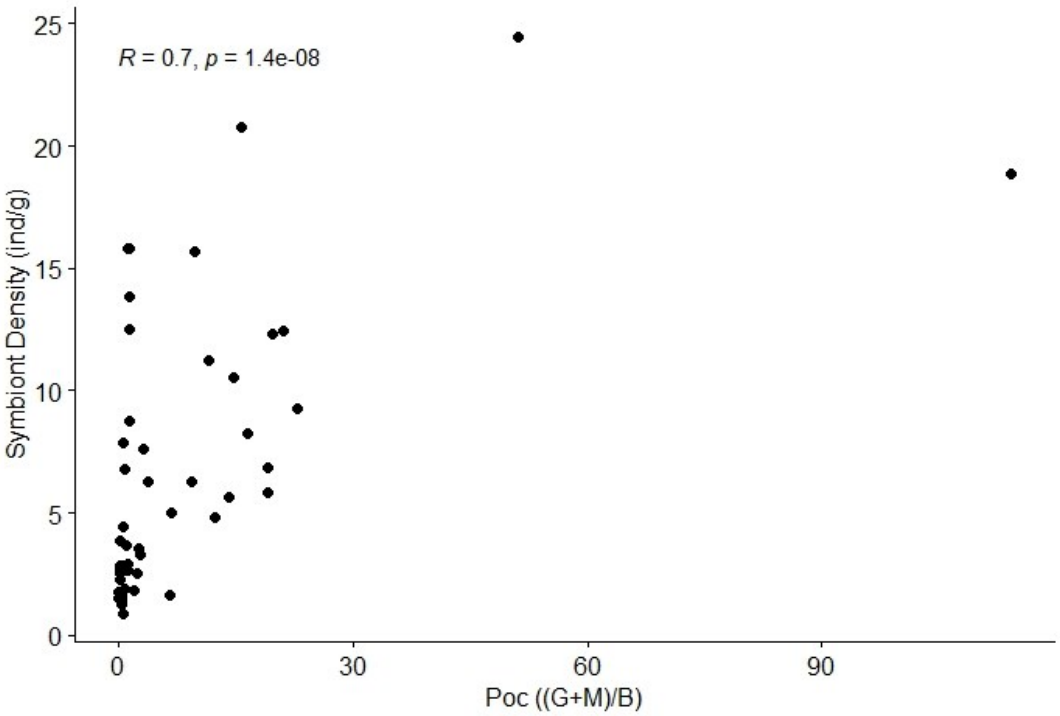

Figure 3.11 Spearman correlation between the ratio of *Pocillopora* in good (G) and intermediate (M) taphonomic condition to *Pocillopora* in bad (B) taphonomic condition and symbiotic foraminiferal density at Saboga.

The core logs for Canales de Tierra are depicted in Figure 3.12. Peaks in the ratio of heterotrophic to symbiotic Foraminifera are out of phase with peaks of the *Pocillopora* ratio down-core. Although the density of symbiotic Foraminifera tends to follow the overall pattern of *Pocillopora* growth (the abundance of *Pocillopora* in good and intermediate taphonomic condition), surprisingly, the density of

symbiotic Foraminifera stays relatively high through time.

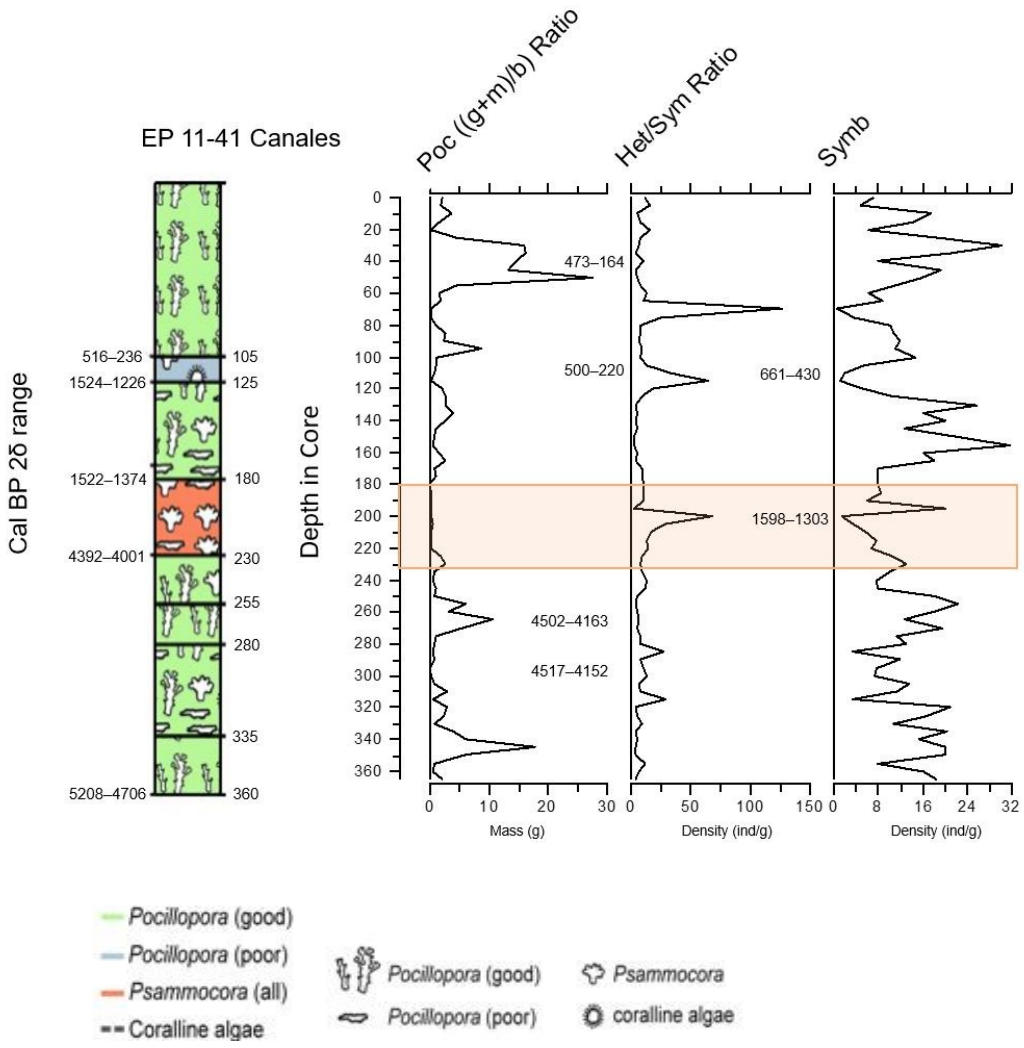

Figure 3.12 Core log for Saboga Island (Core 09-33). The legend refers to the core diagram showing coral genera and taphonomic condition. Ages within the *Pocillopora* ratio graph refer to corals dated for this study. Ages within the Heterotroph to Symbiont Ratio graph refer to foraminifers dated for this study.

BCP analysis shows three significant change-points in the coral growth log (Fig. 3.13). The first occurs within the 345–350 cm interval around 5200–4700 cal BP, where the ratio of *Pocillopora* increases to 17.3:1. This peak declines to a posterior mean of ~1.8 and remains steady until it peaks again at ~473–164 cal BP,

where the *Pocillopora* ratio increases to 27:1 within the 50–55 cm interval. The final change-point represents the decrease of the *Pocillopora* ratio from 27:1 to the posterior mean of 14.7 and then the final decrease to a posterior mean of 2.4. There are three significant change-points in the ratio of heterotrophic to symbiotic Foraminifera. The first occurs toward the end of the hiatus in reef growth ~1600–1300 within the 200–205 cm interval, where the ratio of heterotrophs/symbionts increases from 9:1 to a peak of 67.8:1. The next significant change point occurs within the 115–120 cm interval, where the foraminiferal ratio peaks at 63.9:1. After decreasing to a posterior mean of ~12, the heterotrophs drastically increase to a peak of 127:1 within the 60–65 cm interval around 500–160 cal BP.

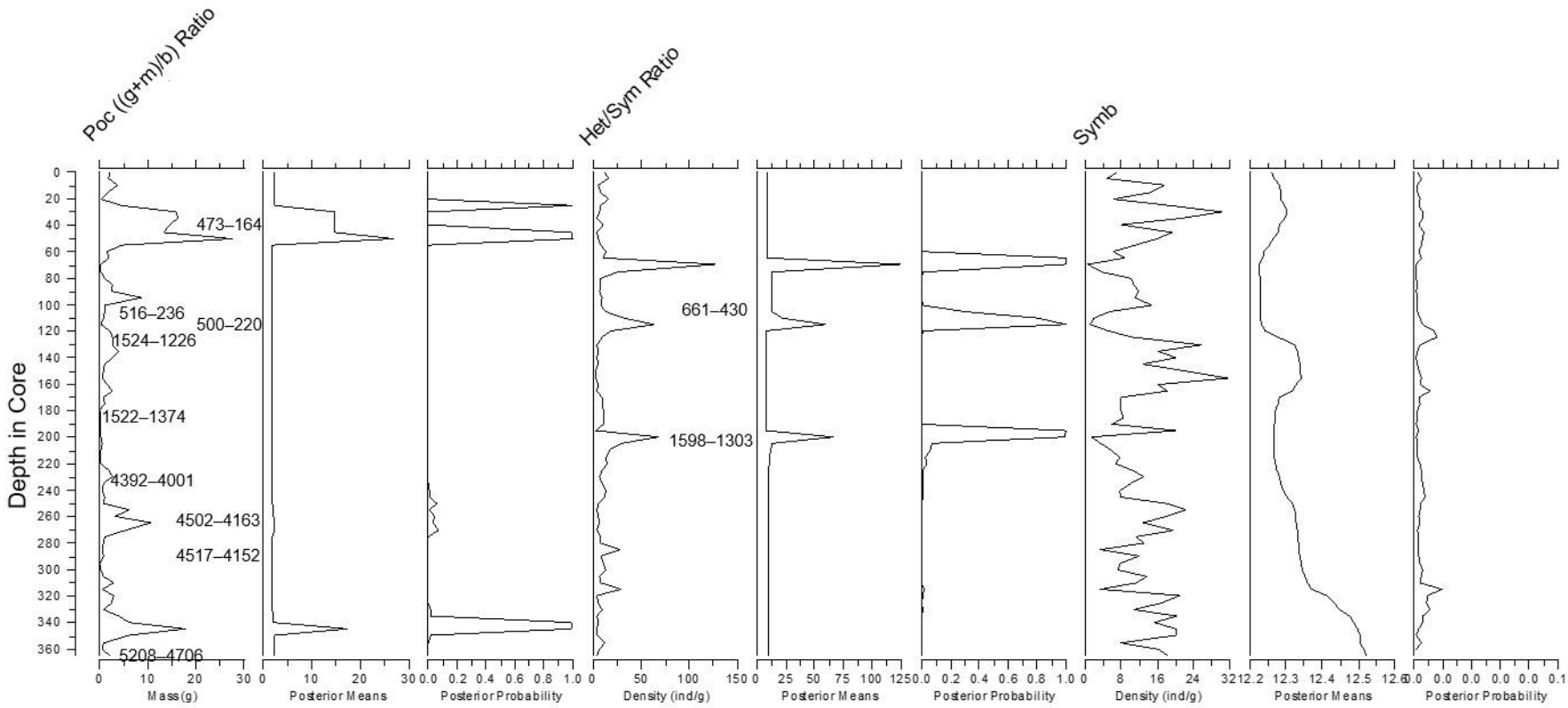

Figure 3.13 Saboga core log plotted with the Bayesian change-point algorithms for the ratio of *Pocillopora* in good and intermediate condition to poor condition, the ratio of heterotrophic to symbiotic Foraminifera, and the density of symbionts. Ages posted on the right side of the columns reflect radiocarbon dates analyzed for this study. Ages that are skewed to the left side of the *Pocillopora* ratio column represent previous dates reported in Toth (2013).

The peaks and valleys of symbiont density appear to follow the same trend exhibited by the *Pocillopora* ratio. However, when considering the BCP analysis, the posterior means do not change beyond 0.3 ind/g. For this reason, the probability of a change is functionally zero, and one cannot conclude that there was a significant change in the density of symbionts through time within the Canales de Tierra core. The correlation between symbiotic foraminiferal density and *Pocillopora* measurements are still significant, although the correlations are not as strong as those of Contadora and Saboga. Symbiotic foraminiferal density is positively correlated with both *Pocillopora* in good and intermediate condition (r = 0.59, p = 2.6×10^{-8}; Fig. 3.14) and the *Pocillopora* ratio (r = 0.62, p = 4.5×10^{-9}; Fig. 3.15). The correlation between heterotroph density and *Pocillopora* in good and intermediate condition as well as the *Pocillopora* ratio were not significant (r = 0.0034, p = 0.98 and r = -0.059, p = 0.62 , respectively).

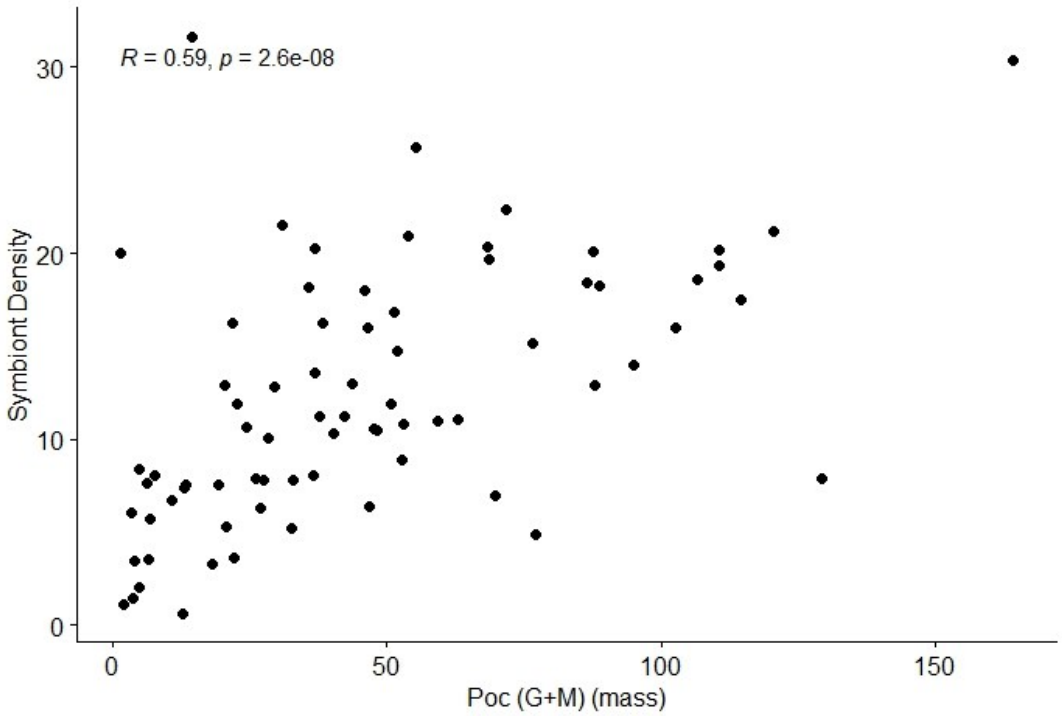

Figure 3.14 Spearman correlation between the mass of *Pocillopora* in good (G) and intermediate (M) taphonomic condition and symbiotic foraminiferal density at Canales de Tierra.

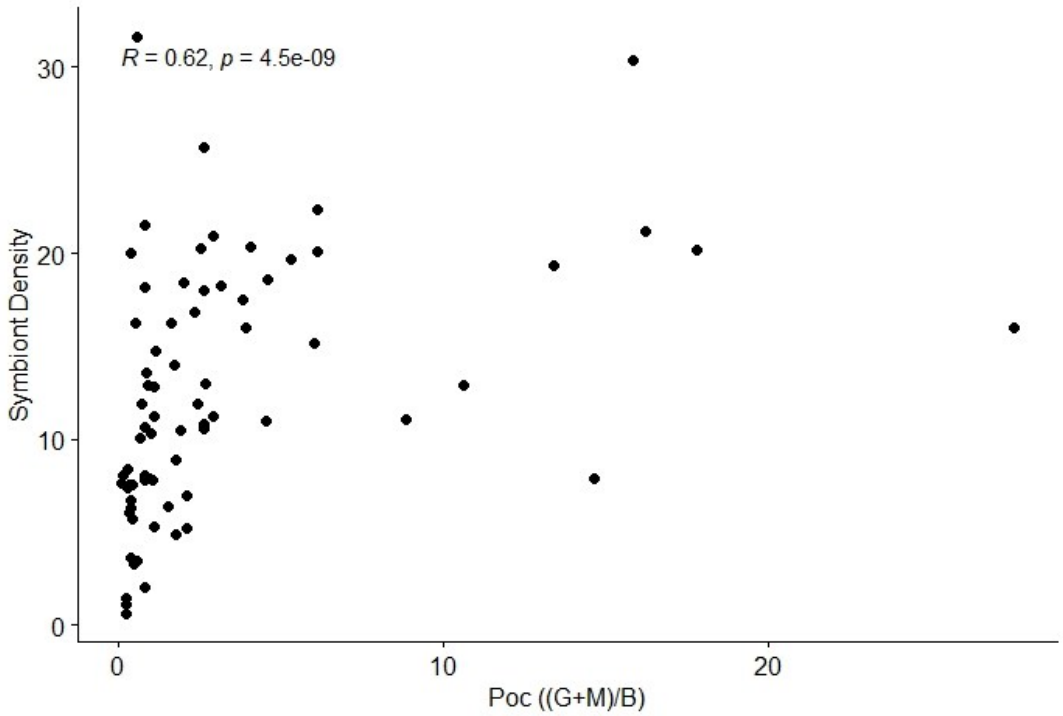

Figure 3.15 Spearman correlation between the ratio of *Pocillopora* in good (G) and intermediate (M) to bad (B) taphonomic condition and symbiotic foraminiferal density at Saboga.

Although the correlations between heterotroph and symbiotic foraminiferal density were not statistically significant, the bivariate plots in Figure 3.16 show that there were distinctively fewer symbiotic Foraminifera in Contadora and Saboga (Figs. 3.16 A and 3.16 B, respectively) compared with Canales de Tierra (Fig. 3.16 C) during the hiatus in reef growth. The bivariate plots also show that symbiotic foraminiferal density rebounded after the hiatus.

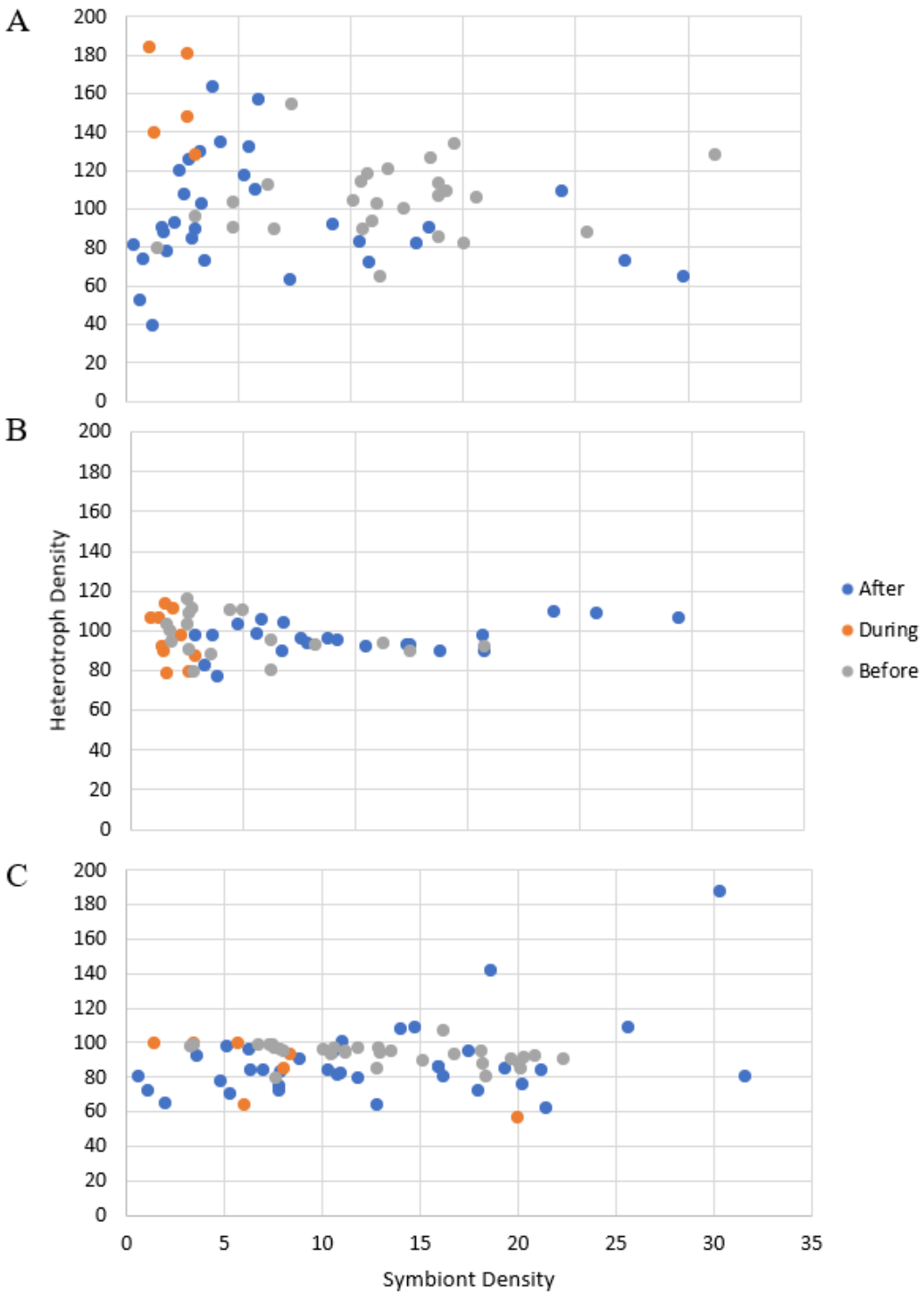

Figure 3.16 Bivariate plots showing the density of heterotrophs and symbiotic foraminiferal density (ind/g) for each core, where (A) is Contadora, (B) is Saboga, and (C) is Canales de Tierra.

Foraminiferal Assemblages

Foraminiferal assemblages in the cores were consistent with those found in modern sediments, with miliolids and rotaliids dominating throughout time. At Saboga and Contadora, rotaliids outnumbered miliolids within almost every interval (Fig. 3.17 A, B). The bivariate plots in Figure 3.17 show apparent changes in the densities of rotaliids and miliolids at Saboga and Contadora depending on if the samples were taken before, during, or after the hiatus in reef growth. In contrast, densities of rotaliids and miliolids at Canales de Tierra overlapped independent of the time period (Fig. 3.17 C).

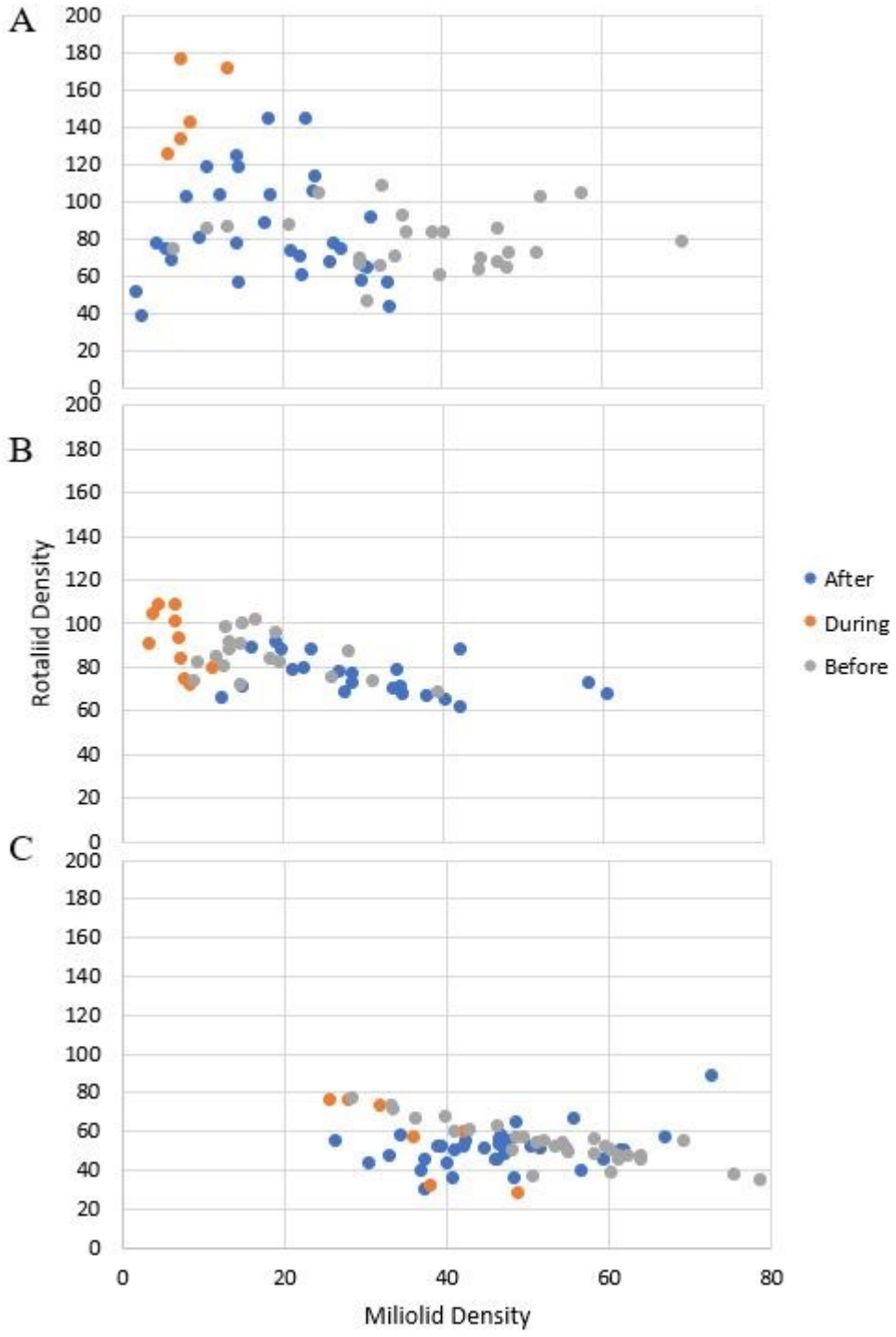

Figure 3.17 Bivariate plots showing the density of rotaliid and miliolid density (ind/g) for each core, where (A) is Contadora, (B) is Saboga, and (C) is Canales de Tierra.

To determine when the shifts in densities occurred and if they are significant, I performed another BCP analysis, this time on the densities of miliolids and rotaliids at each site. At Contadora (Fig. 3.18), there was a decrease in miliolids within the interval of 190–195 cm, corresponding to the initiation of the hiatus ~4300–3900 cal BP; however, the probability that a change occurred at this point is only 60%, which is lower than the 95% threshold for significance. After the decrease in miliolid density, the density of rotaliids began to increase. There is a steep change-point within the 170–175 cm interval corresponding to 3000–2800 cal BP within the hiatus period. Yet this change is not significant as the probability is 77%. Unlike the decreasing trend in the mean density of miliolids, the mean density of rotaliids after the hiatus in reef growth was similar before and after the hiatus. It is important to note, however, that the density of rotaliids was greater than that of miliolids for the entirety of the core, most likely because of depressed pH due to upwelling (Zamora-Duran et al., 2020).

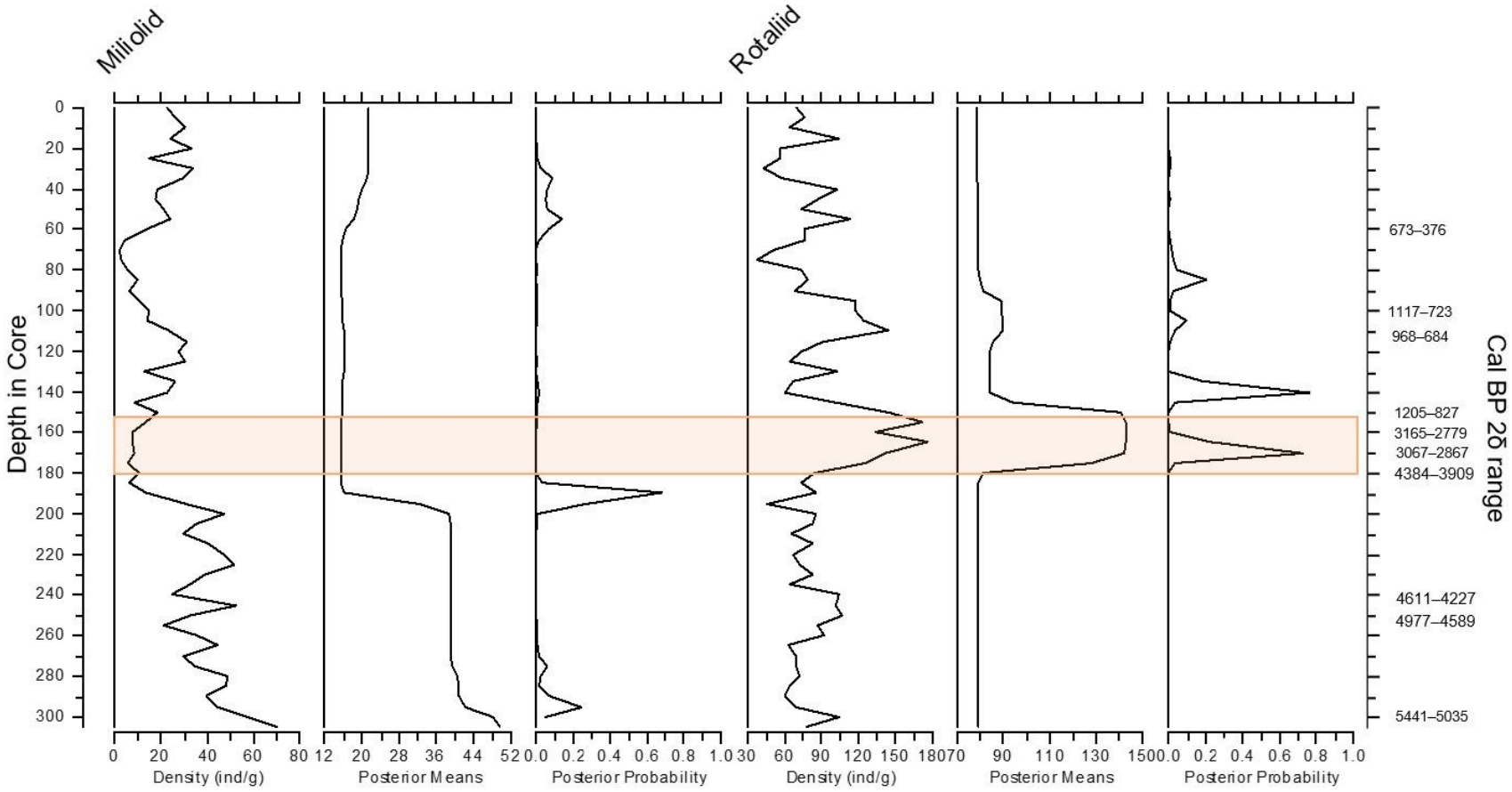

Figure 3.18 Contadora core log plotted with the Bayesian change-point algorithms for miliolid and rotaliid densities. Orange shading represents the period of the hiatus in reef growth.

Interestingly, the density of miliolids at Saboga showed an opposite pattern compared with that of Contadora before and after the hiatus (Fig. 3.19), which is corroborated by the bivariate plots in Figure 3.17 a,b. There is an increasing trend in the mean density of miliolids at the termination of the hiatus, but the uncertainty is too high to determine if the change was significant (Fig. 3.19). There were no significant changes in the mean density of rotaliids throughout time. As was the case with the Contadora core, the density of rotaliids was greater than that of miliolids throughout time.

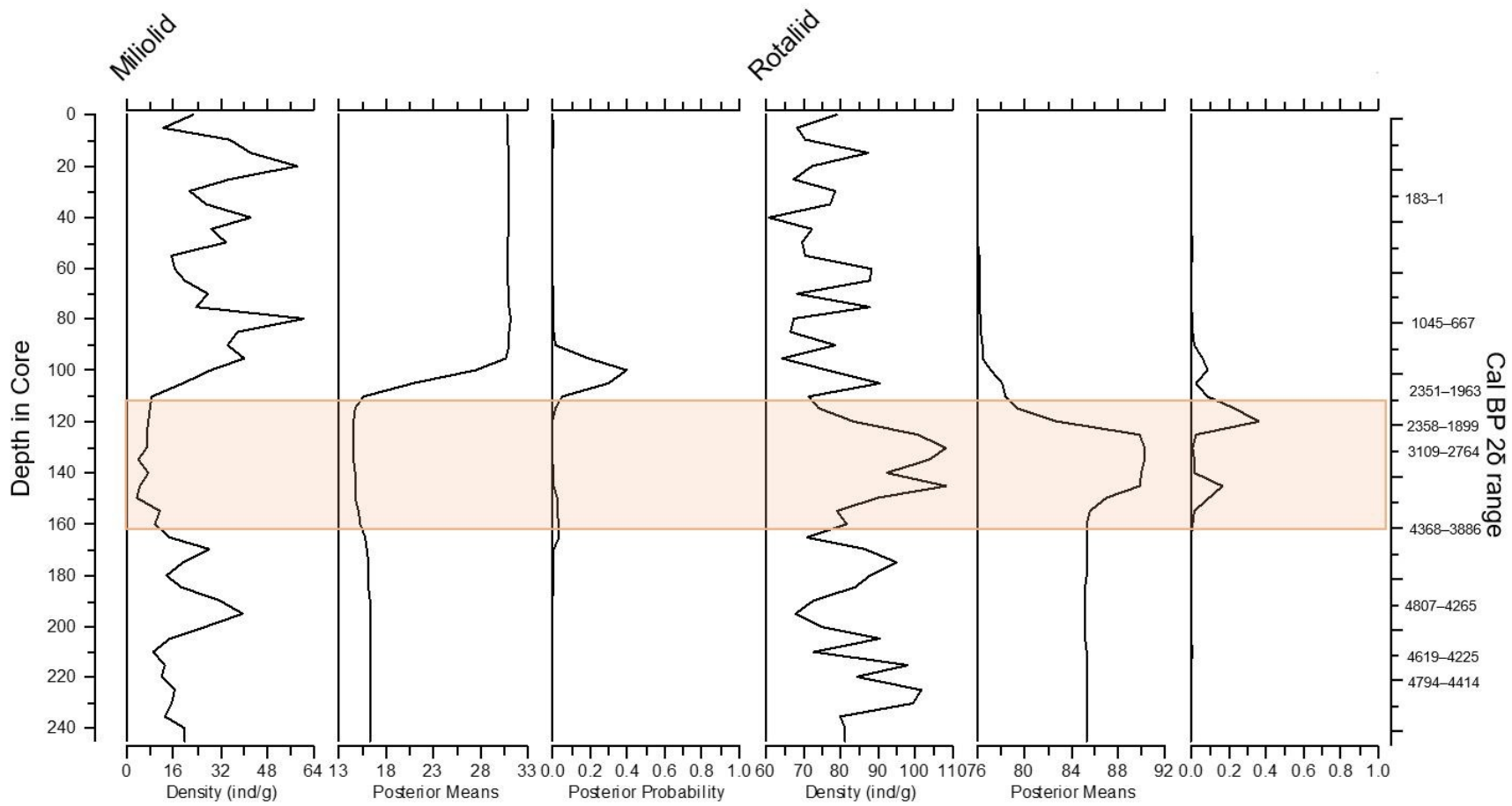

Figure 3.19 Saboga core log plotted with the Bayesian change-point algorithms for miliolid and rotaliid densities. Orange shading represents the period of the hiatus in reef growth.

At Canales de Tierra, the density of miliolids was greater through time compared with Contadora and Saboga. The mean density of miliolids at Canales remained around 45–55 ind/g except for a steep peak within 30–35 cm. The average miliolid densities were greater than the highest mean densities at both Contadora (39 ind/g) and Saboga (30 ind/g). The bivariate plot also shows that the densities of miliolids and rotaliids overlapped at Canales de Tierra, independent of the hiatus in reef growth (Fig. 3.16c).

There is only one significant change-point for miliolid densities between 30–35 cm. This change-point shows an 80% probability that the mean density of miliolids increased to a peak of 98.2 ind/g, corresponding to 473–164 cal BP (Fig. 3.20). There was a significant increase in the mean density of rotaliids from 50.4 to 71.5 at the inception of the hiatus. The mean rotaliid density remained steady at ~71 ind/g until the 200–205 cm interval, where it dropped to 43.5 ind/g. This change-point occurs near the termination of the hiatus, ~1600–1300 cal BP (Fig. 3.20).

There is another prominent peak in rotaliid density at the same depth interval as the peak in miliolid density (30–35 cm). Mean rotaliid density increased from 48.15 ind/g to 90.24 ind/g before dipping back down to 56.4 ind/g at the 15–20 cm interval. This peak was primarily driven by the high densities of two individual genera: one miliolid, and one rotaliid. The miliolid, *Quinqueloculina,* reached a density of 75.4 ind/g and the rotaliid, *Rosalina,* exhibited a density of 62.3 ind/g. These two genera were also the most abundant in the modern sediments

(Chapter 2). The average percentage of miliolids made up of *Quinqueloculina* and rotaliids made up of *Rosalina* are shown in Table 3.4.

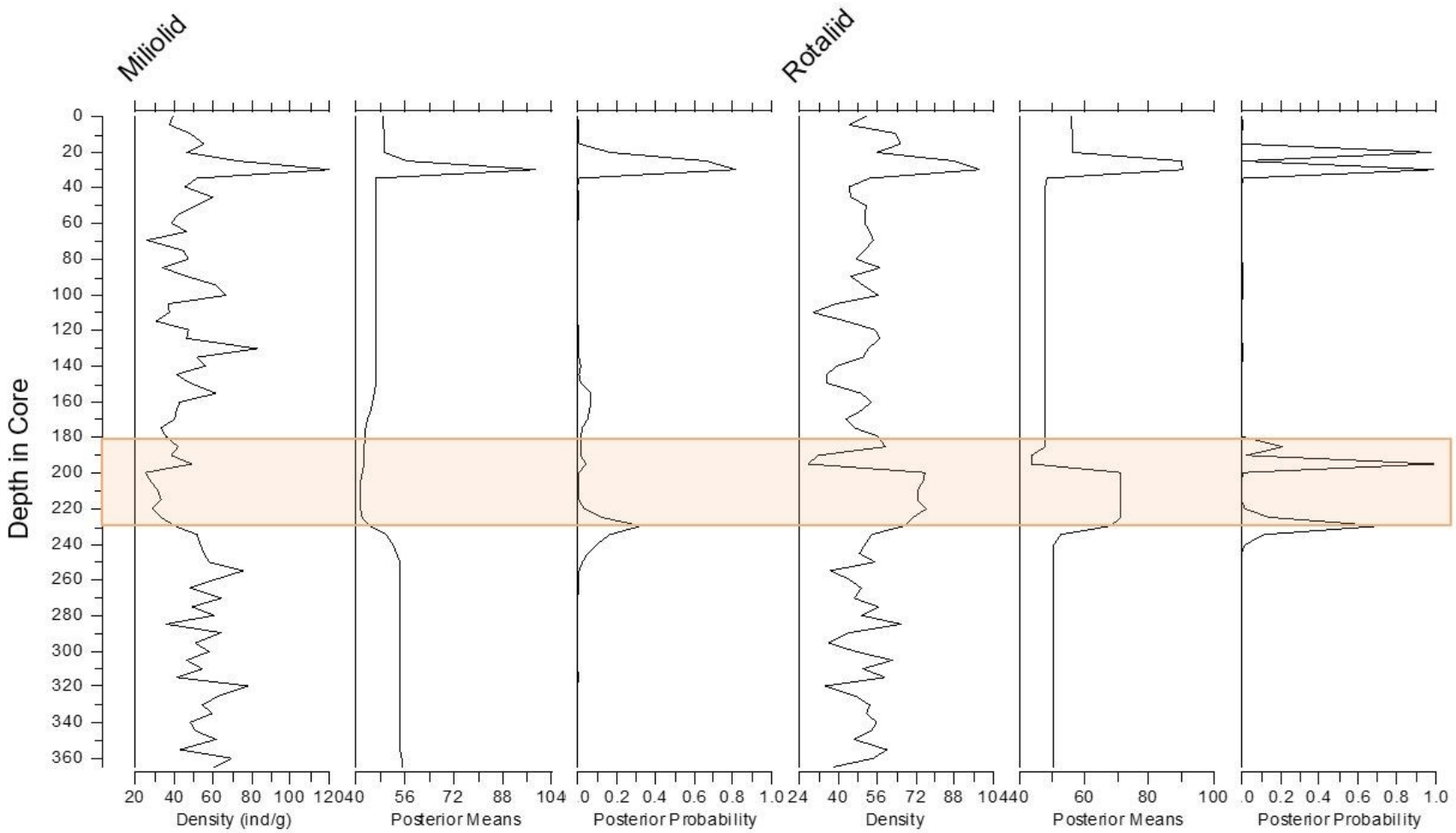

Figure 3.20 Canales core log plotted with the Bayesian change-point algorithms for miliolid and rotaliid densities. Orange shading represents the period of the hiatus in reef growth.

Table 3.4 Average percentage (±SE) of miliolids and rotaliids made up of *Quinqueloculina* and *Rosalina* within each core.

	Mean Percent *Quinqueloculina*	Mean Percent *Rosalina*
Contadora	50±14.2	81±10.8
Saboga	49±12.3	81±13.2
Canales	59±11.7	68±11.4

Although only two genera contributed to the majority of the two most-common orders, rare species may have led to differences in community composition. In order to determine if community composition differed based on location a Detrended Correspondence Analysis (DCA) was completed for each site. The DCA plot in Figure 3.21 shows relationships among genera from Contadora. For the most part, miliolids are grouped together and rotaliids are grouped together along DCA axis 1. The eigenvalues are notably low (DCA1=0.054, DCA2=0.046) suggesting that there is little variance in the matrix.

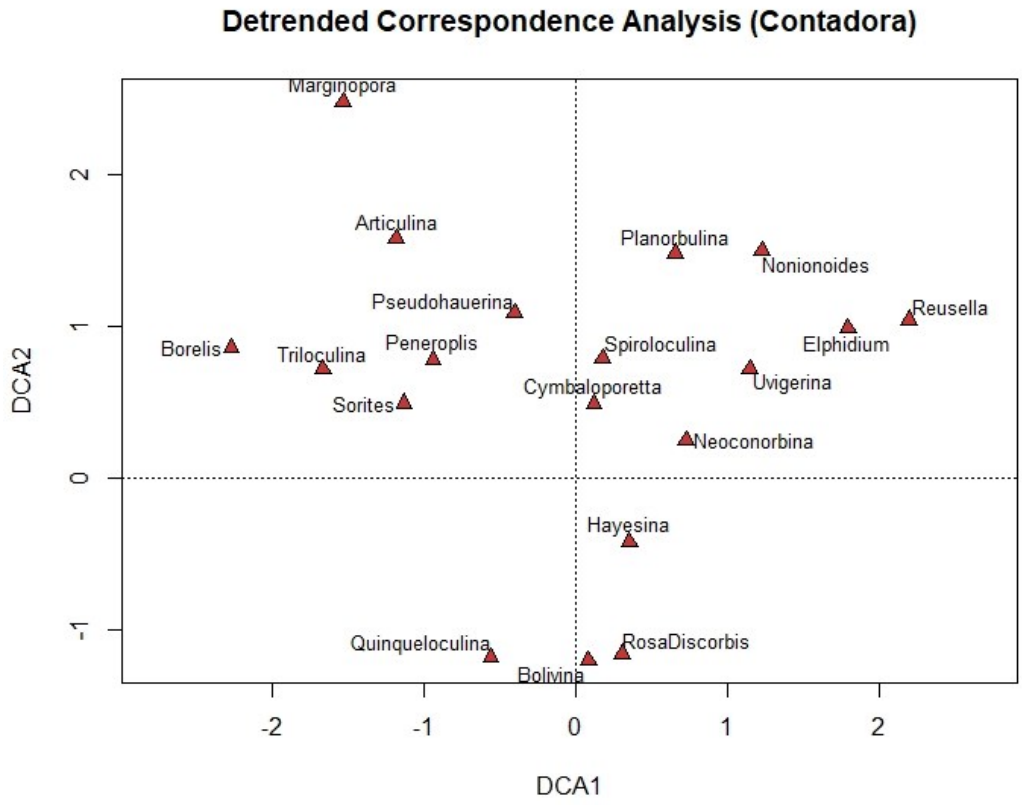

Figure 3.21 DCA plot depicting foraminiferal genera within 5-cm interval samples from Contadora.

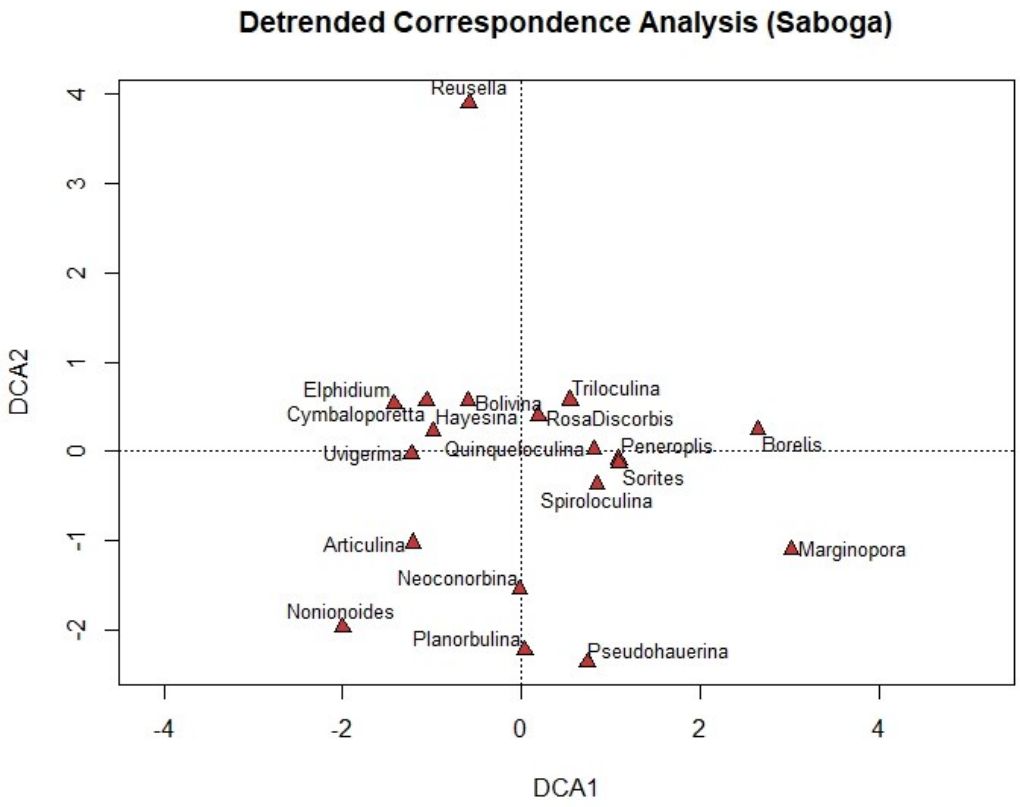

Figure 3.22 DCA plot depicting foraminiferal genera within 5-cm interval samples from Saboga.

The DCA on the foraminiferal composition in Saboga (Fig. 3.22) is similar to that of Contadora, with miliolids grouping together and rotaliids grouping together along DCA axis 1. There is an obvious outlier with *Reusella* being separate from the rest of the foraminiferal genera. The eigenvalue for DCA 1 was higher at Saboga than that of Contadora (0.07 versus 0.05), whereas the eigenvalue for DCA 2 was lower at Saboga (0.026 versus 0.046). The DCA for Canales (Fig. 3.23) shows a separation of heterotrophs and symbiont bearing genera along Axis 2

with the eigenvalue of DCA 1 being 0.042 and for DCA 2 being 0.031 lower than those from both Contadora and Saboga.

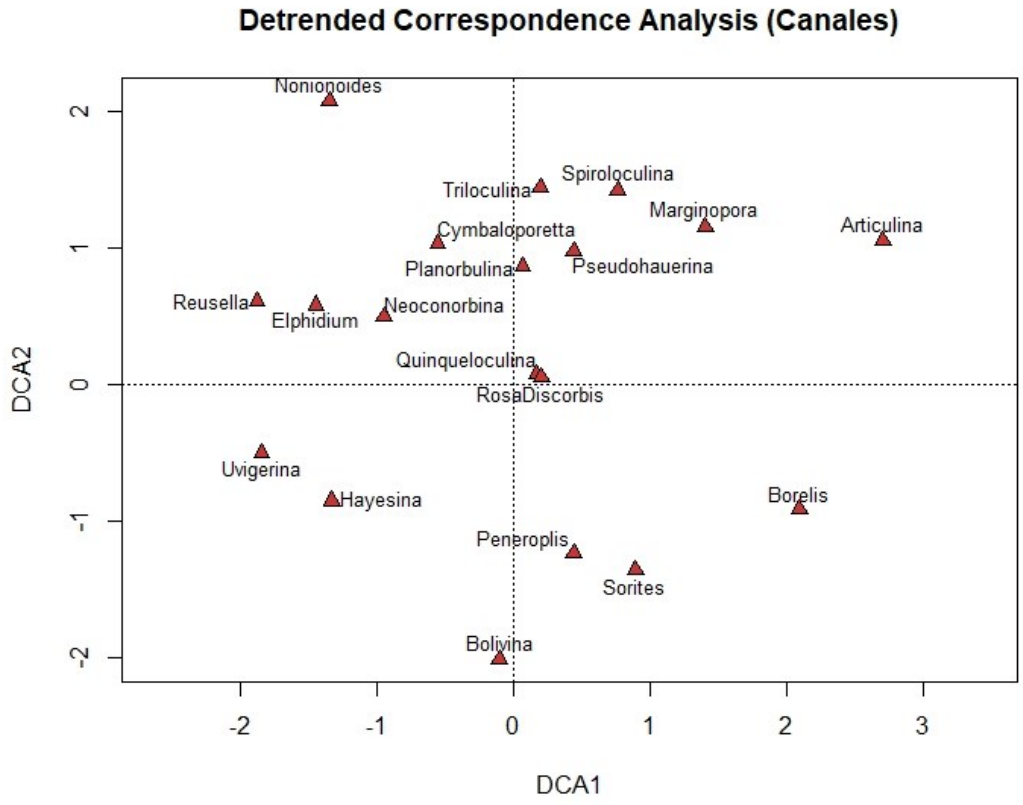

Figure 3.23 DCA plot of foraminiferal genera within 5-cm interval samples from Canales de Tierra.

PERMANOVA was used to evaluate if there are statistically significant differences in foraminiferal species composition based on site, hiatus period, and the interaction of the two. The results of the PERMANOVA (Table 3.5) show that the time period, the site, and the interaction between hiatus period and site significantly influence community composition. Yet, the R^2 values for each are

very low, suggesting that there is substantial variation that the model does not explain (indicated by the high R^2 of the residuals).

Table 3.5 PERMANOVA table shows the relationship between hiatus period, site, and interaction between hiatus period and location and species composition.

	Df	SS	MeanSq	F	R^2	p-value
Hiatus	1	0.13	0.13	4.25	0.019	0.002**
Site	2	1.34	0.67	22.5	0.19	0.001***
Hiatus x Site	2	0.33	0.03	5.56	0.05	0.001***
Residuals	182	5.37	0.03		0.79	
Total	185	7.18			1	

Similarity Percentage (SIMPER) analysis using the Bray-Curtis dissimilarity matrix was used to determine the genera that contributed the most to the differences between the hiatus period and location. Comparisons were made for differences between each site and intervals before and after the hiatus in reef growth, after and during the hiatus, and before and during the hiatus. Figure 3.22 shows the DCA plots for each site. The DCA plots (Figures 3.22 A, B, C) show differences in community composition between sites. Table 3.6 shows the overall dissimilarity between the sites based on the Bray-Curtis dissimilarity index.

Table 3.6 Overall dissimilarity between sites based on the Bray-Curtis dissimilarity index.

Sites	Percent Dissimilarity
Saboga + Contadora	29%
Saboga + Canales	29%
Contadora + Canales	32%

The same five genera contributed to 70 percent of the dissimilarity between sites: *Quinqueloculina* (a heterotrophic miliolid), *Peneroplis* (a symbiotic miliolid), *Triloculina* (a heterotrophic miliolid), *Haynesina* (a heterotrophic rotaliid), and *Sorites* (a symbiotic miliolid). *Quinqueloculina* was the genus that contributed the most to the dissimilarity between Saboga and Contadora and between Saboga and Canales, whereas *Haynesina* was the main contributor to the dissimilarity between Contadora and Canales. It is important to note that although these five species contribute the greatest to the dissimilarity between sites, the cumulative sum of their contribution is only ~34–36%. A full table of species and their contributions to the dissimilarity between sites is shown in Appendix B. The overall dissimilarity at all sites is low most likely because two heterotrophic genera, *Quinquloculina* and *Rosalina* dominate at each site.

In order to determine if community composition differed due to hiatus period, I conducted a SIMPER analysis for each site. At Contadora, 11 genera contributed the most to the differences in community composition when comparing

all intervals. Not surprisingly, *Quinqueloculina* (the genus that constitutes the highest percentage of miliolids) was the highest contributor to the differences in composition between each of the intervals. When comparing the composition after and during the hiatus in reef growth, ten other genera contributed ~70% to the difference in the community composition: *Nonionoides*, *Sorites*, *Triloculina, Peneroplis, Reusella, Rosalina, Uvigerina, Haynesina, Elphidium* and *Neoconorbina* (with genera listed in descending order of their contributions to mean dissimilarity). Only two of these genera are symbiotic (*Sorites* and *Peneroplis*), whereas the others are heterotrophic. Four of these genera are miliolids (*Quinqueloculina*, *Sorites*, *Triloculina* and *Peneroplis*), whereas the other seven are rotaliids. The differences in community composition before and during the hiatus in reef growth were defined by *Sorites, Peneroplis, Nonionoides, Cymbaloporetta, Rosalina, Reusella, Triloculina, Uvigerina, Borelis* and *Neoconorbina*. Finally, when comparing community composition before and after the hiatus, the ten genera (besides *Quinqueloculina*) that contributed to ~70% of the difference are *Triloculina, Peneroplis, Sorites, Borelis, Cymbaloporetta, Planorbulina, Nonionoides, Uvigerina, Articulina* and *Elphidium*.

Within the Saboga core, *Quinqueloculina* was the greatest contributor to differences in community composition only when comparing the communities after and during the hiatus in reef growth and before and during the hiatus. When comparing the communities before and after the hiatus in growth, *Nonionoides* contributed the most to the differences in composition. The other genera that

contributed to the differences in composition at Contadora were the same for Saboga except for *Pseudohauerina*, which contributed a small percentage to the differences after and during the hiatus in reef growth (4%) and before and after the hiatus in growth (6%).

Within the Canales core, 12 genera contributed the most to the differences in community composition when comparing all intervals. *Triloculina* was the top contributor to the difference when comparing community composition during and after and before and during the hiatus in reef growth, unlike *Quinqueloculina* in Contadora and Saboga. The eleven other genera that contributed ~70% to the difference in the community composition during and after the hiatus (in descending order of their contributions to mean dissimilarity) were *Haynesina*, *Sorites*, *Peneroplis, Neoconorbina, Pseudohaureina, Spiroloculina, Bolivina, Cymbaloporetta, Elphidium* and *Uvigerina.* There are five miliolids within this group: *Triloculina*, *Sorites*, *Peneroplis, Pseudohauerina* and *Spiroloculina*.

The differences in community composition before and during the hiatus at Canales were caused by variability in the same genera except for *Borelis* (a symbiotic miliolid), *Articulina* (a heterotrophic miliolid), and *Reusella* (a rotaliid). These genera contributed 6%, 5%, and 4.5% of the difference, respectively. Finally, when comparing community composition before and after the hiatus, the 11 genera that contributed to ~70% of the difference are *Haynesina*, *Triloculina, Peneroplis, Sorites, Borelis, Cymbaloporetta, Planorbulina, Nonionoides, Uvigerina, Articulina* and *Elphidium*.

DISCUSSION

As was the case within the modern foraminiferal assemblages (Chapter 2), two primary patterns are evident within the cores: heterotrophic dominance overall and rotaliid dominance in the Gulf of Panamá. The core from Canales is characterized by a greater density of symbiont-bearing Foraminifera and miliolids than the cores from the Gulf of Panamá. Oceanographic variability produced by the persistence of strong wind-gap upwelling for the last ~6750 years (Martinez et al., 2006; Toth et al., 2012, 2015a, b, Arellano-Torres et al., 2013) is likely the key driver of differences in foraminiferal assemblage between the two gulfs. Greater productivity caused by upwelling leads to blooms of heterotrophic Foraminifera in reef ecosystems if sufficient oxygen is available (Hallock et al., 2003). Low abundances of porcelaneous, miliolid taxa within the Gulf of Panamá may be a result of low pH, which is known to affect porcelaneous forms more strongly than hyaline forms (i.e., the rotaliids; Bentov and Erez, 2006). Strong upwelling would have lowered the pH in the Gulf of Panamá, resulting in an increased cost of calcification for miliolids and overall lower densities (Bentov and Eres, 2006; Knorr, 2015).

In addition to the differences in regional oceanography caused by upwelling, foraminiferal assemblages likely responded to climatic variability through time. In Pacific Panamá, El Niño-like periods are characterized by a warm, dry climate and a reduction in seasonal upwelling. La Niña-like periods lead to

wetter, cooler conditions, and increased seasonal upwelling. Decreases in foraminiferal density would have been expected during El Niño-like periods due to bleaching in symbiont-bearing taxa and decreased food sources available for heterotrophic Foraminifera (Kelmo and Hallock, 2013). La Niña, on the other hand, should have resulted in increased densities of heterotrophic taxa because of increased productivity (greater food sources) and decreases in symbiotic taxa because of low-light conditions caused by increased turbidity (Hallock, 2003; Kelmo and Hallock, 2013).

Existing records from the mid-Holocene suggest high oceanic productivity and low ENSO variability in the ETP (Kouvatas and Joaides, 2012; Pennington et al., 2006). During that same time period (~7000–5000 cal yr BP), the geochemistry of corals from a Contadora core indicates a cool, wet period characterized by moderate upwelling (Toth et al., 2015a). Sr/Ca ratios from Contadora coral samples showed increased warming from ~19°C to 25.5°C between ~5100–4600 cal yr BP with a stable $\delta^{18}O$, suggesting a warm, dry period characteristic of stronger El Niño events and weaker upwelling (Toth et al., 2015a). The newly calibrated dates in this study based on coral samples show that the inception of the hiatus in the Gulf of Panamá occurred ~4300–4000 cal BP. Reconstruction of oceanic radiocarbon variability combined with paleoclimate reconstructions suggested that upwelling strength increased ~4300 ka and intensified for the next 500 years (Toth et al., 2015a, 2015b). Around 3900 cal BP, paleoclimate reconstructions are consistent

with a cooler, wetter climate suggesting La Niña-like conditions (Toth et al., 2015a).

In the Gulf of Panamá, the ratio of heterotrophic to symbiotic Foraminifera began to increase drastically around the same time as the inception of the hiatus in reef growth. Although a negative correlation between *Pocillopora* in good and intermediate taphonomic condition (which suggests a good coral growth phase) and heterotrophic density was not determined to be significant, there was a significant positive correlation between symbiotic foraminiferal density and *Pocillopora* growth. This non-significant correlation between heterotrophs and *Pocillopora* reflects the fact that heterotrophs are, and have always been, dominant in Pacific Panamá, whereas symbiotic foraminifers respond to oceanographic/climatic events similarly to corals.

In Saboga and Contadora, the heterotroph/symbiont ratio peaked ~3100–2700 cal BP. The high density of heterotrophic compared with symbiotic Foraminifera from ~4300 cal BP to its peak ~2900 cal BP align with other studies that hypothesize a transition to more frequent La Niña events from 3500–3000 cal BP (Thompson et al., 2017). Other studies have suggested that El Niño events peaked around 3000 cal BP (Sandweiss et al., 2001; Moy et al., 2002), which could explain the reason that the ratio of heterotrophic to symbiotic Foraminifera started to decline around that time: due to of reduced food supply. The increased climatic variability between ~4200–2000 (Rein et al., 2005; Thompson et al., 2017) was not only the most likely cause of the hiatus in reef growth, but also the reason for the

drastic changes in foraminiferal assemblages. Declines in the heterotrophic/symbiotic ratio at the termination of the hiatus in reef growth at Saboga and Contadora were most likely due to a reduction in the variability/strength of El Niño and La Niña. Reef accretion resumed ~1200–800 cal BP in Contadora and intermittent accretion was seen ~2400–1900 in Saboga, suggesting that the hiatus was longer in Contadora. Including foraminiferal and *Psammocora* samples into the age model provided evidence of intermittent deposition in Saboga ~2100 cal BP and in Contadora ~2600 cal BP. More sampling will be necessary to confirm the second hiatus.

Interestingly, there is a peak in the ratio of heterotrophic to symbiotic Foraminifera again at Contadora during "modern" times that is not present in Saboga. Symbiont-bearing foraminifers increase in density at Saboga to a mean of ~8.7 ind/g after the hiatus, whereas symbiont-bearing densities remain around 4 ind/g in the core from Contadora until a peak of ~15 ind/g in the 15–20 cm interval. This discrepancy could indicate oceanographic differences potentially due to the reefs of Saboga being more protected from oceanic influences than those of Contadora (Glynn and Macintyre, 1977, Macintyre et al. 1992).

The patterns seen in the foraminiferal assemblage from the Gulf of Chiriquí from the Canales de Tierra core differed from those in the Gulf of Panamá. There were three peaks in the heterotrophic/symbiotic ratio, with the first peak occurring at the termination of the hiatus in reef growth ~1500–1300 cal BP. Except for those three increases in the heterotroph/symbiotic ratio, the ratio remained constant and

did not significantly change through time. Even the density of symbionts did not change significantly at Canales de Tierra. Foraminiferal assemblages, therefore, could be more affected by upwelling strength than climatic effects in the ETP. The fact that heterotrophic dominance is a pattern seen through time in both gulfs suggests that the Gulf of Chiriquí historically exhibited weak upwelling, supporting the conclusion of Toth et al. (2015b). The peaks in heterotrophic densities could have resulted from pulses of increased productivity. Although the overall ratio of heterotroph to symbiont-bearing Foraminifera does not change significantly at the inception of the hiatus, the decrease in miliolids coupled with the increase in rotaliids when reef growth is halted (Fig. 3.18) could suggest a La Niña-like state. Increased nutrients could have led to increases in rotaliid heterotrophs, yet the low pH would have resulted in a decrease in miliolid heterotrophs and symbiotic foraminfers.

The decrease in density of miliolids in the Gulf of Chiriquí at the inception of the hiatus in reef growth was minor compared with samples within the Gulf of Panamá. Whereas the mean density decreased from 54 to 44 ind/g at Canales de Tierra, Contadora experienced a decrease from 39 to 15 ind/g in the interval right before the hiatus. In addition, miliolid density rebounded to pre-hiatus levels in Canales de Tierra, but in Contadora miliolid densities remained low after the initial decrease. Interestingly, miliolid density at Saboga remained constant at ~15 ind/g before and during the hiatus and increased to 30 ind/g after the hiatus. This

discrepancy could be another indicator of differences in regional oceanography between these two sites.

The PERMANOVA suggests that foraminiferal assemblages were distinct based on location and hiatus period; however, there was substantial variation that could not be explained by the model. The differences in community assemblages in the Gulf of Panamá were driven by the lower densities of primarily symbiotic and miliolid taxa during the hiatus, most likely due to increases in upwelling strength. Rare genera seemed to contribute to differences in community assemblages in the Gulf of Panamá. The densities of individual genera did not show a significant change through time, most likely because the densities of all genera (except for *Quinqueloculina* and *Rosalina*) were low. In addition, each of the rare genera contributed to less than 10% of the differences in community composition.

Although the DCA did not explicitly show differences in functional groups or foraminiferal orders correlated with the hiatus, change-point analysis did show significant shifts through time. Increasing climatic and oceanic variability during the period of the hiatus influenced functional groups and foraminiferal taxa. Increased nutrients induced by a La Niña-like state appeared to result in increases in heterotroph densities. At the same time, low pH and high turbidity could have led to decreases in high-Mg-calcite Foraminifera as well as symbiont-bearing taxa. Strong upwelling seems to have persisted in the Gulf of Panamá during the hiatus in reef growth. The combined ENSO–ocean acidification effect, in concert with the predicted increase in the frequency of strong ENSO events (Cai et al., 2014, 2018)

and declining oceanic pH (Uthike et al., 2013) in the future, could result in a decrease of foraminiferal diversity due to the enhanced dominance of heterotrophic rotaliids, accompanying a shutdown of reefs in the ETP similar to the historical hiatus.

Chapter 4: Variability of Holocene climate in the ETP during the hiatus in reef growth

INTRODUCTION

The results from Chapter 3, as well as previous research on coral in core samples from the ETP (Toth, 2012), suggest that climatic variability during the late Holocene was the primary influence on reef development. For much of the work that has been completed on corals, however, researchers have only been able to characterize conditions before and after the hiatus in reef growth (Toth et al., 2012; 2015), when corals were available in the reef cores. The analyses of Foraminifera presented here allow for the reconstruction of some aspects of environmental conditions *during* the hiatus ~4100–1200 cal BP yet should be interpreted with caution.

Measuring the elemental ratio of magnesium to calcium in tests of benthic foraminifera has been used successfully to reconstruct past ocean temperatures (e.g., Gillups and Schrag, 2002; Elderfield et al., 2006; Lear et al., 2000; Martin et al., 2002). During test construction, a small amount of magnesium is incorporated and can form impurities in the calcite. The amount of magnesium in calcite precipitated from seawater is temperature-dependent; Foraminifera incorporate more magnesium into their tests in warmer water. In present-day seawater which

has a Mg/Ca ratio of ~5, the kinetically preferred mineral to be precipitated inorganically is aragonite because calcite growth is inhibited by Mg and possibly other ions (Davis et al., 2000; Morse and Bender, 1990). Aragonite is also the mineral deposited by corals and many mollusks. It has previously been shown that in shallow coral-reef environments, Foraminifera dominated when corals became rare during the Paleocene (Scheibner and Speijer, 2008). Therefore, by using the geochemistry of Foraminifera, I will test predictions of changes in regional environmental conditions even in the absence of corals in core records. Geochemical reconstructions using foraminifera make it possible to analyze climatic and oceanographic variability during the hiatus between ~4100–1200 cal BP, for which there are currently limited data.

Although there have been successful temperature reconstructions using benthic Foraminifera, most of the literature on this subject focuses on planktonic species or benthic individuals from deep ocean environments. Therefore, constraints on using benthic Foraminifera to reconstruct temperature in coral-reef ecosystems have not been fully explored. In this chapter, I provide a review of relevant literature regarding Mg/Ca paleothermometry and attempt to determine the constraints to using foraminiferal reconstructions in comparison with Sr/Ca paleothermometry from corals.

By understanding the environmental drivers during the hiatus, I aimed to determine how coral populations were suppressed by climate in the past and what is probable for the future. Impacts of future climate change are thought to increase the

amplitude of El Niño and La Niña events in the ETP, leading to increased ENSO variability (Cai et al., 2014, 2018). Analyzing the geochemistry of foraminiferal tests will provide insight into the environmental conditions leading up to and during the suppression of coral-reef growth. I tested the following hypothesis in this study:

1. Does the geochemistry (Mg/Ca) of *Sorites marginalis* suggest a change in temperature leading up to the hiatus in coral reef growth and/or reef recovery?
    - H_1: Increased temperature variability led to and persisted during the hiatus in reef growth.

MG/CA PALEOTHERMOMETRY IN FORAMINIFERA

The distribution coefficient relating temperature to the Mg composition of calcite formed from seawater is:

$$D = \frac{\left(\frac{Mg}{Ca}\right)calcite}{\left(\frac{Mg}{Ca}\right)seawater} \quad (2)$$

with Mg/Ca referring to the molar ratio of Mg^{2+} to Ca^{2+} in calcite and seawater. More Mg is incorporated into calcite with increasing temperature, which increases the distribution coefficient. The modern molar Mg/Ca ratio in seawater is high (i.e., 5.2), which leads to inorganic calcite with greater than 5 mol % $MgCO_3$, or high-Mg calcite (Mucci, 1987). High-Mg calcite forms naturally in marine sediments except in the deep oceans where the low temperatures and low pH

produce low-Mg calcite (Mucci, 1987). Early experiments showed an increase of 3.1% in Mg/Ca per degree Celsius in inorganic calcite precipitated from seawater over a temperature range of 10–50 °C (Oomori et al., 1987).

Marine organisms that secrete calcite can control the chemical composition of their calcite skeletons, but the uptake of Mg varies with temperature (Chave, 1954). Distribution coefficients are specific for each calcifer. Most planktic Foraminifera precipitate low-Mg calcite, with Mg/Ca ratios less than inorganic calcite precipitated from seawater (Lea, 2003). Porcellaneous benthic foraminifers, on the other hand, precipitate high-Mg calcite.

By measuring both Mg/Ca and $\delta^{18}O$ in planktic foraminifera, temperature and local variations in evaporation and rainfall (i.e., salinity) can be estimated (Lea et al., 2000). The Mg/Ca temperature proxy is calibrated to show the relationship between calcite shell Mg/Ca and seawater temperature. Mg-temperature relationships were first established in planktonic foraminiferal shells by using controlled culture experiments, sediment trap timeseries, and analysis of foraminifers from the tops of sediment cores (core-top studies; Rosenthal and Linsey, 2006). Mg/Ca calibrations are expressed as an exponential dependence of temperature in the form:

$$\text{Mg/Ca (mmol mol}^{-1}) = be^{mT} \qquad (3)$$

where Mg/Ca is measured from marine calcite, T is temperature, and m and b are the constants (Lea et al., 2003). The exponential fit to the empirical data is based on the thermodynamic prediction of exponential response. The exponential

relationship assumes that Mg/Ca responds to a given temperature change (in mmol mol^{-1} per °C reflected by the constant), implying increased sensitivity with increasing temperature. Mg/Ca correlates well with Atlantic and Pacific mean annual sea-surface temperatures (SST), but there is an intraspecific offset attributed to different depths of habitat between/among species (Dekens et al., 2002). Although planktic Foraminifera secrete lower Mg-calcite than benthics, the temperature dependence in planktic Foraminifera is larger than that of benthic foraminifers with exponential constants of ~10% compared with ~2.5%, respectively (Rosenthal et al., 1997, Lea 2003).

The first temperature calibration for benthic species was based on the rotaliid, epibenthic species *Cibicidoides pachyderm*a from a shallow bathymetric transect (~300–1500 meters) on the Little Bahama Bank (LBB) spanning a temperature range of 5–18°C (Rosenthal et al., 1997). Core-top calibrations conducted by Lear et al., 2002 and Martin et al., 2002 determined that the temperature sensitivity of *Cibicidoides* Mg/Ca agreed with the findings of Rosenthal et al. 1997, showing a ~10% increase in Mg/Ca per °C observed in planktonic foraminifera. However, differences in Mg uptake do exist for different species of *Cibicidoides* (Elderfield et al., 2006). Lear et al. (2002) also observed a temperature sensitivity of ~10% in other benthic species including *Planulina* spp., *Oridorslis umbunatus*, and *Melonis* spp. whereas other species, *Uvigerina* spp. and *Planulina aremenensis*, showed a sensitivity of about 6% per °C. Elderfield et al. (2010) suggested that *Uvigerina* may be the best species to use for temperature

reconstructions because, being an infaunal species, it is less affected by bottom-water carbonate-ion differences.

In addition to differences attributed to habitat depth, the pattern of Mg/Ca variation is also significantly different between symbiont-bearing and symbiont-free, heterotrophic species. Shells of symbiont-bearing Foraminifera show cyclic variations between high- and low- Mg/Ca layers within individual chambers, which are absent from heterotrophic species (Sadekov et al., 2005). In symbiotic planktic species, high-Mg/Ca bands (~8–11 mmol/mol) are intercalated between broader low Mg/Ca bands (~1–5 mmol/mol) equating to an apparent calcification temperature change of 10°C or more. This variation is more likely due to biological effects on the co-precipitation of Mg in foraminiferal calcite, as such high variability in temperature is highly improbable (Sadekov et al., 2005). The intercalated growth bands are consistent with a diurnal origin, modulated by changing pH within the foraminiferal microenvironment due to the day–night, photosynthesis–respiration cycle of algal symbionts (Eggins et al., 2004).

Light not only affects variability due to banding but also trace element incorporation in foraminiferal shells. Researchers have shown bands of high-Mg calcite are associated with calcite formed in dark conditions (Spero et al., 2015; Holland et al., 2017) Al-Horani et al. (2003) found light dependent Ca^{2+}-ATPase in corals, suggesting a mechanistic link between light and elemental incorporation. Similar mechanisms in Foraminifera could make elemental incorporation in foraminiferal shells light dependent (Erez, 2003). This effect could be enhanced by

migration of planktonic species in the water column, which would affect symbiont activity (Köhler-Rink and Kühl, 2000; 2005).

A recent study showed that light not only impacts variability due to banding but also significantly affects the average concentration of Mg/Ca within chambers of the large benthic, symbiont-bearing foraminifer *Amphistegina lessonii*. Mg/Ca ratios of Foraminifera that calcify for longer in the dark were 23 mmol mol $^{-1}$ higher than those formed completely in the light (Dämmer et al., 2019). This difference in Mg/Ca translates to an increase of about 2.3 mmol/mol Mg/Ca per 10% decrease of light exposure duration during calcification, implying a change of ~1.4°C. When comparing temperature reconstructions based on symbiotic Foraminifera Mg/Ca from different latitudes, it is important to consider how substantial differences in day lengths affect the Mg/Ca ratio. There should be no bias when comparing a single population's average Mg/Ca, as the population is subject to the same amount of light exposure in terms of seasons and latitude.

Segev and Erez (2006) revealed a positive correlation of shell Mg/Ca with Mg/Ca in the culturing media with slightly different curves for two symbiont-bearing species, *Amphistegina lessonii* and *Amphistegina lobifera*. The researchers determined that calcification rates were sensitive to Mg/Ca ratio rather than the concentration of either Ca^{2+} or Mg^{2+}. The concentration ratios of Mg^{2+} in seawater to Mg^{2+} in the foraminiferal shell, known as the partition coefficients of Mg^{2+} (D_{Mg}), for *A. lobifera* and *A. lessonii* were intermediate between deep benthic and shallow benthic species, at 0.012 and 0.010 respectively. Partition coefficients of

Mg^{2+} display a large range from 0.028 in hyaline benthic species (Toyofuku et al., 2000) to 0.0006 in planktonic species (Nürenberg et al., 1996). Toyofuku et al. (2000) determined that salinity does not influence D_{Mg} so the variability among species is most likely caused by biomineralization effects on the incorporation of Mg into foraminiferal calcite. On the other hand, Dueñas-Bohórquez et al. (2011) determined that alteration of Ca^{2+} concentrations changes the calcite saturation state which, in turn, affects the incorporation of Mg in two species of shallow benthic Foraminifera.

SALINITY AND PH EFFECTS

A weak positive relationship between planktonic foraminiferal Mg/Ca and seawater salinity was determined (Lea et al., 1999; Nürnberg et al., 1996), whereas Mg/Ca showed an inverse dependence on pH (Lea et al., 1999; Russell et al., 2004). A 7±4% change in Mg/Ca per salinity unit (SU) was determined for *G. sacculifer* and *O. universa* translating to an uncertainty of ~0.3–1°C (Lea, 2003). In both species, Mg/Ca ratios decrease by about 7±6% per 0.1 ppm pH, reflecting a change of 0– -1.2 °C per pH unit (Russell et al., 2004). Arbuszewski et al. (2010) also attributed salinity to be the cause of the ~1–2 mmol/mol difference in Mg/Ca ratios from equatorial foraminiferal samples compared with those from more saline subtropical gyres. However, excess Mg/Ca in the subtropical gyres may skew estimates by several degrees C, as laboratory culture experiments observed salinity effects that were an order of magnitude smaller than those suggested by

Arbuszewski et al. (Lea et al., 1999; Russel et al., 2004; Kisakurek et al., 2008; Dueñas-Bohórquez et al., 2009).

DISSOLUTION EFFECTS

Core-top studies along bathymetric transects show a decrease in Mg/Ca ratios of planktonic foraminifera with increasing depth, independent of the overlying sea-surface temperatures, thereby suggesting that foraminiferal Mg/Ca is altered by partial dissolution after deposition on the seafloor, driven by the decrease in carbonate saturation levels with increasing depth (Dekens et al., 2002; Rosenthal et al., 2000). Mg-rich calcite that forms in warmer surface waters is more susceptible to dissolution (Brown and Elderfield, 1996). Therefore, the shell's bulk Mg/Ca is shifted toward the composition acquired in colder waters below the thermocline (Rosenthal et al., 2000). Dissolution effects on Mg/Ca concentration are more prevalent in deep-dwelling species than in shallow dwelling species, since deep-dwelling species calcify over a larger range of temperatures (Brown and Elderfield, 1996; Dekens et al., 2002).

Besides temperature, dissolution is the main cause of Mg/Ca variability. Various approaches have been offered to correct for dissolution effects on Mg/Ca, including adding an ocean-depth correction to calibration equations (Lea et al., 2000; Dekens et al., 2002). The applied dissolution correction suggests a potential error of 0.5°C in estimates for recent Atlantic sediments that are deeper than 2.8 km and Pacific sediments >1.6 km but must be adjusted for times when the lysocline depth differed from modern conditions (i.e. glacials; Dekens et al., 2002). In

addition, this approach does not quantify the dissolution effects on specific samples, which might respond more to changes in pore-water chemistry than shifts in lysocline depth.

To address dissolution effects on specific samples, Rosenthal and Lohmann (2002) suggested that the relationship between shell weight and the decrease in Mg/Ca could be used. Further studies demonstrated that the shell size-weight relationship depends on the carbonate content of seawater in which they grow and not just dissolution (Barker and Elderfield, 2002), so the initial shell weight would have to be known in order to correct Mg/Ca ratios for dissolution effects. Recent studies of calcite dissolution in planktic Foraminifera suggest a percent loss of Mg in individuals rather than a molar loss of Mg in individuals or a loss of the highest-Mg individuals from a population (Rongstad et al., 2017).

Diagenetic alteration is also a concern in the use of Mg/Ca as a temperature proxy. Foraminiferal shells may be altered in the water column and at and within bottom sediments even at depths above the lysocline (Berger et al., 1982). $MgCO_3$ is more soluble than $CaCO_3$, resulting in the dissolution of Mg and lower Mg/Ca ratios (Dekens et al., 2002). Mg/Ca in benthic foraminifers appears to be more resistant to partial dissolution (Elderfield et al., 2006).

SUMMARY OF SR/CA PALEOTHERMOMETRY IN CORALS

Sr/Ca in hermatypic coral skeletons has been shown to be highly correlated with monthly or seasonal variations in water temperature (Beck et al., 1992, Alibert

and McCulloch, 1997; Linsley et al., 2000; Linsley et al., 2004; Marshall and McCulloch, 2002). More Sr is incorporated into the coral skeleton at lower temperatures than at higher temperatures. The relationship between Sr/Ca and temperature is:

$$(Sr/Ca)coral\ (mmol\ mol^{-1}) = B + A(SST) \quad (4)$$

where SST is given in °C, and the slope A= 0.062 mmol mol^{-1} per °C (Beck et al., 1992). Similar to foraminiferal Mg/Ca paleothermometry, using Sr/Ca in corals to reconstruct temperature also has constraints that can limit the use of this proxy. Similar to dissolution effects in Foraminifera, coral Sr/Ca ratios are highly susceptible to diagenesis (Cohen and Hart, 2004; Allison 2005). Even moderately altered sections of the same fossil coral can show Sr/Ca estimates that are 0.6 mmol too high, roughly equivalent to -6 °C SST (Sayani et al., 2021). A variety of imaging tools (i.e., x-ray diffraction, scanning electron microscopy) are used to screen corals for diagenetic alteration, which is effective in heavily altered corals. Yet light to moderately altered corals can escape detection. Including even 1% of altered powders can introduce differences of 1–2 °C in temperature reconstructions (Allison et al., 2007; Sayani et al., 2011). In addition, pH and dissolved inorganic carbon have shown contrasting effects on skeletal Sr/Ca depending on the coral species (Cohen, et al., 2009; Gagnon et al., 2013).

The incorporation of Sr (along with other trace elements) in the aragonite coral skeleton is influenced by physiological processes (Cardinal et al., 2001; Cohen et al., 2006; Gagnon et al., 2013; Kuffner et al., 2012). Yet the

understanding of biological mechanisms whereby corals form their skeleton and how they incorporate materials into that skeleton as a function of the concentrations in the surrounding seawater is still somewhat limited. Therefore, Sr/Ca concentrations can differ within and among species requiring the need for species-specific and site-specific calibrations that relate Sr/Ca concentrations to temperature (Rosenthal and Lindsay, 2006). For example, the sensitivity of coral Sr/Ca to SST varies among *Porites* spp. colonies, both within and across different sites. Differences in Sr/Ca-SST calibrations for *Porites* spp. corals growing at different sites are well documented (e.g., Alibert & McCulloch, 1997), and published Sr/Ca-SST slopes ranging from −0.04 to −0.12 mmol mol^{-1} $°C^{-1}$, with an average of −0.06 mmol mol^{-1} $°C^{-1}$ (Corrège, 2006; Sinclair, 2015). Some of the observed spread may be a result of differences in methodology, (Corrège, 2006; Hathorne et al., 2013; DeLong et al., 2013), yet studies examining contemporaneous corals from the same site also have reported a similar range of Sr/Ca-SST slopes (−0.03 to 0.09 mmol mol^{-1} $°C^{-1}$; Alibert & McCulloch, 1997; Alpert et al., 2016; DeCarlo et al., 2016). Without a site-specific calibration, only relative changes in SST can be accurately constructed (+/- 0.5°C; Marshall and McCulloch, 2002). These calibrations, however, are sometimes based on annual cycles to infer interannual or longer-term variations (Rosenthal and Lindsay, 2006; Sayani et al., 2019).

Paired measurements of coral Sr/Ca and coral $\delta^{18}O$ allow for the quantification of both SST and salinity variations in the past (e.g., Ren et al., 2002;

Cahyarini et al., 2008). This paired approach allows for a more complete understanding of natural versus anthropogenic temperature and/or hydrological changes across the tropics (Felis et al., 2009; Nurhati et al., 2009; Hetzinger et al., 2010; Nurhati et al., 2011; Carilli et al., 2014; Toth et al., 2015a). Nonetheless, the use of paired coral Sr/Ca and $\delta^{18}O$ are subject to the same challenges listed above. For example, numerous studies on *Porites* spp. show intercolony offsets in Sr/Ca and $\delta^{18}O$ that cannot be attributed to small-scale environmental variability (Cobb et al., 2003; Felis et al., 2003; Stephans et al., 2004; Linsley et al., 2008; Dassié et al., 2014) These offsets can be as large as 0.14 mmol/mol for Sr/Ca and up to 0.4‰ for $\delta^{18}O$, equivalent to ~2°C. It is unclear whether these intercolony offsets differ from site to site or, as stated above, represent differences in biomineralization of elements during calcification.

METHODS

To test whether temperature variability changed over time within the Gulf of Panamá and the Gulf of Chiriquí, foraminiferal tests from existing cores were processed to develop temperature reconstructions based on Mg/Ca ratios using Inductively Coupled Plasma-Optical Emission spectroscopy (ICP-OES). The high-Mg calcite tests of *Sorites marginalis*, a symbiont-bearing species, were picked from cores from Contadora and Saboga in the Gulf of Panamá and Canales de Tierra in the Gulf of Chiriquí. All the 5-cm intervals within the hiatus in reef growth were sampled from each core, as well as intermittent intervals from before

and after the hiatus. A total of 24 intervals were sampled from within the Contadora core, 18 intervals from Saboga, and 20 intervals from Canales. Around 10–20 individuals in good taphonomic condition were picked from each interval, which were analyzed to compare the variability of Mg/Ca ratios within and between the three cores. The methods for sample preparation described in Chapter 2 were used for the core samples: sonication, oxidation, and leaching (Barker et al., 2003). Bayesian change-point (BCP) analysis was used to estimate the locations where Mg/Ca changed over time. The full list of Mg/Ca results are recorded in Appendix C, with the samples that had Ca concentrations less than 10 ppm highlighted in red to indicate those samples that fell below QA/QC requirements.

RESULTS

As depicted in Figure 4.1, Mg/Ca concentrations changed dramatically in Contadora during the hiatus compared with those in Saboga and Canales de Tierra. In fact, the variability of the Mg/Ca results in Contadora were so unexpected that new samples were collected, and a second analysis was performed (Contadora Round 2, Fig. 4.1). The second round of analyses showed similar results, with dramatic increases in Mg/Ca during the hiatus in reef growth. At a constant temperature of 25°C, Mg/Ca ranges 144±1 mmol/mol. Slight increases or decreases around this ratio are expected with varying temperatures, as is seen in Saboga and Canales, yet temperature variations alone cannot explain the anomalously high/low ratios seen in Contadora.

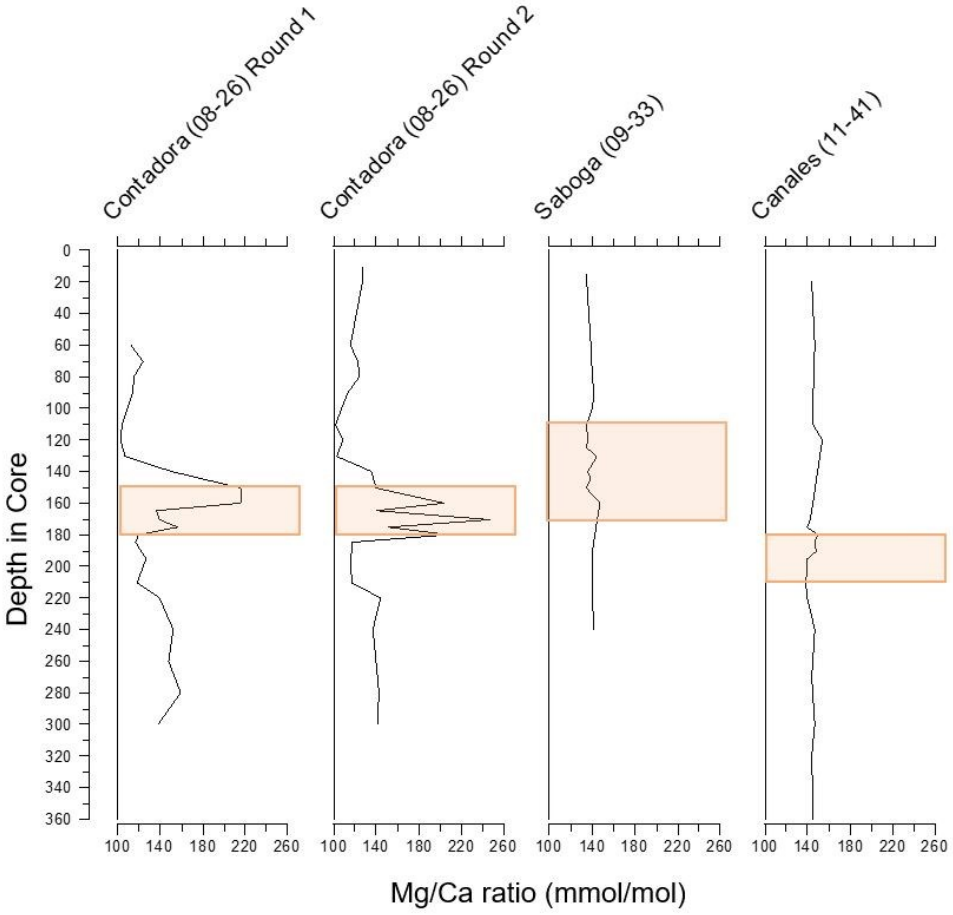

Figure 4.1 Mg/Ca ratios from all three cores. Contadora Round 1 and Round 2 represent the two rounds of samples that were analyzed. Shaded areas represent the hiatus in reef growth. The same scale is used for each axis to emphasize the high variability in Contadora. Shading represents the period of the hiatus for each core.

The linear relationship between Mg/Ca and temperature developed for *Operculina ammonoides* (Evans et al., 2015; Chapter 2, Equation 2) was used to estimate temporal variability in temperature within each core. The temperature reconstructions for the Contadora core are shown in Figure 4.2 (based on the second round of samples analyzed); however, these temperatures are not realistic and suggest that the Mg/Ca ratios are influenced by other factors in Contadora.

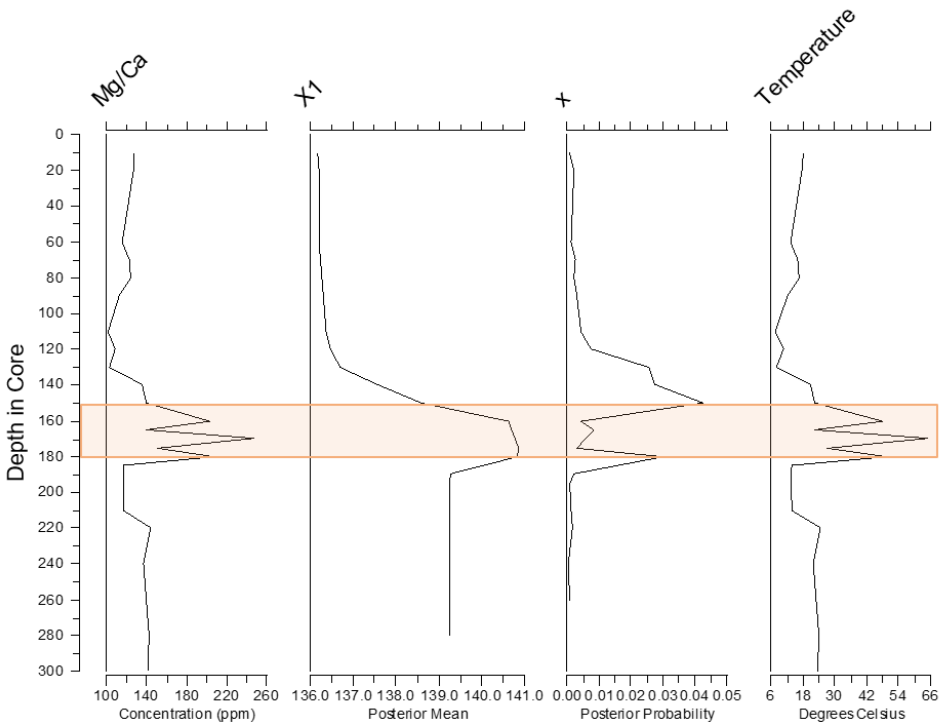

Figure 4.2 Mg/Ca ratios, posterior mean and probability from Bayesian change point analysis, and temperature reconstructions from the Contadora core. X1 and x represent the posterior mean and posterior probabilities, respectively.

As shown in Figure 4.2, Mg/Ca ratios at Contadora increased leading up to the hiatus in reef growth and fluctuated within the hiatus before decreasing at the termination of the hiatus in reef growth. The temperature reconstructions based on the linear equation from *Operculina ammonoides* shows temperature ranging from 8–64°C, which is not realistic. Therefore, I used the posterior means from the BCP analysis instead of the measured Mg/Ca to calculate a more reasonable temperature reconstruction ranging from 21.4–23.3°C (Fig. 4.3). The Mg/Ca analysis shows a likely increase in temperature leading up to the hiatus in reef growth at Contadora,

yet the probability calculated by BCP analysis does not suggest a significant change in Mg/Ca.

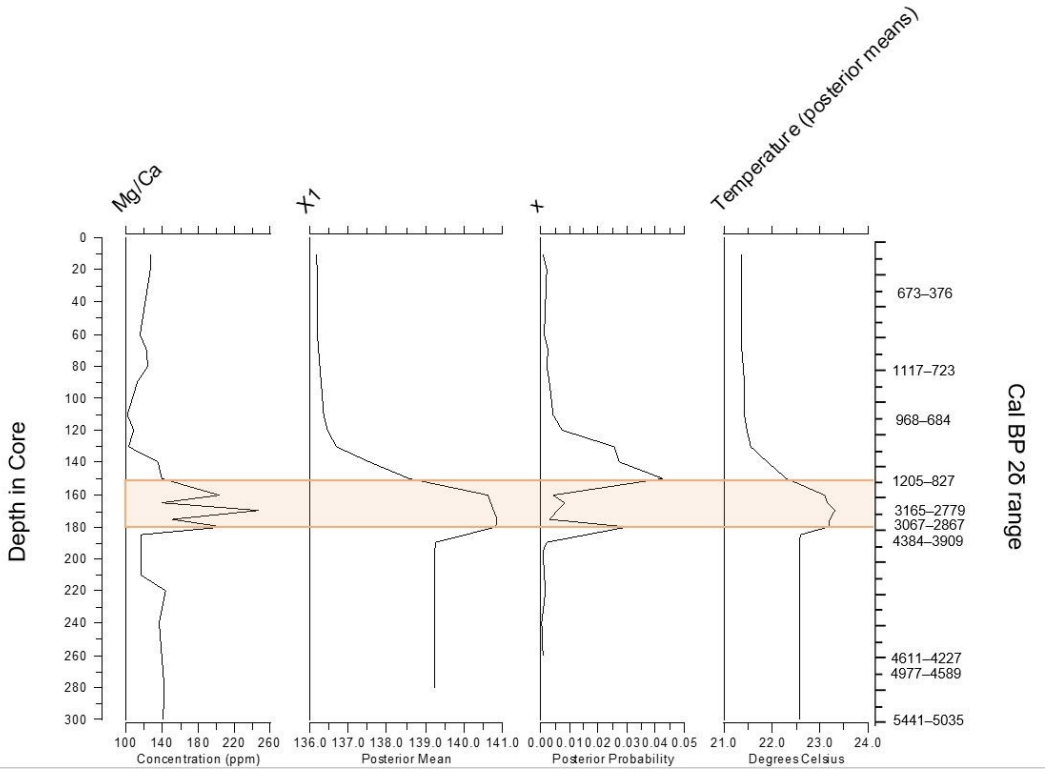

Figure 4.3 Mg/Ca ratios, posterior mean and probability from Bayesian change point analysis, and temperature reconstructions based on the posterior means from the Contadora core.

When compared with the high variability seen at Contadora, the Mg/Ca ratios at Saboga seem relatively stable through time (Fig. 4.1). The difference of scale for Mg/Ca concentration in Figure 4.4 compared with Figure 4.1 better shows the changes that occurred at Saboga. There is greater variability within the hiatus period at Saboga, with temperature increasing up to the inception of the hiatus to a maximum of 25.8°C and then dropping to 21.7°C at the 160–165 cm interval. Another, change occurs during the hiatus ~130 cm with the increase in temperature

from ~21°C to ~25°C before dropping back down to ~21°C. As with Contadora, the variability in Mg/Ca and temperature is greater during the hiatus in reef growth. However, it is important to note that the changes in Mg/Ca (and therefore temperature) are not significant according to BCP analysis with all probabilities being <0.015.

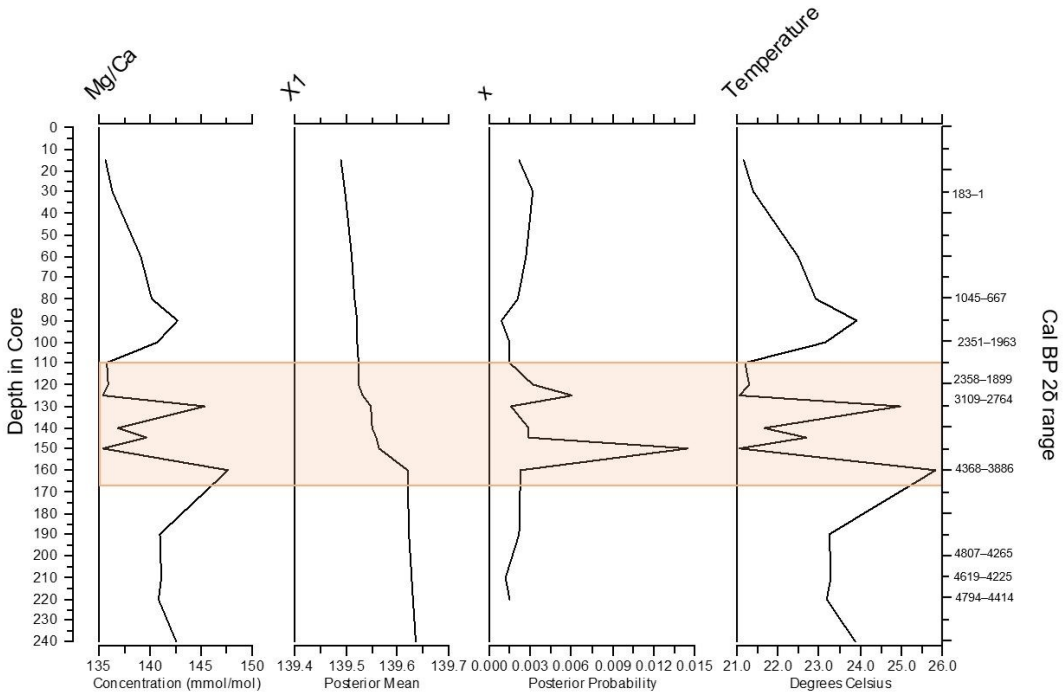

Figure 4.4 Mg/Ca ratios, posterior mean and probability from Bayesian change point analysis, and temperature reconstructions from the Saboga core.

The Mg/Ca results from Canales de Tierra are similar to those of Saboga, showing relatively stable ratios through time with some variability during the period of the hiatus in reef growth (Fig. 4.5). At the inception of the hiatus in reef growth, temperatures drop from ~25°C to 22°C between 220–210 cm before increasing again to ~27°C between 180–190 cm. There is a subsequent decrease in temperature at the end of the hiatus to ~22°C and then an increase to ~28°C at the

120–125 cm interval, which is associated with 1524–1226 cal BP. Again, the probability calculated by BCP analysis does not show a significant change in Mg/Ca as the probability of a change occurring at any point is <0.008.

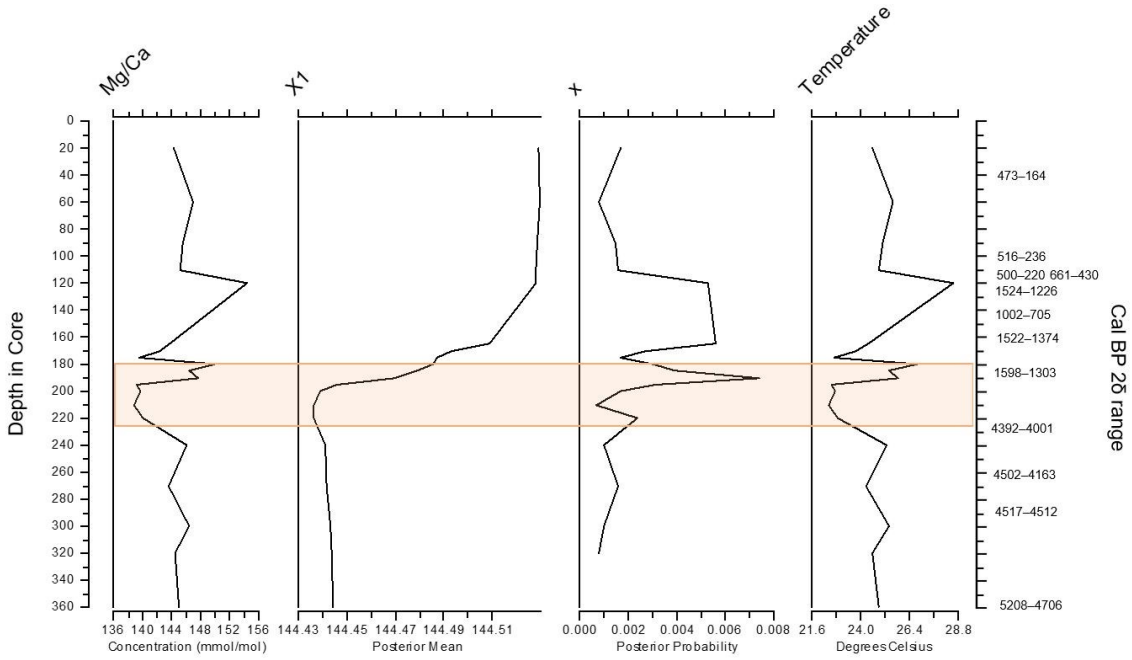

Figure 4.5 Mg/Ca ratios, posterior mean and probability from Bayesian change point analysis and temperature reconstructions from the Canales de Tierra core**.**

The linear relationship between temperature and Mg/Ca for *Operculina ammonoides* (Evans et al., 2015) seems to hold up for downcore temperature reconstructions using *Sorites marginalis*, at least for samples from Saboga and Canales de Tierra. The mean temperatures calculated for the Canales de Tierra core are higher than those calculated for Saboga and relate to the modern *in situ* temperatures reported in Chapter 2. In the temperature reconstructions for Saboga, temperatures ranged from ~21–26 °C, which is similar to the recorded minimum mean temperatures and mean annual temperatures measured in the Gulf of Panamá of 21.6 ± 1.8 SE and 26.9 °C ± 0.38, respectively. The *in situ* temperatures

measured in the Gulf of Chiriquí were higher than the reconstructed temperatures from the Canales core. *In situ* temperatures ranged from 27.5 °C–30.4 °C with a mean annual average of 28.8 °C ± 0.08 SE compared with a range of 22.4 °C–28.5 °C and a mean of ~24.6°C C ± 1.22 SE calculated from the temperature reconstruction. The higher *in situ* temperatures recorded in the Gulf of Chiriquí compared with lower temperatures reconstructed from downcore samples could indicate increased contemporary warming due to climate change.

DISCUSSION

Foraminiferal Mg/Ca ratios have proven to be a useful proxy of temperature (e.g., Lea et al., 2000; Billups and Schrag, 2002, 2003; Lear et al., 2003; Martin et al., 2002; Marchitto and deMenocal, 2003; Skinner et al., 2003) and seem to provide realistic temperature reconstructions from two cores analyzed in this study using the Mg/Ca-temperature relationship for *Operculina ammonoides*. However, the Mg/Ca ratios from Contadora are highly variable, especially during the hiatus, and are apparently influenced by other variables besides temperature. Geochemical reconstructions show higher variability in Mg/Ca during the hiatus within all three cores. However, Mg/Ca ratios from the foraminiferal samples did not show significant differences through time based on BCP analysis.

The high variability in Mg/Ca in the Contadora samples is cannot be solely a result of temperature, as the calculated temperatures would not be realistic for that site. As described above, other environmental variables can offset Mg-

incorporation, for example, salinity and carbonate chemistry, dissolution effects, or even light availability (Lea et al., 1999; Dueñas-Bohórquez et al., 2011; Hönish et al., 2013; Geerken et al., 2018). However, those environmental variables are expected to be similar in Saboga due to the proximity (<3 km) of the two reefs. The availability of light could affect Mg/Ca ratios, as a 23 mmol/mol difference in Mg/Ca was observed between carbonate formed entirely in the dark versus. completely in the light in large benthic, symbiont-bearing Foraminifera (Dämmer et al., 2019). Yet even if high turbidity led to lower light levels in Contadora, the light reduction would not have been comparable to the latter study and could not explain the ~130 mmol/mol increase during the hiatus. The fact that analyses of two different rounds of samples presented higher-than-expected Mg/Ca ratios during the hiatus at Contadora shows that there is most likely a local influence on Mg/Ca concentrations. This local influence could be the reason why a discrete hiatus was seen in Contadora and not in Saboga.

Geochemical analysis of another Contadora core completed by Toth et al. (2012) showed highly variable, but realistic ranges of Sr/Ca-based temperatures during the Holocene, even when the reef was accreting. This pattern is not directly shown based on Mg/Ca records of foraminiferal tests. In fact, BCP analysis shows relatively stable Mg/Ca ratios outside of the hiatus within all cores, with the highest variability occurring at Contadora. Mg/Ca-based temperature reconstructions before the hiatus were stable, consistent with published reconstructions of ENSO that show a Holocene minimum in variance from ~4 to 5 cal BP (Kouvatas and

Joanides, 2012; Cobb et al., 2013; Carré et al., 2014; Emile-Geay et al., 2016). These same reconstructions, however, show large variations in ENSO variance before ~6 ka and after ~4 ka.

The first change-points for Mg/Ca from samples within each core occur ~4300–3900 cal BP, depicting an increase in temperature of ~2°C in Saboga and Contadora and a decrease in temperature of ~3°C in Canales de Tierra. However, the probability of a change occurring at that interval within each of these cores is <1%. The increased temperature recorded in the Gulf of Panamá could reflect the stronger El Niño events after 4 ka (Rein, 2007; Carré, 2014). The initial increase in temperature at Saboga, followed by a sharp decline to ~21°C within the 150–155 cm interval occurring between ~4300 and ~2700 cal BP, could represent the postulated increased La Niña activity between 3800 and 3200 cal BP (Conroy et al., 2008). Mg/Ca-based temperature reconstructions in Contadora begin to decrease ~3067–2867 cal BP before decreasing to a stable mean temperature around ~21.4 °C. The first (though non-significant) change-point at Canales de Tierra occurred within the 190–195 cm interval, representing a temperature range of ~6°C around ~1598–1303 cal BP.

Numerous models of ENSO variability have been published based on a variety of reconstructions of Holocene paleoclimate. Yet predicting the long-term behavior of ENSO with ongoing climate change has been difficult, leading to conflicting evidence on the external forcing of ENSO (Clement, 2010; Cobb et al., 2013; Carré et al., 2014; Emile-Geay et al., 2016). More recent studies using paired

measurements of $\delta^{18}O$ and Mg/Ca in foraminiferal shells to account for salinity and temperature differences show promise, yet the same challenges presented above are prevalent. A recently developed model, *Foraminifera as Modelled Entities* (FAME), takes into account the potential modulation of $\delta^{18}O_{calcite}$ and the temperature recorded in the calcite by planktonic foraminiferal growth (an estimate of the proxy Mg/Ca) to determine if these parameters directly record the ENSO cycle (Roche et al., 2017). Using this model, Metcalfe et al. (2019) showed that foraminiferal-based proxies offer sufficient spatiotemporal continuity allowing for the reconstruction of past changes of ENSO for a large part of the Pacific Ocean, but that slow sedimentation rates and proximity to the calcite compensation depth reduce the available area for reconstructions.

The data presented here show that there was likely increased climatic variability associated with the hiatus and a potential local effect at Contadora. Few studies have investigated whether shallow benthic Foraminifera can reconstruct long-term variability in ENSO. Future studies using paired measurements of $\delta^{18}O$ and Mg/Ca could potentially provide deeper insight into ENSO effects on the hiatus in the ETP as well as local influences on foraminiferal-calcite Mg/Ca.

Chapter 5: Synthesis

How marginal reef systems responded to past climatic variability provides clues to their prospects for persisting through contemporary climate change. Reefs along the Pacific coast of Panamá experience a natural gradient of nutrients, pH, and temperature because of stronger seasonal upwelling in the Gulf of Panamá than in the Gulf of Chiriquí. These reefs are also strongly affected by climatic variability due to the El Niño–Southern Oscillation (ENSO). Increased ENSO variability at the beginning of the Late Holocene is thought to have caused a 2500-year hiatus in reef-building in Pacific Panamá (Toth, 2012). However, the environmental conditions that drove the shutdown were inferred from the geochemistry of a limited number of coral samples. Foraminifera are useful indicators of reef-ecosystem condition because they are abundant in reef settings, secrete calcium carbonate and can host symbionts, respond rapidly to environmental variation, and persist in the absence of corals. By examining benthic Foraminifera in modern (Chapter 2) and fossil sediments (Chapter 3 and 4) collected from the Gulf of Panamá and the Gulf of Chiriquí, regional oceanography and climatic drivers were determined to influence foraminiferal assemblage changes that were contemporaneous with shifts in coral growth.

ANALYSIS OF CONTEMPORARY FORAMINIFERAL ASSEMBLAGES

Contemporary foraminiferal samples from both gulfs were dominated by heterotrophic Foraminifera, which was likely the result of overall nutrient enrichment due to upwelling, even in the weakly upwelling Gulf of Chiriquí. However, the Gulf of Chiriquí had higher abundances of symbiont-bearing taxa than the Gulf of Panamá. Temperature loggers deployed from 2016 to 2019 showed that water temperatures were lower on average (26.9 °C ± 0.38 SE) and more variable (22 °C–29 °C) in the Gulf of Panamá than in the Gulf of Chiriquí (average 28.9 °C ± 0.08; range 28 °C–30°C) due to stronger seasonal upwelling. Geochemical analysis of contemporary, symbiont-bearing miliolids, *Sorites marginalis*, revealed that foraminiferal Mg/Ca ratios were lower in the Gulf of Panamá (131.9 mmol/mol ± 2.10 SE) than in the Gulf of Chiriquí (145.2 ± 2.30 SE), consistent with the lower mean annual temperature observed in the Gulf of Panamá.

Whereas heterotrophic dominance reflects nutrient enrichment caused by upwelling in both gulfs, the lower densities of miliolids in the Gulf of Panamá could be a result of depressed pH due to stronger upwelling compared with the Gulf of Chiriquí. Lower pH results in an increased cost of calcification for miliolids, as their shells contain high-Mg calcite that is subject to dissolution (Bentov and Eres, 2006; Knorr, 2015). Miliolids contributed ~26% of the mean foraminiferal density in the Gulf of Panamá, compared with 48% in the Gulf of Chiriquí, potentially due to the increased cost of calcification (Bentov & Erez,

2006). Overall, the composition of contemporary foraminiferal assemblages and their geochemistry reflect regional oceanography in the eastern tropical Pacific.

ANALYSIS OF FORAMINIFERAL ASSEMBLAGES ASSOCIATED WITH THE HIATUS IN REEF GROWTH

Increased variability of the El Niño–Southern Oscillation (ENSO) beginning around ~4.2 ka was proposed to have led to a shutdown in coral growth for ~2500 years (Toth, 2012; Toth et al., 2015a, 2015b). Updated analyses of radiocarbon dates from coral and foraminiferal samples were used to create Bayesian age models that showed all sites exhibited a hiatus in *Pocillopora* growth between 4000–4250 cal BP but terminated at different times. Contadora experienced the longest hiatus, lasting ~3000 years, with the second being Canales, lasting ~2700 years. Saboga exhibited intermittent reef growth, evidenced by radiocarbon dates of *Pocillopora* in poor taphonomic condition during the hiatus. Although a discrete hiatus was not seen at Saboga, reef development was effectively shut down for 2000 years. Toth (2013) reviewed concurrent hiatuses at other reefs in the Pacific, surmising that climatic changes, rather than local or regional influences, had widespread effects that led to the shutdown of reef growth.

By adding foraminiferal samples to the age models, a possible second hiatus was observed at Contadora and Saboga around 2600 cal BP and 2100 cal BP, respectively. A second hiatus could be possible for Canales, but additional samples would have to be dated to detect it, if it occurred. This second hiatus could be associated with the decline in the variability of the mean position of the

Intertropical Convergence Zone ~2500 cal BP (Haug et al., 2001; Sachs et al., 2018). A more northerly ITCZ have decreased ENSO variability but enhanced eastern-Pacific upwelling and produced cooler sea temperatures in the ETP. That would have inhibited the production of the symbiont-bearing *Sorites marginalis* which were dated in this study.

Shifts in the structure of foraminiferal assemblages during the hiatus in reef growth suggest that foraminifers respond not only to oceanographic effects but also to climatic variations. Core logs from each site showed increases in the ratio of heterotrophic to symbiotic Foraminifera associated with the hiatus in reef growth. These shifts in foraminiferal assemblage did not predict the hiatus in reef growth, but instead occurred within the period of the hiatus at all sites. The peak in the heterotroph-to-symbiont-bearing foraminiferal ratio within the Gulf of Panamá occurred ~3100–2700 cal BP, concurrent with the inferred peak of El Niño strength ~2800 cal BP (Rein 2005; Tudhope 2001). It is surprising that the peak in the heterotroph ratio is seen during the previously predicted peak in El Niño strength, when productivity and, therefore, food sources were low; however, the ratio declined drastically leading up to the termination of the hiatus suggesting that densities were influenced by the heightened El Niño.

The decrease in miliolids within the Gulf of Panamá was evident prior to the inception of the hiatus ~4300 cal BP. This decline could have been associated with the change to a La Niña-like state, which would have caused increased upwelling leading to dampened pH and low light levels. In addition, all of the

symbiont-bearing foraminifers found at these sites were miliolids and would be affected by the low-light conditions caused by increased turbidity from La Niña. Interestingly, there are no significant changes in foraminiferal composition in the Gulf of Chiriquí within the period of the hiatus, which could suggest that foraminiferal abundances can rebound more quickly than corals. The peak in the heterotroph ratio occurred closer to the termination of the hiatus ~1600–1300 cal BP, and the decrease in the density of miliolids at the inception of the hiatus was not significant.

GEOCHEMICAL ANALYSIS OF HOLOCENE CLIMATE

Attempts to reconstruct temperature using Mg/Ca proxies from foraminiferal shells proved difficult in this study. Mg/Ca ratios from samples in Saboga and Canales de Tierra aligned with expected concentrations (~138–145 mmol/mol) and translated to realistic temperatures for Pacific Panamá (~21–29 °C). Based on Mg/Ca analyses, there was an increase in temperature of ~2°C in Saboga and a decrease in temperature of ~3°C in Canales de Tierra around ~4300–3900 cal BP, yet the changes were not significant according to Bayesian change-point analysis. Both sites showed a pattern of decreasing temperature following the initiation of the hiatus ~4300–3900 cal BP. The initial increase in Mg/Ca (and therefore temperature) at Saboga was followed by a decrease in Mg/Ca, which could reflect a switch to a La Niña-like state.

Further confounding the Mg/Ca-temperature reconstructions were the geochemical results from Contadora, where Mg/Ca concentrations ranged from 101–247 mmol/mol. This would translate to an unrealistic range of 8–64°C. The signal is not thought to be erroneous, as the same pattern was shown in two rounds of analyses. However, the absolute temperatures calculated from these Mg/Ca concentrations are problematic. Therefore, some local effect(s) most likely led to the increase in Mg/Ca concentrations during the hiatus. Low light has been shown to increase Mg/Ca concentrations in foraminiferal shells (Dämmer et al., 2019), as has higher Mg/Ca ratios of the ambient seawater (Segev and Erez, 2006). However, even these factors would only explain up to a 23 mmol/mol increase in Mg/Ca, whereas this study found a difference of ~145 mmol/mol between the lowest and highest measured concentrations. A local effect on Mg/Ca concentrations in Contadora could suggest a reason why a discrete hiatus was seen at Contadora, whereas the reef at Saboga experienced intermittent growth. The pattern of increased Mg/Ca concentrations during the hiatus shown in this study suggests changes in ocean conditions. This observation could be strengthened by future studies using simultaneous measurements of $\delta^{18}O$, Sr/Ca and Mg/Ca, which, by making it possible to parse out the effects of temperature and salinity, and would provide deeper insight into ENSO effects on the hiatus in the ETP, as well as local influences on foraminiferal-calcite Mg/Ca.

CONCLUDING REMARKS

In Pacific Panamá, oceanographic and climatic variability affected foraminiferal composition during the Holocene. Persistent, strong seasonal upwelling in the Gulf of Panamá and weaker upwelling in the Gulf of Chiriquí explain the dominance of heterotrophs seen at all times in the core records. Symbiotic Foraminifera were significantly correlated with *Pocillopora* growth and increases in the ratio of heterotrophic to symbiotic Foraminifera coincided with the initiation of the ~2500 year hiatus in reef growth beginning 4000–4250 cal BP. Evidence from corals and Foraminifera from these cores suggests that climatic variability related to ENSO led to the hiatus and continued to suppress reef growth within the Gulf of Panamá and the Gulf of Chiriquí. Although geochemical reconstructions of climate were apparently confounded by other environmental variables in this study, the results suggest that local effects can influence widely used geochemical proxies. Enhanced dominance of heterotrophic rotaliids, due to the potential bleaching of symbiotic miliolids, combined with a potential shutdown of reefs similar to the historical hiatus are predicted for the current trajectory of climate change. As climate change is predicted to increase the frequency of extreme ENSO events (Cai et al., 2014, 2018), and ocean acidification will increase with increased anthropogenic emissions of CO_2, it is likely reefs of the ETP and their foraminiferal assemblages will shift increasingly toward a heterotrophic state.

References

Ahmed, M., Magnayon-Umali, G., Kieok Chong, C., Franz Rull, M., Garcia, M. 2007. Valuing recreational and conservation benefits of coral reefs. The case of Bolinao, Philippines. *Ocean and Coastal Management* 50: 103–118.

Alexander, M.A., Seo, H., Xie, S.P,, and Scott, J.D. 2012. ENSO's impact on the gap wind regions of the eastern tropical Pacific Ocean. *Journal of Climate* 25: 3549–3565.

Alibert, C. and McCulloch, M.T., 1997. Strontium/Calcium ratios in modern Porites corals from the Great Barrier Reef as a proxy for sea surface temperature: Calibration of the thermometer and monitoring of ENSO. *Paleoceanography* 12: 345-363.

Allison, N., Finch, A.A., Webster, J.M., Clague, D.A. 2005. Palaeoenvironmental records from fossil corals: the effects of submarine diagenesis on temperature and climate estimates. *Geochimica et Cosmochimica Acta*. 71: 4693–4703.

Al-Horani, F.A., Al-Moghrabi, S.M., De Beer, D. 2003. The mechanism of calcification and its relation to photosynthesis and respiration in the scleractinian coral *Galaxea fascicularis*. *Marine Biology* 142: 419–426.

Allmon, W. D., Rosenberg, G., Portell, R. W., and Schindler, K. S. 1993 Diversity of Atlantic Coastal Plain mollusks since the Pliocene. *Science* 260: 1626–1629.

Altenbach, A. V and Sarnthein, M. (1989). Productivity record in benthic Foraminifera, in Berger, W. H., Smetacek, V. S., and Wefer, G. (eds.), Productivity of the Ocean: Present and Past. John Wiley and Sons Ltd., New York, 255–269.

Alve, E. 1995. Benthic Foraminiferal responses to estuarine pollution: a review. *Journal of Foraminiferal Research* 25: 190–203.

Andersson, J.E.C. 2007. The recreational cost of coral bleaching. A stated and revealed preference study of international tourists. *Ecological Economics* 62: 704–715.

Arbuszewski, J., deMenocal., P., Kaplan, A., Farmer, E.C. 2010. On the fidelity of shell derived $\delta^{18}O$ seawater estimates. *Earth and Planetary Science Letters* 300: 185–196.

Baker, A. C., Glynn, P. W., Riegl, B. 2008. *Climate change and coral reef bleaching: An ecological assessment of long-term impacts, recovery trends and future outlook: Estuarine, Coastal and Shelf Science* 80: 435–447.

Barbosa, C.F., Prazeres, M.dF., Ferreira, B.P., Seoane, J.C.S. Foraminiferal assemblage and reef check census in coral reef health monitoring of East Brazilian Margin. 2009. *Marine Micropaleontology* 73: 62–69.

Barker, S., Greaves, M., and Elderfield, H. 2003. A study of cleaning procedures used for foraminiferal Mg/Ca paleothermometry: *Geochemistry, Geophysics, Geosystems* 4: 1–20.

Beck, W.J. et al., 1992. Sea-Surface temperature from coral skeletal strontium/calcium ratios. *Science* 257: 644-647.

Bentov, S., and Erez, J., 2006, Impact of biomineralization processes on the Mg content of foraminiferal shells: A biological perspective: *Geochemistry, Geophysics, Geosystems* 7: 1–11.

Berger, W.H., Bonneau, M.C. Parker, F.L. 1982. Foraminifera on the deep-sea floor: lysocline and dissolution rate. *Oceanologica Acta* 5: 249–258.

Billups, K., and Schrag, D. P., 2002, Paleotemperatures and ice volume for the past 27 Myr revisited with paired Mg/Ca and $^{18}O/^{16}O$ measurements on benthic foraminifera: *Paleoceanography* 17: 1–11.

Billups, K., and Schrag, D. P., 2003, Application of benthic foraminiferal Mg/Ca ratios to questions of Cenozoic climate change: *Earth Planetary Science Letters* 209: 181–195.

Birkeland, C. 1977. The importance of rate of biomass accumulation in early succession stages of benthic communities to the survival of coral recruits. *Proc. 3rd Int. Coral Reef Symp.* 16–21.

Birkeland, C. 1988. Geographic comparisons of coral-reef community processes. *Proc. 6th Coral Reef Symp.* 1–21.

Bouchet VMP, Alve E, Rygg B, and Telford RJ. 2012. Benthic Foraminifera provide a promising tool for ecological quality assessment of marine waters. *Ecological Indicators* 23: 66–75.

Bradshaw JS. 1957. Laboratory studies on the rate of growth of the foraminifer, *Streblus beccarii* (Linné) var *tepida* Cushman. *Journal of Paleontology* 31: 1138-1147.

Brown, S.J. and Elderfield, H. 1996. Variations in Mg/Ca and Sr/Ca ratios of planktonic foraminifera caused by postdepositional dissolution: Evidence of shallow Mg-dependent dissolution. *Paleoceanography* 11: 543-551.

Buzas M. A., and Culver, S. J. 1991. Species diversity and dispersal of benthic Foraminifera. *Bioscience* 41: 483–489.

Buzas M. A., and Culver, S. J., 1998. Assembly, disassembly, and balance in marine paleocommunities. *Palaios* 13: 263–275.

Cai, W., Borlace, S., Lengaigne, M., van Rensch, P., Collins, M., Vecchi, G., Timmermann, A., Santoso, A., McPhaden, M.J., Wu, L., England, M.H., Wang, G., Guilyardi, E., Jin, F. 2014. Increasing frequency of extreme El Niño events due to greenhouse warming. *Nature Climate Change* 4: 111–116.

Cai, W., Wang, G., Dewitte, B., Wu, L., Santoso, A., Takahashi, K., Yang, Y., Carréric, A., and McPhaden, M. J. 2018. Increased variability of eastern Pacific El Niño under greenhouse warming. *Nature* 564: 201–206.

Carballo, J. L., Cruz-Barraza, J. A., Vega, C., Nava, H., and Chávez-Fuentes, M. d. C. 2019. Sponge diversity in Eastern Tropical Pacific coral reefs: An interoceanic comparison. *Scientific Reports* 9: 1–15.

Cardinal, D., Hamelin, B., Bard., E., Patzold, J. 2001. Sr/Ca, U/Ca and δ^{18}O records in recent massive corals from Bermuda: relationships with sea surface temperature. *Chemical Geology* 176: 213–233.

Carpenter et al. 2008. One-third of reef-building corals face elevated extinction risk from climate change and local impacts. *Science* 321: 560–563.

Cesar, H.J.S., Burke, L., and Pet-Soede, L. 2003. The Economics of Worldwide Coral Reef Degradation. Cesar Environmental Economics Consulting, Arnhem, and WWF-Netherlands, Zeist, The Netherlands. p. 1–23.

Chambers, J. M., Freeny, A., and Heiberger, R. M., 1992, *Analysis of variance; designed experiments, in* Chambers, *J.* M. and Hastie, T. J. (eds.), *Statistical Models in S:* Wadsworth & Brooks/Cole, Pacific Grove, California, p. 145–193.

Chesher R. H. 1972. The status of knowledge of Panamanian echinoids, 1971, with comments on other echinoderms. *Bulletin of the Biological Society of Washington* 2: 139–158.

Cockey, E., Hallock, P., and Lidz, B. H. 1996. Decadal-scale changes in benthic foraminiferal assemblages off Key Largo, Florida. *Coral Reef* 15: 237–248.

Collins, L. S. 1999. The Miocene to recent diversity of Caribbean benthic foraminifera from the Central American isthmus, *in* Collins, L. S. and Coates, A. G. (eds.), A

Paleobiotic Survey of Caribbean Faunas from the Neogene of the Isthmus of Panama: Bulletins of American Paleontology, Ithaca, New York, p. 91–108.

Cohen, A.L., Ries, J.B., McCorkle, D.C. 2009. Marine calcifiers exhibit CO_2-induced ocean acidification. *Geology* 37: 1131–1134.

Cohen, A.L. and Hart, S.R. 2004. Deglacial sea surface temperatures of the western tropical Pacific: A new look at old coral. *Paleoceanography* 19.

Cortés, J. 1997. Biology and geology of eastern Pacific coral reefs: *Coral Reefs* 16: 539–546.

Cortés, J., Enochs, I. C., Sibaja-Cordero, J., Hernández, L., Alvarado, J. J., Breedy, O., Cruz-Barraza, J. A., Esquivel-Garrote, O., Fernández-García, C., Hermosillo, A., Kaiser, K. L., Medina-Rosas, P., Morales-Ramírez, A., Pacheco, C., and Pérez-Matus, A. 2017, Marine biodiversity of eastern tropical Pacific coral reefs, *in* Glynn, P. W., et al. (eds.), Coral Reefs of the Eastern Tropical Pacific: Persistence and Loss in a Dynamic Environment: Springer, Dordrecht, Netherlands, p. 203–250.

Cottey, T.L. and Hallock, P. 1988. Test surface degradation in *Archaias angulatus*. *Journal of Foraminiferal Research* 18: 187.

Crouch, R. W., and Poag, C. W. 1979. *Amphistegina gibbosa* d'Orbigny from the California Borderlands: The Caribbean connection. *Journal of Foraminiferal Research* 9: 85–105.

Cushman, J.A. and Waters, J.A. 1928. Upper Paleozoic Foraminifera from Sutton County, Texas. *Journal of Paleontology* 1: 358-371.

Dämmer, L.K., de Nooijer, L., van Sebille, E., Haak, J.G. and Reichart, G.J. 2020. Evaluation of oxygen isotopes and trace elements in planktonic foraminifera from the Mediterranean Sea as recorders of seawater oxygen isotopes and salinity. *Climate of the Past* 16: 2401-2414.

Davis, C.V., Fehrenbacher, J.S., Hill, T.M., Russell, A.D. and Spero, H.J. 2017. Relationships between temperature, pH, and crusting on Mg/Ca ratios in laboratory-grown Neogloboquadrina foraminifera. *Paleoceanography* 32: 1137-1152.

D'Croz, L., and O'Dea, A. 2007. Variability in upwelling along the Pacific shelf of Panamá and implications for the distribution of nutrients and chlorophyll: Estuarine, Coastal and Shelf *Science* 73: 325–340.

de Nooijer, L. J., van Dijk, I., Toyofuku, T., and Reichart, G. J. 2017. The impacts of seawater Mg/Ca and temperature on element incorporation in benthic foraminiferal calcite: *Geochemistry, Geophysics, Geosystems* 18: 3617–3630.

Dekens, P.S., Lea, D.W., Pak, D.K. and Spero, H.J. 2002. Core Top Calibration of Mg/Ca in Tropical Foraminifera: Refining Paleo-temperature Estimation. *Geochemistry, Geophysics, Geosystems* 3: 1–29.

Dimiza, M.D., Koukousioura, O., Triantaphyllou, M.V. and Dermitzakis, M.D. 2016. Live and dead benthic foraminiferal assemblages from coastal environments of the Aegean Sea (Greece): Distribution and diversity. *Revue de Micropaléontologie* 59: 19–32.

Dueñas-Bohórquez, A., da Rocha, R.E., Kuroyanagi, A., Bijma, J. and Reichart, G.J. 2009. Effect of salinity and seawater calcite saturation state on Mg and Sr incorporation in cultured planktonic foraminifera. *Marine Micropaleontology* 73: 178–189.

Dujardin, F. 1835. Observations mouvelles sur les Cephalopodes microscopiques. Ibid. 1: 312.

Eiler, J.M., 2011. Paleoclimate reconstruction using carbonate clumped isotope thermometry. *Quaternary Science Reviews* 30: 3575-3588.

Eggins, S., De Deckker, P. and Marshall, J. 2003. Mg/Ca variation in planktonic foraminifera tests: implications for reconstructing palaeo-seawater temperature and habitat migration. *Earth Planetary Science Letters* 212: 291-306.

Elderfield, H., and Ganssen, G., 2000, Past temperature and $\delta^{18}O$ of surface ocean waters inferred from foraminiferal Mg/Ca ratios: *Nature* 405: 442– 445.

Erez, J., 2003. The source of ions for biomineralization in foraminifera and their implications for paleoceanographic proxies. *Reviews in mineralogy and geochemistry* 54: 115-149.

Evans, D., Erez, J., Oron, S., and Müller, W. 2015. Mg/Ca-temperature and seawater-test chemistry relationships in the shallow-dwelling large benthic foraminifera *Operculina ammonoides*: *Geochimica et Cosmochimica Acta* 148: 325–342.

Falkowski, P.G., Dubinsky, Z., Muscatine, L. and McCloskey, L. 1993. Population control in symbiotic corals. *Bioscience* 43: 606-611.

Fajemila, O. T., Langer, M. R., and Lipps, J. H. 2015. Spatial patterns in the distribution, diversity and abundance of benthic Foraminifera around Moorea (Society Archipelago, French Polynesia): *PLoS ONE*, 10 (e0145752): 1–25.

Fiedler, P. C., 1992, Seasonal climatologies and variability of eastern tropical Pacific surface waters: NOAA/National Marine Fisheries Service Technical Report NMFS, v. 109, p. 1–65.

Fiedler, P. C., 2002, Environmental change in the eastern tropical Pacific Ocean: Review of ENSO and decadal variability: Marine Ecology Progress Series, v. 244, p. 265–283.

Fiedler, P. C. and Lavin, M. F., 2017, Oceanographic conditions of the eastern tropical Pacific, *in* Glynn, P. W., et al. (eds.), Coral Reefs of the Eastern Tropical Pacific: Persistence and Loss in a Dynamic Environment: Springer, Dordrecht, Netherlands, pp. 59–83.

Gagnon, A.C., Adkins, J.F. and Erez, J. 2012. Seawater transport during coral biomineralization. *Earth and Planetary Science Letters* 329: 150-161.

Glynn, P. W., 1972, Observations on the ecology of the Caribbean and Pacific coasts of Panamá, *in* Jones, M. L. (ed.), The Panamic Biota: Some Observations Prior to a Sea-level Canal. Bulletin of the Biological Society of Washington: 2, Washington, D.C, p. 13–30.

Glynn, P. W., 1984, *Widespread coral mortality and the 1982–83 El Nino warming events: Environmental Conservation* 11: 133–146.

Glynn, P. W., 2004, High complexity food webs in low-diversity eastern Pacific reef-coral communities: *Ecosystems* 7: 358–367.

Glynn, P. W., 2017, History of eastern Pacific coral reef research: *in* Glynn, P. W., et al. (eds.), Coral Reefs of the Eastern Tropical Pacific: Persistence and Loss in a Dynamic Environment: Springer, Dordrecht, Netherlands, p. 1–37.

Glynn, P. W. and Ault, J. S., 2000, A biogeographic analysis and review of the far eastern Pacific coral reef region: Coral Reefs 19: 1–23.

Glynn, P. W., and Maté, J. L., 1997, Field guide to the Pacific coral reefs of Panamá: 8th International Coral Reef Symposium 1: 145–166.

Glynn, P. W., Alvarado, J. J., Banks, S., Cortés, J., Feingold, J. S., Jiménez, C., Maragos, J. E., Martínez, P., Maté, J. L., Moanga, D. A., Navarrete, S., Reyes-Bonilla, H., Riegl, B., Rivera, F., Vargas-Ángel, B., Wieters, E. A., and Zapata, F. A., 2017, Eastern Pacific coral reef provinces, coral community structure and composition: an overview, *in* Glynn, P. W., et al. (eds.), Coral Reefs of the Eastern Tropical Pacific: Persistence and Loss in a Dynamic Environment: Springer, Dordrecht, Netherlands,, pp. 107–176.

Goldstein ST. 2002. Foraminifera: a biological review. In Sen Gupta, BK (ed.), Modern Foraminifera, 2nd edn. Boston: Kluwer, 37-55.

Goldstein ST and Barker WW. 1988. Test ultrastructure and taphonomy of the monothalamous agglutinated foraminifer Cribrothalammina n. gen. alba (Heron-Allen and Earland). *Journal of Foraminiferal Research* 18: 130-136.

Goldstein ST and Corliss BH. 1994. Deposit feeding in selected deep-sea and shallow-water benthic Foraminifera. *Deep Sea Research* 41: 229-241.

Gooday AJ. 2003. Benthic Foraminifera (Protista) as tools in deep-water palaeoceanography: environmental influences of faunal characteristics. *Advances in Marine Biology* 46: 1-90.

Grell KG. 1973. Protozoology. New York: Springer.

Groeneveld, J., Ho, S.L., Mackensen, A., Mohtadi, M. and Laepple, T. 2019. Deciphering the variability in Mg/Ca and stable oxygen isotopes of individual foraminifera. *Paleoceanography and Paleoclimatology* 34: 755-773.

Halfar, J., and Ingle, J. C. 2003. Modern warm-temperate and subtropical shallow-water benthic Foraminifera of the southern Gulf of California, Mexico: *Journal of Foraminiferal Research* 33: 309–329.

Hallock, P., 2000, Symbiont–bearing Foraminifera: Harbingers of global change?. *Micropaleontology*, 46: 95–104.

Hallock P. 2002. Symbiont-bearing Foraminifera. In Sen Gupta, BK (ed.), Modern Foraminifera, 2nd edn. Boston: Kluwer, 123-139.

Hallock, P., Lidz, B. H., Cockey-Burkhard, E.M., and Donnelly, K. B., 2003, Foraminifera as bioindicators in coral reef assessment monitoring: The FORAM index. Environmental *Monitoring and Assessment* 81: 221–238.

Haug, G.H., Hughen, K.A., Sigman, D.M., Peterson, L.C. and Rohl, U. 2001. Southward migration of the intertropical convergence zone through the Holocene. *Science* 293: 1304-1308.

Havach, S. M., and Collins, L. S., 1997, The distribution of recent benthic Foraminifera across habitats of Bocas del Toro, Caribbean Panamá. *Journal of Foraminiferal Research* 27: 232–249.

Henderson, G.M. and O'nions, R.K., 1995. $^{234}U^{238}U$ ratios in quaternary planktonic foraminifera. *Geochimica et cosmochimica acta* 59: 4685-4694.

Hendricson, K. J., 2014, Climatic Control of Coral Communities in the Galápagos Islands, Ecuador: MSc Thesis, Nova Southeastern University, Dania Beach, Florida, 103 p.

Hoegh-Guldberg, O., 1999. Climate change, coral bleaching and the future of the world's coral reefs. *Marine and freshwater research* 50: 839-866.

Hoegh-Guldberg, O., Mumby, P. J., Hooten A. J., Steneck, R. S., Greenfield, P., Gomez, E., Harvell, C. D., Sale P. F., Edwards, A. J., and Caldeira, K., 2007, Coral reefs under rapid climate change and ocean acidification: *Science* 318: 1737–1742.

Hofker J. 1927. The Foraminifera of the Siboga Expedition. Leiden: E.J. Brill.

Hohenegger, J., 2006. The importance of symbiont-bearing benthic foraminifera for West Pacific carbonate beach environments. *Marine Micropaleontology* 61: 4-39.

Holland, K., Eggins, S.M., Hönisch, B., Haynes, L.L. and Branson, O., 2017. Calcification rate and shell chemistry response of the planktic foraminifer *Orbulina universa* to changes in microenvironment seawater carbonate chemistry. *Earth and Planetary Science Letters* 464: 124-134.

Hottinger, L. C., 2000. Functional morphology of benthic foraminiferal shells, envelopes of cells beyond measure. *Micropaleontology* 46(Suppl. 1), 57–86.

Hottinger, L. C., 2006. The depth-depending ornamentation of some lamellar-perforate Foraminifera. *Symbiosis* 42: 141–151.

Hughes, T. P., Baird, A. H., Bellwood, D. R., Card, M., Connolly, S. R., Folke, C., Grosberg, R., Hoegh-Guldberg, O., Jackson, J. B. C., Kleypas, J., Lough, J. M., Marshall, P., Nyström, M., Palumbi, S. R., Pandolfi, J. M., Rosen, B., and Roughgarden, J., 2003, *Climate change, human impacts, and the resilience of coral reefs*: *Science*, 301: 929–933.

Humphreys, A. F., Halfar, J., Ingle, J. C., Manzello, D., Reymond, C. E., Westphal, H., and Riegl, B., 2019, Shallow-water benthic Foraminifera of the Galápagos archipelago: Ecologically sensitive carbonate producers in an atypical tropical oceanographic setting: *Journal of Foraminiferal Research* 49: 48–65.

Jones, D. S., and Hasson, P. F., 1985, History and development of the marine invertebrate faunas separated by the Central American isthmus: *in* Stehli, F. G., and Webb, S. D. (eds.), The Great America Biotic Interchange: Plenum Press, New York, NY, p. 325–355.

Kelmo, F., and Hallock, P., 2013, Responses of foraminiferal assemblages to ENSO climate patterns on bank reefs of northern Bahia, Brazil: A 17–year record: *Ecological Indicators* 30: 148–157.

Kısakürek, B., Eisenhauer, A., Böhm, F., Garbe-Schönberg, D. and Erez, J., 2008. Controls on shell Mg/Ca and Sr/Ca in cultured planktonic foraminiferan, *Globigerinoides ruber* (white). *Earth and Planetary Science Letters* 273: 260-269.

Klicpera, A., Michel, J., and Westphal, H., 2015, Facies patterns of a tropical heterozoan carbonate platform under eutrophic conditions: The Banc d'Arguin, Mauritania: *Facies* 61: 1–24.

Knorr, P. O., Robbins, L. L., Harries, P. J., Hallock, P., and Wynn, J., 2015, Response of the miliolid *Archais angulatus* to simulated ocean acidification. *Journal of Foraminiferal Research* 45: 109–127.

Köhler-Rink, S. and Kühl, M., 2000. Microsensor studies of photosynthesis and respiration in larger symbiotic foraminifera. I The physico-chemical microenvironment of Marginopora vertebralis, *Amphistegina lobifera* and *Amphisorus hemprichii*. *Marine Biology* 137: 473-486.

Köhler-Rink, S. and Kühl, M., 2005. The chemical microenvironment of the symbiotic planktonic foraminifer Orbulina universa. *Marine Biology Research* 1: 68-78.

Kuffner, I.B., Jokiel, P.L., Rodgers, K.U.S., Andersson, A.J. and Mackenzie, F.T., 2012. An apparent "vital effect" of calcification rate on the Sr/Ca temperature proxy in the reef coral Montipora capitata. *Geochemistry, Geophysics, Geosystems* 13.

Laws, E.A. and Redalje, D.G., 1979. Effect of sewage enrichment on the phytoplankton population of a subtropical estuary. *Pacific Science* 33: 129–144.

Lea, D. W., Pak, D. K., and Spero, H. J. 2000, Climate impact of late Quaternary equatorial Pacific sea surface temperature variations: *Science* 289: 1719–1724.

Lear, C. H., Elderfield, H., and Wilson, P. A., 2000, Cenozoic deep-Sea temperatures and global ice volumes from Mg/Ca in benthic foraminiferal calcite: *Science* 287: 269–272

.

Lear, C.H., Rosenthal, Y. and N., S., 2002. Benthic foraminiferal Mg/Capaleothermometry: A revised core-top calibration. *Geochimica Cosmochimica Acta*, 66: 3375-3387.

Lear, C. H., Rosenthal, Y., and Wright, J. D., 2003, The closing of a seaway: Ocean water masses and global climate change. *Earth and Planetary Science Letters* 210: 425–436.

Lee JJ. 1990. Phylum Granuloreticulosa (Foraminifera). In Margulis L, Corliss JO, Melkonian M, and Chapman DJ (eds.), Handbook of Protoctista: the Structure, Cultivation, Habitats and their Life Histories of the Eukaryotic Microorganisms and Their Descendants Exclusive of Animals, Plants and Fungi. Boston: Jones and Bartlett, 524-548.

Lea, D.W., 2003. Elemental and Isotopic Proxies of Past Ocean Temperatures. In: K. Turkien (Editor), Treatise On Geochemistry. Elsevier.

Lee, J. J., 2006. Algal symbiosis in larger foraminifera. *Symbiosis* 42: 63–75.

Lee, J.J., Faber Jr., W.W., Anderson, O.R., and Pawlowski, J. 1991. Life cycles of Foraminifera. In J.J. Lee and O.R. Anderson (eds.), Biology of Foraminifera. London: Academic Press, 295-334.

Le Calvez J. 1946. Place de la reduction chromatique et alternance des phases nucléaires dans le cycle des Foraminiferes: Développement et reproduction. *Arch. Zool. Esp. Gen.* 80: 163-333.

Legeckis, R., 1988, Upwelling off the Gulfs of Panamá and Papagayo in the Tropical Pacific during March 1985: Journal of Geophysical Research 93: 15485–15489.

Linsley, B.K. et al., in press. Tracking the extent of the South Pacific Convergence Zone since 1619 AD. Geophys. Geochem. Geosys.

Linsley, B.K., Wellington, G.M. and D.P. Schrag, 2000. Decadal Sea Surface Temperature Variability in the Sub-tropical South Pacific from 1726 to 1997 A.D. Science, 290: 1145-1148.

Linsley, B.K. et al., 2004. Coral evidence for changes in the amplitude and spatial pattern of South Pacific interdecadal climate variability over the last 300 years. *Climate Dynamics* 22: 1-11.

Loeblich AR and Tappan H. 1992. Resent status of Foraminiferal classification. *Studies in Benthic Foraminifera, Proceedings of the 4th International Symposium on Benthic Foraminifera, Sendai, 1990.* Tokyo: Tokai University Press, 93-102.

Longet D and Pawlowski J. 2007. Higher-level phylogeny of Foraminifera inferred from the RNA polymerase II (RPBI) gene. *European Journal of Protisology* 43: 171-177.

Loubere, P. and Banonis, G., 1987. Benthic foraminiferal assemblage response to the onset of northern hemisphere glaciation: paleoenvironmental changes and species trends in the northeast Atlantic. *Marine Micropaleontology* 12: 161-181.

Lutze GF and Coulbourn WT, 1984. Recent benthic foraminifera from the continental margin of northwest Africa: community structure and distribution. *Marine Micropaleontology* 5: 361–401.

Manzello, D. P., 2010, Ocean acidification hotspots: Spatiotemporal dynamics of the seawater CO_2 system of eastern Pacific coral reefs. *Limnology and Oceanography* 55: 239–248.

Manzello, D. P., Kleypas, J. A., Budd, D. A., Eakin, C. M., Glynn, P. W., and Langdon, C., 2008, Poorly cemented coral reefs of the eastern tropical Pacific: Possible insights into reef development in a high-CO_2 world: Proceedings of the National Academy of Sciences of the United States of America, v. 105, p. 10450–10455.

Manzello, D. P., Eakin, C. M., and Glynn, P. W., 2017, Effects of global warming and ocean acidification on carbonate budgets of eastern Pacific coral reefs, *in* Glynn, P. W., et al. (eds.), Coral Reefs of the Eastern Tropical Pacific: Persistence and Loss in a Dynamic Environment: Springer, Dordrecht, Netherlands, pp. 517–533.

Marchitto, T. M., and deMenocal, P. B., 2003, Late Holocene variability of upper North Atlantic Deep Water temperature and salinity: *Geochemistry, Geophysics, Geosystems* 4: 1–12.

Martin, P. A., Lea, D. W., Rosenthal, Y., Shackleton, N. J., Sarnthein, N., and Papenfuss, T., 2002, Quarternary deep sea temperature histories derived from benthic foraminiferal Mg/Ca: *Earth Planetary Science Letters* 198: 193–209.

Martínez-Colón, M., Hallock, P., and Green-Ruíz, C., 2009, Strategies for using shallow-water benthic foraminifers as bioindicators of potentially toxic elements: A review. *Journal of Foraminiferal Research* 39: 278–299.

McKee, E.D., Chronic, J. and Leopold, E.B., 1959. Sedimentary belts in lagoon of Kapingamarangi Atoll. *AAPG Bulletin* 43: 501-562.

Morse, J.W. and Bender, M.L., 1990. Partition coefficients in calcite: Examination of factors influencing the validity of experimental results and their application to natural systems. *Chemical Geology* 82: 265-277.

Moy CM, Seltzer GO, Rodbell DT, Anderson DM. 2002. Variability of El Niño/Southern Oscillation activity at millennial timescales during the Holocene epoch. *Nature* 420: 162–165.

Mucci, A. 1987. Influence of temperature on the composition of magnesian calcite overgrowths precipitated from seawater. *Geochimica et Cosmochimica Acta* 51: 1977–1984.

Murray, J. W., 1991, Ecology and distribution of benthic Foraminifera *in* Anderson, O.R. (ed.), Biology of Foraminifera: Academic Press, London, p. 221–253.

Murray JW. 2006. Ecology and Applications of Benthic Foraminifera. Cambridge: Cambridge University Press.

Naqvi, S.W.A., 1994. Denitrification processes in the Arabian Sea. *Proceedings of the Indian Academy of Sciences-Earth and Planetary Sciences* 103: 279-300.

National Oceanographic and Atmospheric Administration, 2018, El Niño SST Index. NOAA Earth System Research Laboratory, 31 July 2018, www.esrl.noaa.gov/psd/gcos_wgsp/Timeseries/Nino3.

Nurenberg, D., Muller, A. and Schneider, R.R., 2000. Paleo-sea surface temperature calculations in the equatorial east Atlantic from Mg/Ca ratios in planktic foraminifera: A comparison to sea surface temperature estimates from Uk037, oxygen isotopes and forminiferal transfer function. *Paleoceanography* 15: 124-134.

Nyholm, K.G. 1975. Orientation and binding power of recent monothalamous Foraminifera in soft sediments. *Micropaleontology* 3: 76-78.

Oliver, L.M., Fisher, W.S., Dittmar, J., Hallock, P., Campbell, J., Quarles, R.L., Harris, P. and LoBue, C., 2014. Contrasting responses of coral reef fauna and foraminiferal assemblages to human influence in La Parguera, Puerto Rico. *Marine Environmental Research* 99: 95-105.

Oomori, T., Kaneshima, H., Maezato, Y. and Kitano, Y., 1987. Distribution coefficient of Mg2+ ions between calcite and solution at 10–50 C. *Marine Chemistry* 20: 327-336.

Parker, J. H., and Gischler, E., 2011, Modern foraminiferal distribution and diversity in two atolls from the Maldives, Indian Ocean: Marine Micropaleontology 78: 30–49.

Pawlowski J and Holzmann M. 2008. Diversity and geographic distribution of benthic Foraminifera: a molecular perspective. *Biodiversity and Conservation* 17: 317-328

Pennington JT, Mahoney KL, Kuwahara VS, Kolber DD, Calienes R, Chavez FP. 2006. Primary production in the eastern tropical Pacific: a review. Prog Oceanogr 69:285–317.

Pochon, X., Garcia-Cuetos, L., Baker, A.C., Castella, E. and Pawlowski, J., 2007. One-year survey of a single Micronesian reef reveals extraordinarily rich diversity of Symbiodinium types in soritid foraminifera. *Coral Reefs* 26: 867-882.

Prazeres, M., 2018. Bleaching-associated changes in the microbiome of large benthic foraminifera of the Great Barrier Reef, Australia. *Frontiers in Microbiology* 9: 2404.

Raitzsch, M., Dueñas-Bohórquez, A., Reichart, G.-J., de Nooijer, L., and Bickert, T., 2010. Incorporation of Mg and Sr in calcite of cultured benthic foraminifera: impact of calcium concentration and associated calcite saturation state: *Biogeosciences* 7: 869–881.

Randall, C. J., Toth, L. T., Leichter, J. J., Maté, J. L., and Aronson, R. B., 2019, Upwelling buffers climate-change impacts on coral reefs of the tropical eastern Pacific. *Ecology* e02918: 1–15.

Reijmer, J. J. G., Bauch, T., and Schafer, P., 2012, Carbonate facies patterns in surface sediments of upwelling and non-upwelling shelf environments (Panama, East Pacific) *Sedimentology* 59: 32–56.

Rein B, Lückge A, Reinhardt L, Sirocko F, Wolf A, Dullo W-C. 2005. El Niño variability off Peru during the last 20,000 years. Paleoceanography 20:PA4003.

Reymond, C. E., Zihrul, K., Halfar, J., Riegl, B., Humphreys, A., and Westphal, H., 2016, Heterozoan carbonates from the equatorial rocky reefs of the Galápagos Archipelago. *Sedimentology* 63: 940–958.

Rosenthal, Y., Boyle, E. A., and Slowey, N., 1997, Temperature control on the incorporation of magnesium, strontium, fluorine, and cadmium into benthic foraminiferal shells from Little Bahama Bank: Prospects for thermocline paleoceanography. *Geochimica et Cosmochimica Acta* 61: 3633–3643.

Rosenthal, Y., Lear, C.H., Oppo, D.W. and Linsley, B.K., 2006. Temperature and carbonate ion effects on Mg/Ca and Sr/Ca ratios in benthic foraminifera: Aragonitic species *Hoeglundina elegans*. *Paleoceanography* 21.

Rongstad, B.L., Marchitto, T.M. and Herguera, J.C., 2017. Understanding the effects of dissolution on the Mg/Ca paleothermometer in planktic foraminifera: Evidence from a novel individual foraminifera method. *Paleoceanography* 32: 1386-1402.

Russell, A.D., Hoenisch, B., Spero, H.J. and Lea, D.W., 2004. Effects of seawater carbonate ion concentration and temperature on shell U. Mg, and Sr in cultured planktonic foraminifera. *Geochim. Cosmochim. Acta*, 68: 4347-4361.

Sachs, J.P., Blois, J.L., McGee, T., Wolhowe, M., Haberle, S., Clark, G. and Atahan, P., 2018. Southward shift of the Pacific ITCZ during the Holocene. *Paleoceanography and Paleoclimatology* 33: 1383-1395.

Sandweiss DH, Maasch KA, Burger RL, Richardson III JB, Rollins HB, Clement A. 2001. Variation in Holocene El Niño frequencies: climate records and cultural consequences in ancient Peru. *Geology* 29: 603–606.

Sadekov, A.Y., Eggins, S.M. and De Deckker, P., 2005. Characterization of Mg/Ca distributions in planktonic foraminifera species by electron microprobe mapping. *Geochem. Geophys. Geosys.,* 6: 14.

Sayani, H.R., Cobb, K.M., Cohen, A.L., Elliott, W.C., Nurhati, I.S., Dunbar, R.B., Rose, K.A. and Zaunbrecher, L.K., 2011. Effects of diagenesis on paleoclimate reconstructions from modern and young fossil corals. *Geochimica et Cosmochimica Acta* 75: 6361-6373.

Sayani, H.R., Thompson, D.M., Carilli, J.E., Marchitto, T.M., Chapman, A.U. and Cobb, K.M., 2021. Reproducibility of Coral Mn/Ca-Based Wind Reconstructions at Kiritimati Island and Butaritari Atoll. *Geochemistry, Geophysics, Geosystems* 22: p.e2020GC009398.

Schafer, C.T., 2000. Monitoring nearshore marine environments using benthic foraminifera: some protocols and pitfalls. *Micropaleontology* 46: 161-169.

Scheibner, C. and Speijer, R.P., 2008. Late Paleocene–early Eocene Tethyan carbonate platform evolution—A response to long-and short-term paleoclimatic change. *Earth-Science Reviews* 90: 71-102.

Schlesinger WH. 1991. Biogeochemistry: An Analysis of Global Change. San Diego: Academic Press.

Schnitker D, 1974. Ecotypic variation in *Ammonia beccarii* (Linné). *Journal of Foraminiferal Research* 4: 217-223.

Schönfeld J, Alve E, Geslin E, Jorissen F, Korsum S, and Spezzaferri S. 2012. The FOBIMO (Foraminiferal Biomonitoring) initiative—Towards a standardized protocol for soft-bottom benthic Foraminiferal monitoring studies. *Marine Micropaleontology* 94-95: 1-13.

Schrag, D. P., 1999. Rapid analysis of high-precision Sr/Ca ratios in corals and other marine carbonates. *Paleoceanography* 14: 97–102.

Segev, E. and Erez, J., 2006. Effect of Mg/Ca ratio in seawater on shell composition in shallow benthic foraminifera. *Geochemistry, Geophysics, Geosystems* 7.

Sen Gupta BK. 2002. Systematics of modern Foraminifera. In Sen Gupta BK (ed.), Modern Foraminifera, 2nd edn. Boston: Kluwer. 7-36.

Skinner, L. C., Shackleton, N. J., and Elderfield, H., 2003, Millennial-scale variability of deep-water temperature and $\delta^{18}O_{dw}$ indicating deep-water source variations in the Northeast Atlantic 0–34 cal. ka BP: *Geochemistry, Geophysics, Geosystems* 4:1–17.

Spero, H.J., Eggins, S.M., Russell, A.D., Vetter, L., Kilburn, M.R. and Hönisch, B., 2015. Timing and mechanism for intratest Mg/Ca variability in a living planktic foraminifer. *Earth and Planetary Science Letters* 409: 32-42.

Stuiver, M. and Reimer, P.J., 1993. Extended 14C data base and revised CALIB 3.0 14C age calibration program. *Radiocarbon* 35: 215-230.

Timmerman, A., Oberhuber, J., Bacher, A., Esch, M., Latif, M., and Roeckner, E., 1999. Increased El Niño frequency in a climate model forced by future greenhouse warming: *Nature* 298: 694–697.

Toth, L. T., 2013, Holocene reef development in the tropical eastern Pacific: PhD Dissertation, Florida Institute of Technology, Melbourne, Florida, 374 p.

Toth, L. T., Aronson, R. B., Cobb, K. M., Cheng, H., Edwards, R. L., Grothe, P. R., and Sayani, H. R., 2015a, Climatic and biotic thresholds of coral-reef shutdown: *Nature Climate Change* 5: 369–374.

Toth, L. T., Aronson, R. B., Cheng, H., Edwards, R. L., 2015b, Holocene variability in the intensity of wind-gap upwelling in the tropical eastern Pacific: *Paleoceanography* 30: 1113–1131.

Toth, L. T., Aronson, R. B., Vollmer, S. V., Hobbs, J. W., Urrego, D. H., Cheng, H., Enochs, I. C., Combosch, D. J., van Woesik, R., and Macintyre, I. G., 2012, ENSO drove 2500-year collapse of Eastern Pacific coral reefs: *Science* 337: 81–84.

Toth, L. T., Macintyre, I. G., and Aronson, R. B., 2017, Holocene reef development in the Eastern Tropical Pacific, *in* Glynn P. W., et al. (eds.), Coral Reefs of the Eastern

Tropical Pacific: Persistence and Loss in a Dynamic Environment: Springer, Dordrecht, Netherlands, p. 177–201.

Toyofuku, T., Kitazato, H., Kawahata, H., Tsuchiya, M., and Nohara, M., 2000, Evaluation of Mg/Ca thermometry in Foraminifera: Comparison of experimental results and measurements in nature: *Paleoceanography* 15: 456–464.

Tudhope, A.W., Chilcott, C.P., McCulloch, M.T., Cook, E.R., Chappell, J., Ellam, R.M., Lea, D.W., Lough, J.M., Shimmield, G.B. 2001. Variability in the El Niño-Southern Oscillation through a glacial-interglacial cycle. *Science* 291: 1511–1517.

van Dijk, I., de Nooijer, L. J., and Reichart, G. J., 2017, Trends in element incorporation in hyaline and porcelaneous foraminifera as a function of pCO_2: *Biogeosciences* 14: 497–510.

Verhallen, P.J.J.M. 1991. Late Pleistocene to early Pleistocene Mediterranean mud-dwelling Foraminifera, influence of a changing environment on community structure and evolution. *Utrect Micropaleontology Bulletin*. 40: 1-219.

Waelbroeck, C., Labeyrie, L., Michel, E., Duplessy, J.C., Mcmanus, J.F., Lambeck, K., Balbon, E. and Labracherie, M., 2002. Sea-level and deep water temperature changes derived from benthic foraminifera isotopic records. *Quaternary science reviews* 21: 295-305.

Walther, G.R., Post, E., Convey, P., Menzel, A., Parmesan, C., Beebee, T.J., Fromentin, J.M., Hoegh-Guldberg, O. and Bairlein, F., 2002. Ecological responses to recent climate change. *Nature*, 416: 389-395.

Wang, C., Deser, C., Yu, J., DiNezio, P., and Clement, A., 2016, El Niño and Southern Oscillation (ENSO): A Review, *in* Glynn P. W., et al. (eds.), Coral Reefs of the Eastern Tropical Pacific: Persistence and Loss in a Dynamic Environment: Springer, Dordrecht, Netherlands, p. 85–106.

Wang, C., and Fiedler, P. C., 2006, ENSO variability and the eastern tropical Pacific: A review: *Progress in Oceanography* 69: 239–266.

Woodruff, F., 1985. Changes in Miocene deep-sea benthic foraminiferal distribution in the Pacific Ocean: Relationship to paleoceanography. *Geological Society of America Memoir* 163: 131-176.

Wyatt, A. S. J., Leichter, J. J., Toth, L. T., Miyajima, T., Aronson, R. B., and Nagata, T., 2020, Heat accumulation on coral reefs mitigated by internal waves: *Nature Geoscience* 13: 28–34.

van der Zwaan, G.J., 1982. *Paleoecology of late Miocene Mediterranean foraminifera* (Doctoral dissertation, University Utrecht).

Xie, S.-P., Xu, H., Kessler, W. S., and Nonaka, M., 2005, Air-sea interaction over the eastern Pacific warm pool: Gap winds, thermocline dome, and atmospheric convection: *Journal of Climate* 18: 5–20.

Zamora-Duran, M.A., Aronson, R.B., Leichter, J.J., Flannery, J.A., Richey, J.N. and Toth, L.T., 2020. Imprint of Regional Oceanography on Foraminifera of Eastern Pacific Coral Reefs. *Journal of Foraminiferal Research* 50: 279-290.

APPENDIX A

RADIOCARBON DATES

This appendix includes a complete list of radiocarbon Contadora, Saboga, and Canales de Tierra. Radiocarbon dates are calibrated according to the local (Gulf-specific) reservoir correction (ΔR). Both the mean date of the probability distribution of dates and the 2σ ranges are given.

Table A-1. Radiocarbon dates from fore-reef cores at Contadora, Iguana, and Canales de Tierra.

Site	Core #	Depth in core (cm)	Coral genus	Dating technique	Conventional ^{14}C age	ΔR	Cal BP	Cal BP 2σ range
Contadora	EP08-26	40–45	*Pocillopora*	Bulk ^{14}C	Modern			
		55–60	*Porites*	Bulk ^{14}C	1020±50	-83±36.8	534	673–376
		65–70	Foraminifera	Bulk ^{14}C	Modern			
		80–85	*Pocillopora*	Bulk ^{14}C	1450±60	-83±36.8	919	1117–723
		115–125	*Pocillopora*	Bulk ^{14}C	1370±15	-83±36.8	834	1205–827
		145–150	*Pocillopora*	Bulk ^{14}C	1540±50	-83±36.8	1016	1205–827
		165–170	Foraminifera	Bulk ^{14}C	2930±20	-87±35.1	2632	3067–2867
		175–180	*Psammocora*	Bulk ^{14}C	3730±40	419±32.7	2974	3165–2779
		180–185	*Porites*	Bulk ^{14}C	4490±60	256±31.8	4142	4384–3909
		225–230	Foraminifera	Bulk ^{14}C	2100±20	56.5±35.3	1569	1719–1399
		260–265	Foraminifera	Bulk ^{14}C	4700±25	256±31.8	4420	4611–4227
		260–265	*Pocillopora*	Bulk ^{14}C	4840±20	100±38.5	4794	4977–4589
		305–310	*Pocillopora*	Bulk ^{14}C	5060±30	-34±3709	5244	5441–5035

Site	Core #	Depth in core (cm)	Coral genus	Dating technique	Conventional ^{14}C age	ΔR	Cal BP	Cal BP 2σ range
Saboga	EP09-33	25–30	*Psammocora*	Bulk ^{14}C	565±20	-134±37.5	157	183–1
		80–85	Foraminifera	Bulk ^{14}C	1340±20	-83±36.7	807	1045–667

		80–85	*Pocillopora*	Bulk ^{14}C	2920±15	-87±35.1	2621	2289–2086
		105–110	*Pocillopora*	Bulk ^{14}C	3070±50	419±32.7	2175	2351–1963
		125–130	*Psammocora*	Bulk ^{14}C	3050±70	419±32.7	2149	2358–1899
		125–130	Foraminifera	Bulk ^{14}C	3700±20	419±32.7	2934	3109–2764
		160–170	*Pocillopora*	Bulk ^{14}C	4460±60	241±34.5	4122	4368–3886
		190–195	Foraminifera	Bulk ^{14}C	3670±25	419±32.7	2897	3070–2740
		205–210	*Pocillopora*	Bulk ^{14}C	4560±80	163±37.9	4531	4807–4265
		210–215	*Pocillopora*	Bulk ^{14}C	4610±20	163±37.9	4424	4619–4225
		225–230	Foraminifera	Bulk ^{14}C	4740±25	163±37.9	4596	4794–4414
Canales	EP11-41	45–50	*Pocillopora*	Bulk ^{14}C	795±15	-69±37.4	332	473–164
		100–105	*Pocillopora*	Bulk ^{14}C	850±30	-69±37.4	376	516–236
		115–120	*Pocillopora*	Bulk ^{14}C	830±15	-69±37.4	361	500–220
		115–120	Foraminifera	Bulk ^{14}C	1050±15	-69±37.4	547	661–430
		120–125	*Pocillopora*	Bulk ^{14}C	1880±30	-86.5±32.9	1363	1524–1226
		140–145	Foraminifera	Bulk ^{14}C	1390±15	-86.5±32.9	856	1002–705
		165–170	*Pocillopora*	Bulk ^{14}C	2000±30	-104±32.9	1506	1522–1374
		190–195	Foraminifera	Bulk ^{14}C	1950±20	-104±32.9	1450	1598–1303
		225–230	*Pocillopora*	Bulk ^{14}C	4150±30	-125±32.9	4198	4392–4001
		260–265	*Pocillopora*	Bulk ^{14}C	4340±20	-26±32.7	4316	4502–4163
		270–275	Foraminifera	Bulk ^{14}C	3580±20	-53.5±33.1	3250	3400–3071
		290–295	*Pocillopora*	Bulk ^{14}C	4360±20	-26±32.7	4341	4517–4152
		365–370	*Pocillopora*	Bulk ^{14}C	4760±60	-83±34.2	4930	5208–4706

APPENDIX B

SIMPER RESULTS

This appendix includes a complete list of species that contribute to the differences between sites and the cumulative sum of the percent difference.

Table B-1. Genera and their percent contribution to differences between Contadora and Canales de Tierra.

Genus	Average	Standard Deviation	Avg. to SD ratio	Average Abundance A	Average Abundance B	Cumulative Sum
Hayesina	0.03	0.02	1.58	0.67	0.26	0.08
Quinqueloculina	0.03	0.02	1.31	1.46	1.04	0.16
Peneroplis	0.02	0.02	1.41	0.70	0.46	0.23
Triloculina	0.02	0.02	1.34	0.53	0.36	0.30
Sorites	0.02	0.02	1.28	0.74	0.57	0.36
Pseudohauerina	0.02	0.01	1.45	0.44	0.18	0.42
Spiroloculina	0.02	0.01	1.43	0.44	0.19	0.47
Rosalina	0.02	0.01	1.48	1.55	1.83	0.52
Borelis	0.02	0.01	1.25	0.30	0.27	0.57
Uvigerina	0.02	0.01	1.37	0.40	0.47	0.62
Neoconorbina	0.02	0.01	1.32	0.43	0.32	0.67
Bolivina	0.02	0.01	1.31	0.48	0.62	0.72
Cymbaloporetta	0.01	0.01	1.39	0.27	0.32	0.76
Nonionoides	0.01	0.01	1.29	0.24	0.29	0.81
Elphidium	0.01	0.01	1.31	0.34	0.36	0.85

Reusella	0.01	0.01	1.35	0.23	0.29	0.89
Articulina	0.01	0.01	1.08	0.20	0.23	0.93
Planorbulina	0.01	0.01	1.22	0.20	0.27	0.97
Marginopora	0.01	0.01	1.19	0.13	0.11	1.00

Table B-2. Genera and their percent contribution to differences between Saboga and Contadora.

Genus	Average	Standard Deviation	Avg. to SD Ratio	Average Abundance A	Average Abundance B	Cumulative Sum
Quinqueloculina	0.02	0.02	1.31	0.99	1.04	0.08
Hayesina	0.02	0.01	1.51	0.53	0.26	0.15
Peneroplis	0.02	0.01	1.38	0.47	0.46	0.22
Sorites	0.02	0.01	1.36	0.57	0.57	0.29
Triloculina	0.02	0.01	1.37	0.40	0.36	0.35
Nonionoides	0.02	0.01	1.34	0.35	0.29	0.41
Elphidium	0.02	0.01	1.27	0.52	0.36	0.48
Uvigerina	0.02	0.01	1.27	0.45	0.47	0.53
Borelis	0.02	0.01	1.17	0.12	0.27	0.58
Bolivina	0.01	0.01	1.30	0.61	0.62	0.63
Cymbaloporetta	0.01	0.01	1.33	0.19	0.32	0.68
Reusella	0.01	0.01	1.34	0.15	0.29	0.73
Neoconorbina	0.01	0.01	1.29	0.29	0.32	0.78
Planorbulina	0.01	0.01	1.25	0.21	0.27	0.83
Pseudohauerina	0.01	0.01	1.25	0.20	0.18	0.87
Articulina	0.01	0.01	1.22	0.11	0.23	0.91
Spiroloculina	0.01	0.01	1.33	0.22	0.19	0.95
Rosalina	0.01	0.01	1.26	1.82	1.83	0.97

Marginopora	0.01	0.01	0.85	0.05	0.11	1.00

Table B-3. Genera and their percent contribution to differences between Saboga and Canales de Tierra.

Genus	Average	Standard Deviation	Avg. to SD Ratio	Average Abundance A	Average Abundance B	Cumulative Sum
Quinqueloculina	0.03	0.02	1.51	0.99	1.46	0.09
Peneroplis	0.02	0.01	1.47	0.47	0.70	0.16
Triloculina	0.02	0.01	1.43	0.40	0.53	0.22
Hayesina	0.02	0.01	1.35	0.53	0.67	0.29
Sorites	0.02	0.01	1.46	0.57	0.74	0.35
Pseudohauerina	0.02	0.01	1.50	0.20	0.44	0.41
Spiroloculina	0.02	0.01	1.53	0.22	0.44	0.47
Elphidium	0.02	0.01	1.32	0.52	0.34	0.52
Bolivina	0.02	0.01	1.32	0.61	0.48	0.58
Nonionoides	0.02	0.01	1.38	0.35	0.24	0.63
Rosalina	0.02	0.01	1.79	1.82	1.55	0.68
Borelis	0.02	0.01	1.17	0.12	0.30	0.73
Neoconorbina	0.01	0.01	1.39	0.29	0.43	0.78
Uvigerina	0.01	0.01	1.38	0.45	0.40	0.83
Reusella	0.01	0.01	1.32	0.15	0.23	0.87
Cymbaloporetta	0.01	0.01	1.38	0.19	0.27	0.91
Articulina	0.01	0.01	0.90	0.11	0.20	0.94
Planorbulina	0.01	0.01	1.36	0.21	0.20	0.98
Marginopora	0.01	0.01	1.08	0.05	0.13	1.00

APPENDIX C

MG/CA AND SR/CA RATIOS

This appendix includes a complete list of Mg/Ca and Sr/Ca ratios from Contadora, Saboga, and Canales de Tierra.

Table A-1. Mg/Ca and Sr/Ca concentrations from cores at Contadora, Saboga, and Canales de Tierra.

Site	Core #	Depth in core (cm)	Mg/Ca (mmol/ mol)	Sr/Ca (mmol/mol)
Contadora	EP08-26	10	127.51	2.04
		20	126.54	3.52
		60	115.93	2.70
		70	123.04	3.69
		80	123.65	3.99
		90	112.75	5.90
		110	101.65	3.87
		120	109.02	4.38
		130	102.36	5.74
		140	134.96	4.21
		150	139.51	2.22
		160	203.37	3.44
		165	139.60	2.07
		170	247.18	3.50
		175	151.43	3.51
		180	207.71	2.87
		185	116.93	5.10
		190	115.67	5.08
		210	116.79	2.09
		220	143.95	2.28
		240	137.41	2.15
		260	139.74	2.35

		280	143.10	3.06
		300	141.54	3.78
Saboga	EP09-33	15	135.64	2.16
		30	136.30	2.91
		60	139.09	2.35
		80	140.12	2.44
		90	142.69	2.15
		100	140.70	2.08
		110	135.76	2.19
		120	135.97	2.03
		125	135.39	1.95
		130	145.39	1.94
		140	136.91	1.98
		145	139.59	2.02
		150	135.42	2.04
		160	147.58	2.23
		190	140.98	2.04
		210	141.06	2.15
		220	140.82	2.05
		240	142.61	2.12
Canales	11-41	20	144.28	2.17
		60	146.93	2.32
		90	145.60	2.24
		110	145.13	2.32
		120	154.44	2.67
		165	143.86	2.09
		170	142.29	2.09
		175	139.48	2.18
		180	150.04	2.09
		185	146.41	2.08
		190	147.64	2.07
		195	139.25	2.04
		200	139.65	2.21
		210	138.89	2.89
		220	140.02	2.31
		240	146.13	2.23
		270	143.55	2.09
		300	146.42	2.24
		320	144.41	2.13
		360	145.11	2.03